LUND UNIVERSITY

LTH

FACULTY OF ENGINEERING

Degree Project in Applied Biochemistry KBKM05

Affinity exploration of a bispecific ADAPT towards CD22 for therapeutic purposes

January 2024 – June 2024

Nora Jonsson Pagels

Examiner: Johan Bonde, Senior lecturer, Institute of Pure and Applied Biochemistry, LTH
Supervisor at LTH: Solmaz Hajizadeh, Researcher, Institute of Pure and Applied Biochemistry, LTH
Supervisor at KTH: Sophia Hober, Professor, Division of Protein Science, KTH
Co-Supervisor at KTH: Emma Larsson, PhD student, Division of Protein Science, KTH

Abstract

Leukemia is the most common type of cancer in children, with B-cell acute lymphocytic leukemia (B-ALL) being a common type in both children and adults. Different types of treatments are available, such as chemotherapy, stem cell treatment and immunotherapy. However, a recurring problem is relapses, with the survival rate after relapse being very low. In combating this issue new methods have been developed, where the usage of surface protein targeting has been a prominent feature. These new methods, such as antibody therapies and chimeric antigen receptor (CAR)-T cell therapy, targets surface proteins such as CD19 or CD22, which are exclusively expressed on the surface of B-cells. These therapies have shown great results; however, they are expensive with many patients still relapsing due to downregulation of the target protein. An alternative, which could provide cheaper production and high modularity is the usage of albumin-derived affinity proteins (ADAPT), a small triple helical scaffold protein of about 6 kDa. The cheaper production is enabled by the possibility of rapidly producing ADAPTs using a bacterial host. The high modularity means potential for multitargeting, which would be beneficial if downregulation of one targeted protein would occur. ADAPT naturally binds to human serum albumin (HSA), an ability which has been preserved to increase the serum half-life of the small ADAPT to enable therapeutic use. Moreover, other residues in the ADAPT have been found changeable in such a way that it can be modified to have an affinity towards another protein, such as for CD22, while simultaneously binding HSA. For this purpose ADAPT(ABD035)_CD22_10 has been developed. However, even though it binds in rapidly it has a high off rate, which is problematic if to be used for therapeutic purposes. In this study, 20 variants were chosen from a maturation selection with a library based on ADAPT(ABD035)_CD22_10, to investigate is any of these offered a stronger affinity. However, none of them did. Moreover, an alanine scan was executed to evaluate which positions are of great importance for the affinity to CD22 as well as for the stability of the ADAPT. Lastly, a library exploration was made to further investigate one position targeted in the alanine scan as well as a position previously unexplored. With the conclusions drawn from these results, a new design for an affinity maturation library is suggested, hopefully deriving new variants with slower off rate. This with the desire to create an ADAPT which could be used for therapeutic purposes in the future.

KEY WORDS: cancer therapy, ADAPT, ABD, protein engineering, albumin, simultaneous bispecificity, leukemia, B-cells, CD22.

Sammanfattning

Leukemi är den vanligaste cancerformen hos barn, där B-cells akut lymfatisk leukemi (B-ALL) är en vanlig leukemiform hos både barn och vuxna. Det finns olika typer av behandlingar, så som kemoterapi, stamcellsbehandling och immunterapi. Ett återkommande problem med dagens behandlingar är dessvärre återfall, och bland dessa patienter är överlevnadsfrekvensen väldigt låg. I hopp om att lösa detta problem har nya metoder utvecklats, som ofta inriktar sig på proteiner på cellens yta. Dessa nya metoder, såsom antikroppsbehandling och CAR-T-cellsbehandling, målsöker ytproteiner såsom CD19 eller CD22, som enbart uttrycks på B-celler. Trots att behandlingsmetoderna har påvisat bra resultat så är de väldigt dyra och patienter får fortfarande återfall på grund av nedreglering av målproteinet. Ett alternativ till dessa metoder, som skulle kunna innebära billigare produktion och hög modularitet är albumin-derived affinity proteins (ADAPT), ett litet protein på ungefär 6 kDa, i form av en trippelhelix. Den lägre kostnaden kommer ifrån möjligheten att producera ADAPT i bakterier. Hög modularitet innebär att det finns potential att målsöka flera olika proteiner samtidigt, vilket skulle vara fördelaktigt i de fall som nedreglering av ett visst protein sker. ADAPT binder naturligt till mänskligt albumin (HSA), en egenskap som har bevarats för att öka halveringstiden i blodet för ADAPT, vilket är en förutsättning för att kunna användas som läkemedelsbehandling. Vidare har man funnit att andra delar av ADAPT kan modifieras för att skapa affinitet mot ytterligare ett protein, så som CD22, samtidigt som den binder HSA. ADAPT(ABD035)_CD22_10 har tagits fram för detta syfte. Trots att den binder in fort (hög ”on rate”) till CD22 dissocierar den dock hastigt (snabb ”off rate”), vilket är problematiskt om bindaren ska användas för läkemedelsbehandling. I den här studien undersöktes 20 varianter, utvalda från en matureringsselektion som skapats från ett bibliotek baserad på ADAPT(ABD035)_CD22_10, för att se om någon av dem har högre affinitet. Dock visade ingen av de 20 varianterna på förbättrad affinitet. Utöver detta gjordes en alanin skanning för att hitta vilka positioner som har stor betydelse för affiniteten mot CD22 samt stabiliteten av ADAPT. Slutligen gjordes en biblioteksundersökning för att vidare undersöka en specifik position från alanin skanningen, samt en position som tidigare varit orörd. Med slutsatser dragna från dessa resultat föreslås en ny design för ett affinitetsmatureringsbibliotek, med förhoppningen om att nya varianter ska kunna tas fram med långsammare ”off rate”. Detta med målet att skapa en ADAPT som ska kunna användas som läkemedelsbehandling i framtiden.

Acknowledgement

This Master thesis was conducted during the spring of 2024 at KTH Royal Institute of Technology, at the department of Protein Science as a thesis for Lund University, Faculty of Engineering.

I would like to start by thanking Emma, my co-supervisor at KTH who has guided me through this project flawlessly. Always encouraging me, knowing how to challenge me and making me feel right at home from day one. My gratitude goes to Sophia for making it possible for me to join this project. I am so happy to have had the chance to work in your group for a while. It's been a time full of inspiration and growth. A special thanks to all the people in the Hober group, I have so enjoyed this time with you. Thank you for always being prepared to spare a minute for another question!

I also want to thank Solmaz, my LTH supervisor, who is always quick to reply and easy to communicate with!

Thank you to the Secretome group, for kindly providing me with CD22. And lastly, I would like to thank all the people on floor 3 at AlbaNova for being so open and helpful. My sneak-peak at KTH has been very nice because of all of you.

Table of Contents

1. Introduction

Acute lymphocytic leukemia (ALL) is the most common type of cancer in children, accounting for about 25% of all cases. In children, about 85% of the ALL cases develop into B-cell acute lymphoblastic leukemia (B-ALL) (1). The same number for adults corresponds to 75% (2). A report done in Sweden showed that between the years 2007 and 2015, the 5-year survival (OS) was about 46% in the age group 46 to 65 years (3). Available treatments toward B-ALL cancer include for example chemotherapy, stem cell treatment and immunotherapy (2). However, a recurring problem with treatments of ALL is relapses. For children who are treated for ALL, and have been in complete remission, about 15% relapse (4). With only about 40% of adults surviving long term without the disease reoccurring. This is even more of a problem due to the low survival rate after relapse, with one study, published in 2007, recording an OS rate of only 7%, 5 years after relapse (5). To combat these issues, new methods are being developed. One such example is the development of chimeric antigen receptor (CAR)-T cell therapy, a type of immunotherapy which was FDA approved for the first time in 2017 for people under age 25 with B-ALL, in second or later relapse. This is an anti-CD19 CAR-T cell therapy (6). Here T-cells are gathered from the patient, which are thereafter genetically modified to recognize CD19, a protein expressed exclusively on the surface on B-cells, then adding them back to the patient. This is both time consuming and makes it a very expensive method (7). Even though the response has been generally positive with this treatment, a new problem has occurred. For patients which still relapse, the cancer cells have been seen to exhibit less or no CD19 on their surface, thus rendering further treatment ineffective (8,9). One way to work around this is to target another protein on the B-cell surface. Therefore, phase 1 studies have been made, using a mixture of CD19 and CD22 CAR-T cell therapy for B-ALL which has thus far showed promising results (10,11). CD22 is a protein which has regulatory effects on the growth of B-cells. It is a surface transmembrane sialoglycoprotein of 135 kDa that is exclusively expressed on B-lymphocytes, at a concentration which is highest for mature B-cells (Figure 1a). This makes it a good candidate for cancer treatment, since targeting CD22 will specifically target B-cells (12). Additionally, the prevalence of CD22 on B-cells is high, with two studies finding CD22 on all their patients (13,14)

Another type of treatment using specific B-cell targeting is inotuzumab ozogamicin. This is a monoclonal antibody which specifically recognizes CD22 and is covalently linked to a cytotoxin. This was also FDA approved in 2017, for treatment of adults with relapsed or refractory CD22-positive B-ALL (15). Although monoclonal antibodies are less expensive than CAR-T, the prize is still high and relapses still occur, meaning further alternatives is desirable. One such option could be the usage of albumin-derived affinity proteins (ADAPT) which due to its small size, can be produced directly in *E. coli* making it a cheaper and a more easily producible alternative (16). ADAPT is a triple helical scaffold protein, at a mass of only 6 kDa. It is based on one of the albumin-binding domains of streptococcal protein G (SPG), a bacterial surface protein that has been very well characterized (17). ADAPT naturally binds to human serum albumin (HSA) whereafter modifications have been made to create a dual binding capacity (Figure 2a). Thus, the ADAPT can be tailored to have an affinity, a binding strength, towards another target protein of choice, at the same time as that of HSA. To obtain the bispecific binding to another protein, 11 positions on helix 1 and 2 (eight of which are located on helix 1 and three on helix 2) can be randomized to create a novel binding surface. The affinity towards HSA is being kept purposefully. This is due to small proteins, such as ADAPT, having a very short half-life in blood. However, as ADAPT naturally binds to HSA it can take advantage of the abilities HSA possesses when it comes to half-life. Albumin has a half-life of approximately 19 days in humans, which is dependent both on its size, 67 kDa, stopping the

filtration through the glomerular barrier, and it being recycled via binding to the neonatal Fc receptor instead of being sent to lysosomes for degradation (Figure 1b) (18). By albumin association, ADAPT can thus remain longer in the blood without being broken down, to such an extent that it is possible to use it for therapeutic purposes (17).

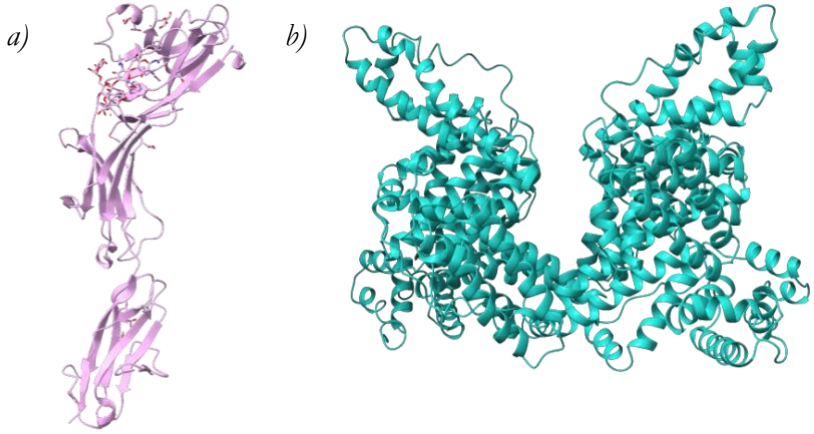

Figure 1. a) The structure of domain 1 to 3 of CD22 (PDB 5vkj). All seven domains of CD22 have a total size of 135 kDa. b) The structure of human serum albumin at a size of 67 kDa (PDB 1ao6).

For the three, antiparallel, helices that create ADAPT, helix 2 and 3 are responsible for the binding towards HSA. Depending on the desired abilities of the ADAPT, different ABD scaffolds can be used, containing small variations on helix 2 and 3 (19). ABD035 has been engineered to have a very high affinity towards HSA of approximately 50 fM, and with a melting temperature (T_m) of 58°C (20). Another scaffold, ABDstab, was developed to increase its stability. ABDstab has an affinity towards HSA of about 50 nM, however a T_m of over 80°C (21). ABDstab thus shows a lower affinity towards HSA compared to ABD035, but is also a more thermostable protein, which can be beneficial.

In a previous study, an ADAPT with the ABD035 scaffold, called ADAPT(ABD035)_CD22_10, has been derived (Figure 2b). The affinity (K_D) describes how strong the interaction is between two molecules and is dependent on how fast the molecules associate (the on rate, k_a) and dissociate (the off rate, k_d) from each other (22). This binder has been shown to have an affinity of 110 nM towards CD22 and dissociates almost instantly. The idea is to use the ADAPT for therapeutic purposes by coupling it to a drug agent, similar to inotuzumab ozogamicin. It would therefore be necessary for the ADAPT to bind to the B-cell to such an extent that the drug would have time to exert its cytotoxic effect. For this to happen, the off rate needs to be lower. The aim of this project is to improve the affinity of the ADAPT binder towards CD22, by decreasing k_d. A maturation library had previously been created based on the original binder but with usage of the ABDstab scaffold, to promote a high stability of the library variants. From the previous affinity maturation selections, 20 variants had been chosen to be characterized in this project. How the affinity and stability was affected by the switch between ADAPT(ABD035)_CD22_10 and ADAPT(ABDstab)_CD22_10 was also studied. Furthermore, an alanine scan was performed on ADAPT(ABD035)_CD22_10, where each of the eleven library positions on helix 1 and 2 was switched out to alanine, one by one, to see how each position influence the binding of ADAPT(ABD035)_CD22_10. Lastly, an exploration of the library was made to see if a certain previously locked position, based on the results from the alanine scan, could be varied, as well as if a completely new position could be altered when creating the next library, beyond the eleven that have been standardized.

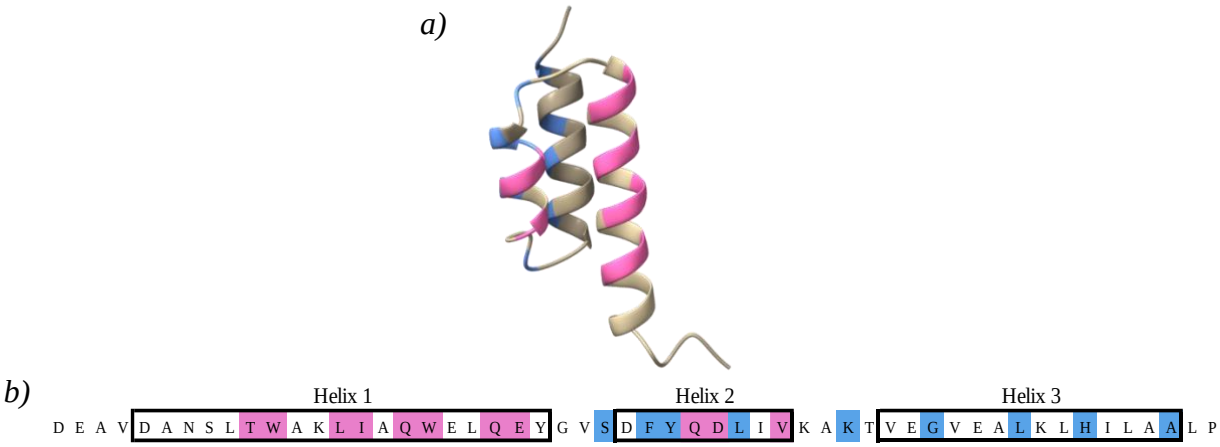

Figure 2. a) ADAPT(ABD035)_CD22_10 structure obtained by homology modeling (to the wild-type albumin binding domain, PDB 1gjt) using SWISS-MODEL (23). The pink coloration are the library positions that previously have been selected for binding against CD22. The blue coloration are the positions responsible for the binding towards HSA. The protein has a size of approximately 6 kDa (17). b) The amino acids of ADAPT(ABD035)_CD22_10. The pink coloration are the library positions that previously have been selected for binding against CD22. The blue coloration are the positions responsible for the binding towards HSA.

2. Material and Methods

2.1 Variants from the Maturation Selection

All PCR reactions were made in accordance with the instructions from the manufacturer of the polymerase. PCR purifications were executed using QIAquick PCR purification kit, gel extractions by QIAquick Gel Extraction Kit and plasmid preparations with QIAprep Spin Miniprep protocol, by the company QIAGEN. DNA concentrations were measured using NanoDrop 1000 spectrometer (Thermo Fisher Scientific) and in accordance with their instructions, unless otherwise specified. All restriction and ligation enzymes were products of New England Biolabs unless stated otherwise.

2.1.1 Cloning of ADAPT Sequences

To produce the 20 different ADAPTs from the affinity maturation selections, the gene encoding the ADAPT was subcloned into a bacterial expression vector. The vector used, HisDummy 4.0, contained a gene for carbenicillin resistance and a T7 promotor, helix 3 of ABDstab, which is identical in all 20 ADAPTs, as well as a dummy fragment, to be switched out for the wanted helix 1 and 2, and an N-terminal 6xHis-tag. The amount of vector had to be amplified, whereafter the dummy fragment could be cut out and the ADAPT gene (helix 1 and 2) ligated in.

2.1.1.1 Preparation of HisDummy 4.0

Firstly, the vector HisDummy 4.0 was chemically transformed into Top10 *E. coli* (made in-house) for amplification. This was done through mixing the plasmid with KCM (to a final concentration of 0.1 M KCl, 30 mM CaCl2, 50 mM MgCl2), whereafter it was incubated on ice for 5 minutes. Thereafter, the competent Top10 *E. coli* was added, after which it was incubated on ice for an additional 20 minutes and then at room temperature (RT) for an additional 10 minutes. Tryptic soy broth (TSB) medium was added, after which the mixture was put on a rotamixer at 150 rpm, 37ºC for 1 hour. When the hour had passed, it was plated on carbenicillin plates, whereafter they were incubated at 37ºC overnight (O/N).

After the incubation one colony was taken from the plate, being inoculated in TSB with 100 µg/ml carbenicillin. This was put in 37ºC O/N at 150 rpm. The day after, a plasmid preparation was made on the culture to obtain the HisDummy 4.0 vector.

The dummy part of the vector was to be cut out, creating sticky ends into which the ADAPT can be ligated. This was done through the HisDummy 4.0 being mixed in 1xrCutSmart buffer the restriction enzymes EcoRI-HF (R3101S) and HindIII-HF (R3104L). This was incubated for 1 hour in 37ºC for the cleavage to occur. To stop the reaction a heat inactivation was made at 80ºC for 20 minutes.

The cleaved HisDummy 4.0 was run through a 0.7% agarose gel and extracted through gel purification. The concentration was measured using Qubit (Thermo Fisher Scientific), in accordance with the manufacturer's instructions.

2.1.1.2 Preparation of ADAPT Fragments Helix 1-2

The primers were delivered from Integrated DNA Technologies. To amplify only the wanted ADAPT helix 1-2 from the phagemid selection output, a 1-step-PCR clone recovery was made, using Phusion DNA Polymerase (F-530L, Thermo Fisher Scientific), together with 2mM dNTP and the template plasmids, from the phage display selections, which was thereafter mixed with the ordered primers. Using a 1% agarose gel, the PCR products were examined, whereafter the

DNA concentration was measured. To produce sticky ends to use for ligation, the same restriction enzyme procedure was used as described for the HisDummy 4.0 vector. Thereafter a PCR purification was made, and then the DNA concentration was measured using Qubit.

2.1.1.9 Ligation of Cleaved ADAPT Fragments into Cleaved HisDummy 4.0
When ligating the cleaved ADAPT fragments with HisDummy 4.0, T4 DNA Ligase (M0202L) was used following the manufacturer's instructions. The samples were incubated at RT for 1 hour, after which the reaction was stopped using heat inactivation at 65ºC for 10 minutes.

The ligation product was then transformed into chemically competent Top10 *E. coli* cells, as described in 2.1.1.1 Preparation of HisDummy 4.0, using the ligation mix. The sample was then plated on carbenicillin plates and incubated at 37ºC overnight.

Colonies were chosen to be screened for each sample. The picked colonies were both regrown on a new carbenicillin plate, put in 37ºC O/N, as well as used for the screening. For the PCR reaction to screen the produced colonies, DreamTaq polymerase (EP0702, Thermo Fisher Scientific) was used with primers spanning the ADAPT insert. Thereafter a gel analysis of the product was conducted on a 1% agarose. Two of each sample which had the correct size were sent to Eurofins for Sanger sequencing, in accordance with their specifications.

2.1.2 Protein Production in BL21(DE3) *E. coli*
Since all 20 ADAPTs were now cloned and sequence confirmed, the next step was to produce the wanted proteins. To be able to compare the new variants to the original binder, ADAPT(ABD035)_CD22_10, this protein was produced as well.

Single Top10 *E.* coli colonies containing each of the respective ADAPT variant were inoculated in TSB with 100 μg/ml carbenicillin and grown O/N at 37 ºC and 150 rpm. A plasmid preparation was made on the cultures, after which the DNA concentration was measured. The plasmids were then transformed into competent BL21(DE3) *E. coli* (in-house made). The cells were mixed with plasmids, and then incubated on ice for 30 minutes, after which they were heat shocked at 42°C for 1 minute, then placed back on ice for 5 minutes. TSB was added, whereafter it was placed at 37°C, 200 rpm for 1 hour. Lastly, they were spread on carbenicillin plates and left at 37°C O/N. The day after, one colony per plate were dipped into TSB medium with 100 μg/ml carbenicillin, this was incubated O/N at 37°C, 150 rpm. The next day 4 ml of tryptic soy broth + yeast (TSB+Y) with 100 μg/ml carbenicillin were added to wells of a 24-deep well plate, after which the overnight cultures were added, to obtain an OD_{600} of approximately 0.1. They were thereafter incubated at 37°C, 200 rpm until OD_{600} reached between 0.5 and 0.8, then isopropyl β-d-1-thiogalactopyranoside (IPTG) was added to a final concentration of 1 mM. It was incubated at 25°C, 150 rpm O/N. The cells were then to be lysed to obtain the ADAPT proteins. The cultures were harvested through centrifugation at 3500xg for 20 minutes at 4°C. After discarding the supernatant, the pellet was resuspended in lysis buffer (0.5 mg/ml lysozyme (Sigma, L-2879), 8 U/ml DNase1, 1 mM $MgCl_2$ in 20 mM Tris-HCl) and then incubated at RT for 1 hour with slow shaking. The cell lysis was then centrifuged at 16.000xg for 20 minutes, 4°C, to remove cell debris.

2.1.3 Screening of Cell Lysates in Octet
To compare the affinity to CD22 of the 20 ADAPT variants and the original binder, biolayer interferometry (BLI) was employed using an Octet RED96 instrument (Sartorius). CD22, kindly provided by the Human Secretome project. The Octet was run, by capturing the ADAPTs from cell lysate on Anti-Penta-HIS (His1K) Biosensors (Satorius) for 600s, followed by

association to CD22 (1 µM) for 300 s and dissociation in PBST (0.15M NaCl, 8mM Na_2HPO_4, 2mM $NaH_2PO_4xH_2O$, 0.05% Tween20) for 600 s. A wash in PBST for 300 s was made between the samples. The sensors were regenerated three times in 10 mM glycine, pH 1.5 for 20 s. The shake speed used was 1000 rpm. The software used for analysis was Octet Data Acquisition and for evaluation ForteBio Data Analysis.

2.2 Alanine Scan

To gain a greater knowledge of which amino acids affect the affinity of the ADAPT towards CD22, an alanine scan was performed. Thus all 11 residues which had been randomized during the formation of the ADAPT library were one by one changed to alanine, generating 11 different variants of ADAPT(ABD035)_CD22_10.

ADAPT(ABDstab)_CD22_10 was also created and produced to evaluate how the difference between scaffolds ABD035 and ABDstab affected the affinity and stability of the ADAPT. This was done through changing one scaffold position on helix 2, switched out using QuickChange, and four scaffold positions on helix 3, made through exchanging the entire helix 3 using HisDummy4.0 (ABDstab). A PCR screen was performed, in accordance with 2.1.1.9 Ligation of cleaved fragments into cleaved HisDummy 4.0. Whereafter the original binder ADAPT(ABD035)_CD22_10 was to be analyzed and compared to the 11 alanine scan variants and ADAPT(ABDstab)_CD22_10.

2.2.1 QuickChange Mutagenesis

A QuickChange mutagenesis was executed to create the 11 variants of ADAPT(ABD035)_CD22_10 for an alanine scan. The primers used had been derived using Kozane (an open-source program for primer design), and then bought from Integrated DNA Technologies. Phusion DNA polymerase (F-530L, Thermo Fisher Scientific) was used together with dNTP (2mM) and template plasmid containing ADAPT(ABD035)_CD22_10, which was mixed with the mutagenesis primers whereafter a PCR was executed, using annealing temperatures of both 63°C and 67°C. Thereafter the PCR products were examined through a gel analysis using a 1% agarose gel. DnpI (R0176S) enzyme was added to the PCR products with incubation at 37℃ for 1 hour, to break down the parental DNA. The DnpI-treated DNA was transformed into chemically competent Top10 *E. coli* cells. This was done as before, with the changes of the heat shock being at 45 seconds in 42℃ (instead of RT for 10 minutes), whereafter they were put on ice for 5 minutes. As before, the mixture was plated on carbenicillin plates, which was put in 37℃ O/N. To make sure the correct sequences had been created a PCR screen was made, as described in 2.1.1.9 Ligation of cleaved fragments into cleaved HisDummy 4.0.

2.2.2 ADAPT(ABD035)_CD22_10 to ADAPT(ABDstab)_CD22_10

To change the single scaffold position on helix 2, a QuickChange mutagenesis was executed, in the same way as described above. Thereafter helix 3 of ADAPT(ABD035)_CD22_10 was to be changed to that of ADAPT(ABDstab)_CD22_10, thus ligating helix 1 and 2 into HisDummy 4.0. Firstly, one Top10 colony from the ADAPT(ABDstab)_CD22_10 QuickChange, were inoculated O/N using TSB with 100 µg/ml carbenicillin in 37℃ at 150 rpm. Thereafter the plasmid was extracted through plasmid preparation. A PCR was then preformed to amplify helix 1 and 2, as described in 2.1.1.2 Preparation of ADAPT fragments Helix 1-2. The PCR product was cleaved with EcoRI-HF (R3101S) and HindIII-HF (R3104L). The reaction was incubated at 37℃ for 1 hour, whereafter heat inactivation was performed at 80℃ for 20 minutes, followed by PCR purification. The cleaved fragments were then ligated into the

HisDummy 4.0 containing helix 3 of ABDstab, whereafter the ligation mix was transformed into Top10 *E. coli*, as previously described. Lastly, a PCR screen was performed, as described in 2.1.1.9 Ligation of cleaved fragments into cleaved HisDummy 4.0.

2.2.3 Protein Production

For ADAPT(ABDstab)_CD22_10 and the 11 alanine scan variants, firstly, the colonies of Top10 containing the correct sequences were inoculated in TSB with 100 µg/ml carbenicillin and incubated O/N at 37ºC and 150 rpm. These cultures were then used for plasmid preparations, whereafter they were transformed into BL21(DE3) *E. coli* as described in 2.1.2 Protein Production in BL21 E. coli. The day after, inoculation in TSB with 100 µg/ml carbenicillin, of a single BL21 colony were made with each of the 12 variants and the original ADAPT(ABD035)_CD22_10. The following day, these were used for protein production, using 100 ml of TSB+Y with 100 µg/ml of carbenicillin, in flasks of 1000 ml. To each flask, overnight culture was added to obtain an OD_{600} of approximately 0.1. These were put on 150 rpm in 37℃ until an OD_{600} of 0.5-0.8 was reached. Thereafter IPTG was added to a final concentration of 1 mM. The cultures were incubated O/N at 25℃ and 150rpm, to produce protein. The following day the cultures were transferred to centrifugation tubes. These were centrifuged at 4000 rpm for 8 minutes. The supernatant was discarded, with the pellet being resuspended using 10 ml TST (with a concentration of 25 mM Tris, 1 mM EDTA, 0.2 M NaCl, 0.05% Tween20). Thereafter lysis of the cells was done using a sonicator (Fisher Scientific, HB505). A microtip of 6 mm was used, with a pulse of 1.0/1.0 for 2:30 minutes at 30% amplitude. Another 10 ml of TST was added, after which the samples were centrifuged at 16000 rpm, 4℃ for 20 minutes. The lysate was then filtered through 0.45 µm syringe filters.

2.2.4 Protein Purification

Gravity flow columns packed with human serum albumin (HSA) sepharose matrix were used to purify the proteins. They columns cleaned with 5 column volumes (CV) of MilliQ and then 5 CV TST. Equilibration was done using 3 CV acetic acid (0.5M, pH 2.8) and then 8 CV TST. The samples were added to the columns, after which washing was made, firstly with 10 CV of TST and then 2 CV NH_4Ac (5mM, pH 6.0). Elution was made with 10x1ml of acetic acid (0.5M, pH 2.8). The fractions with an absorbance over 0.1, measured using a spectrophotometer at 280 nm, were pooled and frozen at -80℃ for at least an hour. These were freeze-dried O/N using ScanVac CoolSafe freeze dryer (LaboGene). The product was then resuspended in PBS (with a concentration of 0.14M NaCl, 2.7mM KCl, 1.8mM KH_2PO_4, 0.01M Na_2HPO_4), adding a few microliters of 1 M NaOH to aid in dissolving, making sure the pH did not go over approximately 8. The protein concentration was measured with Qubit.

2.2.5 SDS-PAGE

To analyze the purity of the protein samples, Sodium Dodecyl Sulphate Polyacrylamide Gel Electrophoresis (SDS-Page) was performed, comparing the cell lysates from 2.2.1 Protein Production to the final product from 2.2.2 Protein purification. For the lysate 5 µl of sample was used, and for the purified protein a volume corresponding to 2 µg of protein. 3xRED (15 mM TCEP, 93.75 mM Tris-HCl, 0.03% Bromophenol blue and 3% SDS, 37.5% glycerol) were added to a final concentration of 1xRED, to the samples. The samples were boiled at 95℃ for 5 minutes. The gel used was mini-protean TGX Stain-Free (Bio-Rad), wherein the samples were loaded together with a low molecular weight ladder (Cytiva, 17044601). The running gel was 1xTris/Glycine/SDS buffer (Bio-Rad), within which the gel was run for 20 minutes at 200V. The gel was washed for 3x 5 minutes in deionized water (on a plate shaker), whereafter it was stained for 1 hour using GelCode Blue Safe Protein Stain (Thermo Scientific) (on a plate shaker). The gel was then destained O/N in deionized water (on a plate shaker).

2.2.6 Mass Spectrometry

With the objective of measuring the molecular mass of the proteins, a mass spectrometry (MS) was made using the matrix-assisted laser desorption/ionization (MALDI) technique. For this a 4800 MALDI-TOF/TOF MS (Applied Biosystems) was used. The samples were diluted between 1:3 and 1:5 in deionized water. The diluted sample was mixed 1:2 with CHCA matrix (5 mg/ml of α-Cyano-4- hydroxy-cinnamic acid) and added to the MALDI plate whereafter the software 4000 Series Explorer was used to analyze it.

2.2.7 Surface Plasmon Resonance

To measure the affinity between the proteins and CD22 and HSA respectively, surface plasmon resonance (SPR) was performed on a Biacore T200 (Cytiva). HSA and CD22 were immobilized on a Series S Sensor chip CM5 (Cytiva), using amine coupling chemistry. HSA was diluted with sodium acetate (10 mM, pH 4) to a concentration of 5 µg/ml and reached an immobilization level of 951.1 RU. CD22 was diluted with sodium acetate (10 mM, pH 5) to a concentration of 5 µg/ml with a final immobilization level of 1221.2 RU, with PBST as running buffer. The ADAPTs to be analyzed were serially diluted 1:1 in PBST, from 250 nM to 15.6nM. Each concentration of all the ADAPTs were then flowed over the chip in a multi-cycle kinetics setup at 30 µl/min with 180 s association and 300 s dissociation, using PBST as the running buffer, followed by regeneration with 10 mM HCl for 30 s. The experiment was run at 25°C. For analysis the software Biacore T200 Control software was used and for evaluation Biacore T200 Evaluation Software 3.2.1.

A dual injection was made, where the ability to bind HSA and CD22 simultaneously for ADAPT(ABD035)_CD22_10 and ADAPT(ABDstab)_CD22_10 could be studied. At a flowrate of 30 µl/min with PBST as running buffer, ADAPT (250 nM) was injected over the chip for 180 s, followed by an injection of a mixture of CD22 (250 nM) and ADAPT (250 nM) for 120 s. This was followed by a dissociation time with PBST for 300 s, and regeneration using 10 mM HCl for 30 s.

Using the SPR, the off rate (k_d) and on rate (k_a) were measured and used to derive the equilibrium dissociation constant K_D. See equation 1.

$$K_D = \frac{k_d}{k_a} \qquad \text{(Equation 1)}$$

Thereafter Gibbs free energy (ΔG) could be calculated, see equation 2, with R being the gas constant (1.987 cal/Kmol), T being the temperature (298.15K), and K_D the obtained value from the SPR.

$$\Delta G = RT * \ln\left(\frac{1}{K_D}\right) \qquad \text{(Equation 2)}$$

2.2.8 Circular Dichroism Spectroscopy

To obtain information on the melting point of the proteins and to analyze the secondary structure and refolding capability, Circular Dichroism Spectroscopy (CD) was used. The software used for analysis and evaluation of data was Chirascan software. This was done with the Chirascan CD spectrometer (Applied Photophysics). The proteins were diluted to a concentration of 0.2 mg/ml in PBS. For the analysis a 1 mm cuvette was used. Information of the secondary structure was analyzed using wavelengths between 195 and 260 nm at 20°C. To

analyze the melting temperature a variable temperature measurement (VTM) was made, at 221 nm with temperatures ranging between 4 and 100℃. After this the temperature was lowered back to 20℃, whereafter the secondary structure was once again measured, same as before, to determine if the protein had refolded.

To be able to easily compare the VTM data collected for the different variants, the data was adjusted to start at a y-value of zero. This was done individually for each variant, through subtracting the value (mdeg) of the first measurement from all subsequent measurements. Thereafter the data was normalized individually between 0 and 1, with a value of 0 being protein with an ordered secondary structure and 1 being completely unstructured.

2.2.9 Size Exclusion Chromatography

To evaluate if the proteins are monomers, aggregation prone or have been degraded, a size exclusion chromatography (SEC) was performed. For the analysis NGC™ Chromatography System (BioRad) was used Software ChromLab was used for the program and analysis of the results. The samples were diluted to 0.4 mg/ml or 0.2 mg/ml in PBS, depending on the amount of protein obtained. The injection loop required 25 µl of each sample, which was injected onto a Superdex 75 Increase 5/150 GL (Cytiva). PBS was used as a running buffer, and a flowrate of 0.15 ml/min was used. As a calibrant five proteins of known molecular weight were used (Conalbumin, Ovalbumin, Carbonic anhydrase, Ribonuclease A and Aprotinin).

2.3 Library Exploration

Two positions on helix 1 were chosen to be further evaluated, to explore how the library could be varied in the future. The positions chosen were N7 and T10. N7 has not been varied before, thus asparagine (N) was exchanged to 16 different amino acids, excluding cysteine, glycine, and proline. T10 was a library position that had been kept constant during the maturation library formation, for which one amino acid from each group was tested in this study.

2.3.1 Creation and Production of Proteins

To exchange the desired amino acids towards another, with the aim to obtain the new variants, QuickChage mutagenesis was made on ADAPT(ABD035)_CD22_10, to create a total of 21 different variants. This was executed as described in 2.2.1 QuickChange Mutagenesis. However, it was done three times, using 64℃, 67℃, and 70℃, for annealing temperature, to successfully create as many of the 21 variants as possible. To see if the correct sequences had been created, a PCR screen was made, as described in 2.1.1.9 Ligation of cleaved fragments into cleaved HisDummy 4.0. However, this time, up to 6 sequences per variant were sent for screening. The colonies with the correct sequences were inoculated in TSB with 100 µg/ml carbenicillin and grown O/N at 37 ºC and 150 rpm. The following day, plasmid preparation was made on the cultures, following which they were transformed into BL21(DE3) *E. coli*, as describes in *2*.1.2 Protein Production in BL21(DE3) E. coli. The day after a single BL21 colony from each of the variants was inoculated with TSB and 100 µg/ml carbenicillin, O/N at 37 ºC and 150rpm. Thereafter the protein was produced in accordance with 2.2.3 Protein Production. The produced protein was then purified as described in 2.2.4 Protein Purification, however this time, elution fractions three to six were saved. The fractions were measured using the spectrophotometer (280 nm), after which they were freeze-dried O/N. The following day they were resuspended in PBS, as described before.

2.3.2. Characterization

To examine the purity of the protein, an SDS-PAGE was made, as described in *2.2.6 SDS-PAGE*. The molecular weight of the proteins was measured using MALDI MS, as describes in 2.2.6 Mass Spectrometry, diluting the samples 1:5 in deionized water. The CD was used to obtain information about the proteins structure, melting temperature and ability to refold after denaturation, as described in 2.2.8 Circular Dichroism Spectroscopy. This was only done on the proteins which had been changed in the N7 position.

For examining the affinity towards CD22, BLI was employed using an Octet RED96 instrument (Sartorius). The Octet was run by capturing the purified ADAPT (20 µg/ml) on Anti-Penta-HIS (His1K) Biosensors (Satorius). Association to CD22 (500 nM) was made for 180s, and disassociation was made during 300 s using PBST. Between the cycles the sensors were regenerated in 10 mM glycine, pH 1.5 for 20 s. The shake speed used was 1000 rpm. The software used for analysis was Octet Data Acquisition and for evaluation ForteBio Data Analysis.

3. Results

3.1 Variants from the Maturation Selection

A selection of 20 ADAPT variants from previously performed affinity maturation selections against CD22 were cloned and produced for evaluation. The affinity maturation library was based on the original low-affinity binder ADAPT(ABD035)_CD22_10, but with an exchange in scaffold from ABD035 to ABDstab, hopefully making the library variants more stable and thus more accepting of variations in the library. In the creation of the maturation library, seven of the original library positions were opened to variation, and four positions were locked based on their importance for CD22 recognition as suggested by earlier explorations. The variable positions can be seen in Figure 3. The sequences of the 20 variants from the maturation selection can be seen in Table 1, together with the amino acids that vary between the original ADAPT(ABD035)_CD22_10 and the affinity maturation scaffold ADAPT(ABDstab)_CD22_10.

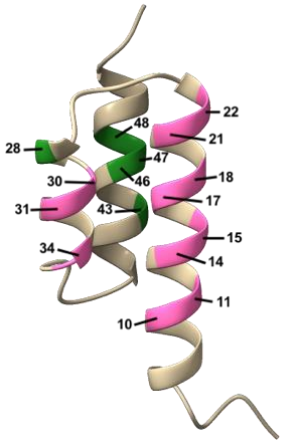

Figure 3. ADAPT structure obtained by homology modeling (to the wild-type albumin binding domain, PDB 1gjt) using SWISS-MODEL (23). The positions marked in green are the ones which differ between the scaffolds ABD035 and ABDstab. The pink positions are the amino acids that can be altered to affect the affinity towards CD22, however positions 10, 11, 14 and 17 has been kept constant in the creation of the maturation library.

Table 1. Table highlighting the differences between the original binder, ADAPT(ABD035)_CD22_10 (in the table called Original), the ADAPT where only the scaffold has been changed, ADAPT(ABDstab)_CD22_10 (in the table called ABDstab) and the 20 variants from the maturation selection, which all have the ABDstab scaffold. The pink color on the original binder marks the library positions which can be varied to alter the affinity towards CD22. The positions among the maturation variants which are identical to the original binder have pink letters. The green marks the scaffold positions that vary between ABD035 and ABDstab.

	Helix 1																							Helix 2											Helix 3														
	1	2	3	4	5	6	7	8	9	10	11	12	13	14	15	16	17	18	19	20	21	22	23	24	25	26	27	28	29	30	31	32	33	34	35	36	37	38	39	40	41	42	43	44	45	46	47	48	49	50	51	52	53	54
Original	D	E	A	V	D	A	N	S	L	T	W	A	K	L	I	A	Q	W	E	L	Q	E	Y	G	V	S	D	F	Y	Q	D	L	I	V	K	A	K	T	V	E	G	V	E	A	L	K	L	H	I	L	A	A	L	P
ABDstab										T	W			L	I		Q	W			Q	E						Y		Q	D			V								K			I	D	E						
mat1										T	W			L	L		Q	D			S	H						Y		F	D			A								K			I	D	E						
mat2										T	W			L	V		Q	A			Q	S						Y		L	D			A								K			I	D	E						
mat3										T	W			L	Q		Q	Y			R	D						Y		L	D			A								K			I	D	E						
mat4										T	W			L	T		Q	S			W	D						Y		H	A			A								K			I	D	E						
mat5										T	W			L	H		Q	S			W	D						Y		I	Y			A								K			I	D	E						
mat6										T	W			L	E		Q	S			W	N						Y		M	N			A								K			I	D	E						
mat7										T	W			L	E		Q	S			W	D						Y		L	D			E								K			I	D	E						
mat8										T	W			L	Q		Q	S			W	D						Y		M	D			A								K			I	D	E						
mat9										T	W			L	L		Q	D			M	N						Y		L	D			A								K			I	D	E						
mat10										T	W			L	T		Q	A			W	D						Y		M	D			A								K			I	D	E						
mat11										T	W			L	Q		Q	S			W	K						Y		L	V			A								K			I	D	E						
mat12										T	W			L	T		Q	A			W	D						Y		F	D			A								K			I	D	E						
mat13										T	W			L	A		Q	S			W	H						Y		I	D			A								K			I	D	E						
mat14										T	W			L	V		Q	D			S	H						Y		M	D			A								K			I	D	E						
mat15										T	W			L	Q		Q	S			R	E						Y		L	Y			A								K			I	D	E						
mat16										T	W			L	V		Q	S			M	D						Y		L	D			A								K			I	D	E						
mat17										T	W			L	Q		Q	S			W	D						Y		M	D			T								K			I	D	E						
mat18										T	W			L	Q		Q	S			W	A						Y		M	D			E								K			I	D	E						
mat19										T	W			L	N		Q	S			W	E						Y		L	D			A								K			I	D	E						
mat20										T	W			L	V		Q	N			W	D						Y		M	D			A								K			I	D	E						

3.1.1 Binding Affinity of Variants from the Maturation Selection

To measure the affinity of the variants from the maturation selections towards CD22, biolayer interferometry (BLI) was employed. Some variants showed affinity towards CD22, namely mat1, mat2, mat6, mat8, mat9, mat10, mat12, mat14, mat16, mat17, mat19 and mat20, and some showed none, namely mat3, mat4, mat5, mat7, mat11, mat13, mat15 and mat18. The results of ADAPT(ABD035)_CD22_10, mat8, mat11 and mat17 can be seen in Figure 4 and have been chosen as representative results. The results for the remaining variants can be found in Appendix, Figure A1. However, even though mat8 and mat17 both show affinity towards CD22, the off rate curve is a bit steeper than that of ADAPT(ABD035)_CD22_10. For mat11 no affinity can be seen. Unfortunately, none of the variants displayed an improvement in affinity compared to the original binder.

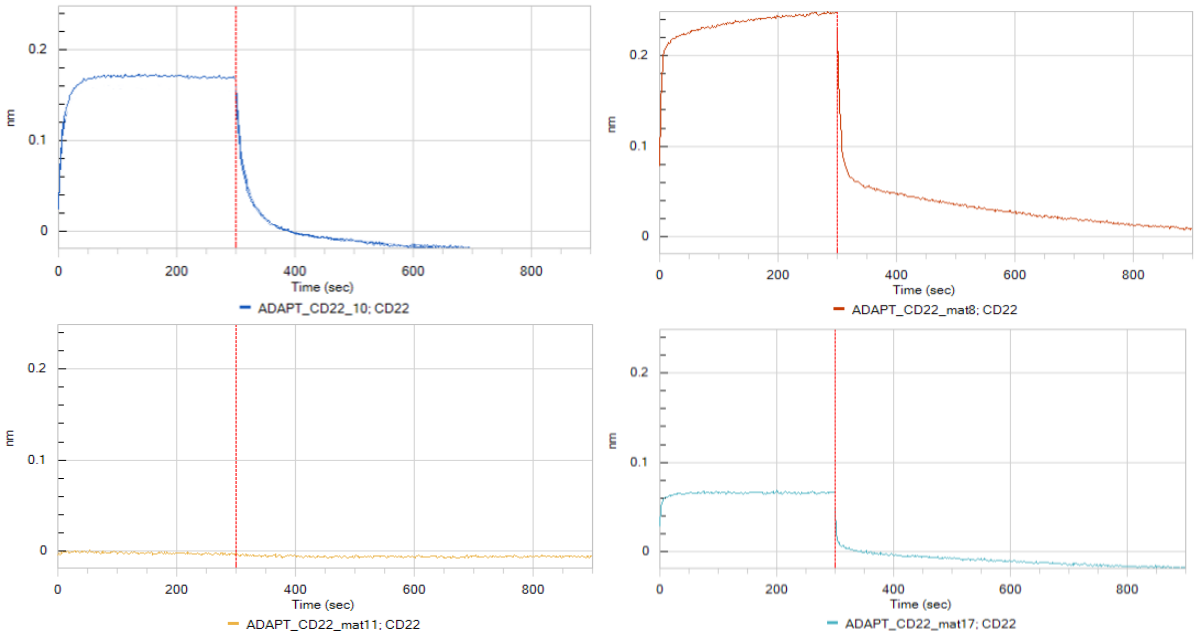

Figure 4. The binding profile of four variants, ADAPT(ABD035)_CD22_10 (in the figure called ADAPT_CD22_10), mat8, mat11 and mat17, towards CD22 using BLI. The sensograms show the binding of captured ADAPT (on anti-His biosenors) to CD22 (1 μM) in solution. At the red, dotted line, after 300s, the sensors are dipped into buffer (PBST) to measure how fast CD22 releases from the ADAPT.

3.1.2 Comparison of ABD035 and ABDstab Scaffolds

A series of experiments were executed to investigate the impact of using ABDstab as the scaffold instead of ABD035. Circular Dichroism (CD) Spectroscopy was used to investigate the thermal stability, the melting point of the proteins, and investigate the secondary structure of the protein. The secondary structure was analyzed both before and after heat denaturation, thus investigating its ability to refold. It could be seen that ADAPT(ABDstab)_CD22_10 had the expected α-helical structure, and the ability to refold after heat denaturation (Figure 5), just as ADAPT(ABD035)_CD22_10 does. An increase in thermostability for ADAPT(ABDstab)_CD22_10 can be seen when looking at the melting temperature which lies about 13ºC above that of ADAPT(ABD035)_CD22_10 (Figure 6 and Table 2). A summarization of the results from the CD spectroscopy can be seen in Table 2. Using size exclusion chromatography (SEC), both variants could be seen to have the expected monomeric form (Table 2 and Appendix Figure A2). Moreover the table contains information about the amount of protein which could be obtained from production of the two variants, which can be seen to be approximately the same. The molecular mass of the proteins was measured using mass spectrometry (MS) with a matrix-assisted laser desorption/ionization (MALDI) technique (Table 2 and Appendix Figure A3).

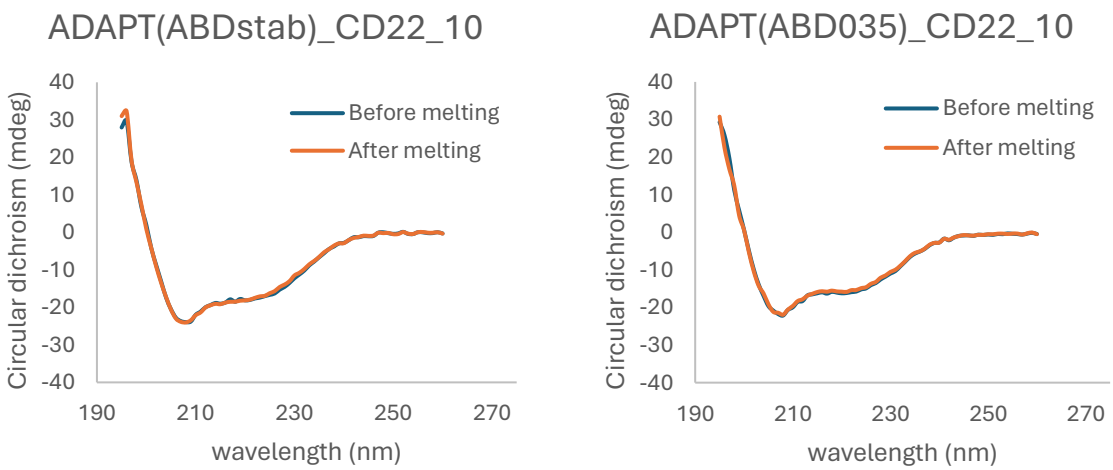

Figure 5. CD spectroscopy of ADAPT(ABDstab)_CD22_10 to the left, and ADAPT(ABD035)_CD22_10 to the right. The experiment was conducted twice, at room temperature, once before heat denaturation of the protein (in blue) and once after (in orange), to study the secondary structure. The α-helical structure can be seen due to the typical dips at 208 and 222 nm. Both variants can be seen to refold completely.

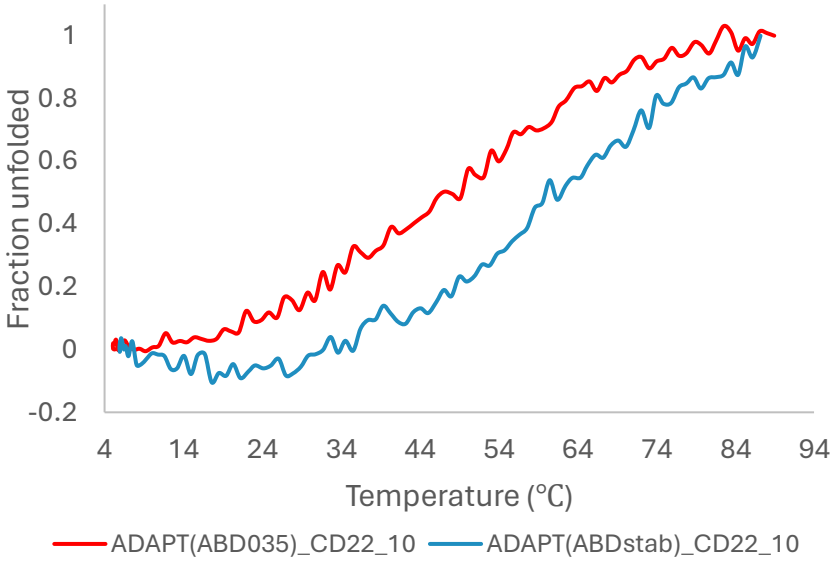

Figure 6. Variable temperature measurement (VTM), showing the melting curve of the proteins, where the difference between ADAPT(ABD035)_CD22_10 and ADAPT(ABDstab)_CD22_10 can be seen. The temperature ranges from 4°C to 100°C.

Table 2. A summary of the biophysical characetrization of the two different scaffolds, comparing the original ADAPT(ABD035)_CD22_10 to the basis of the affinity maturation library, ADAPT(ABDstab)_CD22_10. Showing the amount of obtained protein, the measured molecular weight, the theoretical molecular weight (MW) of the protein, if the protein had an α-helical stucture at 20°C, the ability to refold after heat denaturation, melting temperature and the result of SEC for ADAPT(ABD035)_CD22_10 and ADAPT(ABDstab)_CD22_10.

Variant	Amount of obtained protein (mg protein / 100 ml culture)	MALDI MS (Da)	Theoretical MW (Da)	α-helical structure at 20°C (in CD)	Ability to refold after heat denaturation	Melting temp. (°C)	SEC
ADAPT(ABD035)_CD22_10	0.68	7069	7063	Yes	Yes	48	Monomer
ADAPT(ABDstab)_CD22_10	0.52	7063	7063	Yes	Yes	61	Monomer

To analyze the simultaneous bispecificity of ADAPT to both target proteins, surface plasmon resonance (SPR) was used. ADAPT was injected over immobilized HSA followed by a second injection of CD22. This is to see if both variants can bind HSA and CD22 simultaneously. Expected is that ADAPT(ABDstab)_CD22_10 will bind HSA with a lower affinity, since its affinity towards HSA has been somewhat compromised to increase the stability. In Figure 7, a decrease in the ability to bind HSA can indeed be seen for ADAPT(ABDstab)_CD22_10, which affects how much CD22 can bind in since the amount of captured ADAPT will decrease. Nonetheless, both scaffolds clearly demonstrate an ability to simultaneous interact with HSA and CD22.

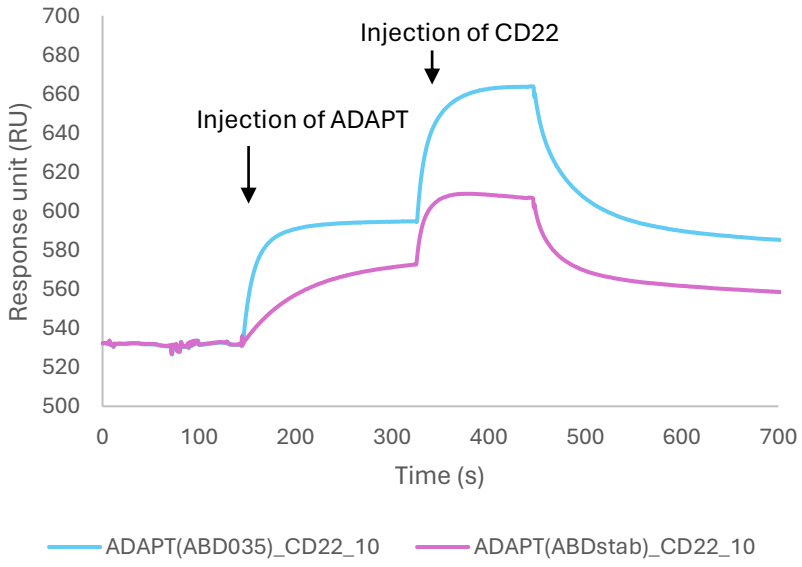

Figure 7. Showing the simultaneous bispecific binding for ADAPT(ABD035)_CD22_10 and ADAPT(ABDstab)_CD22_10, during dual injection, with the first step flushing over ADAPT which binds into the HSA surface, and the second step flushing CD22 over the HAS-captured ADAPT.

Using SPR, affinity measurements were also made for ADAPT(ABDstab)_CD22_10 and ADAPT(ABD035)_CD22_10 towards CD22 and HSA separately. These results, showing the affinity (K_D) for ADAPT(ABDstab)_CD22_10 and ADAPT(ABD035)_CD22_10 for CD22 and HSA, can be seen in Table 3. ADAPT(ABDstab)_CD22_10 shows a slightly lower affinity towards CD22 compared to ADAPT(ABD035)_CD22_10. This difference can be further examined by comparing the binding signal for the two proteins to CD22 in Appendix A, Figure A4, where the signal for ADAPT(ABDstab)_CD22_10 is lower.

Table 3. The affinity measured for ADAPT(ABDstab)_CD22_10 and ADAPT(ABD035)_CD22_10, towards CD22 and HSA using Biacore T200.

Variant	Affinity for CD22, K_D (M)	Affinity for HSA, K_D (M)
ADAPT(ABD035)_CD22_10	1.0E-07	7.2E-10
ADAPT(ABDstab)_CD22_10	5.7E-07	2.1E-08

3.2 Alanine Scan Results

In order to gain more insight into the paratope, an alanine scan was performed on the 11 ADAPT library positions, to analyze how they impact the affinity towards CD22. This was made by changing each of the 11 amino acids one by one to alanine, and then performing experiments on them to see how it affected the properties of the ADAPT. The alanine scan was done on the original binder ADAPT(ABD035)_CD22_10. Amino acid number 10, which was a threonine (T), was changed to alanine (A), thus rendering the name T10A. The tryptophan (W) to alanine at position 11 was named W11A, and so forth. The remaining positions exchanged was L14A, Q17A, W18A, Q21A, E22A, Q30A, D31A and V34A.

The purity of the produced and purified alanine scan mutants was examined using SDS-PAGE, comparing the cell lysates with the purified samples (Figure 8). Only one protein band, of a size smaller than 14.4 kDa, as expected for the ADAPT, can be seen in the purified samples, indicating a high purity of the sample. Some results can be seen two times, since they were produced twice to obtain a large enough amount of protein to perform all desired experiments. The total amount of protein obtained lies between 0.23 and 1.52 mg protein per 100 ml of culture, which can be compared to 0.68 mg per 100 ml for the original binder. The specific amounts for each variant can be seen in Table 4.

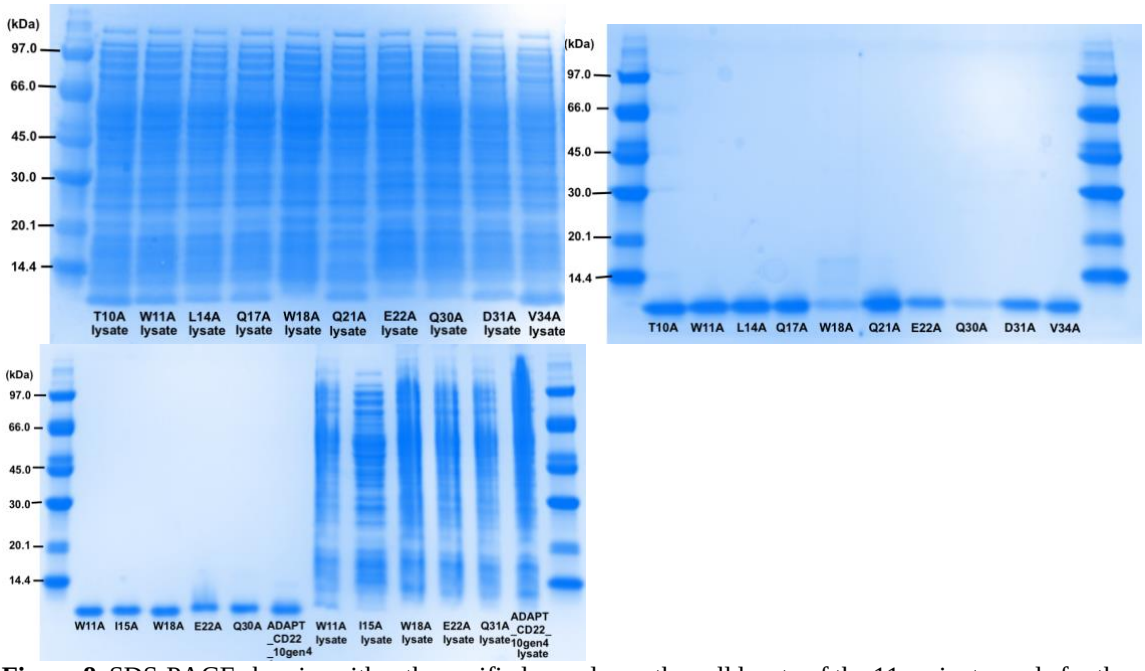

Figure 8. SDS-PAGE showing either the purified samples or the cell lysate of the 11 variants made for the alanine scan, as well as for ADAPT(ABDstab)_CD22_10. W11A, W18A, E22A and Q30A were produced twice since they did not produce enough protein for the desired experiments the first time. All results from the purification can be seen to have one clear band, which lies well below 14.4 kDa (ADAPT with His-tag is 7 kDa), even though some lysates show very faint bands at this size.

3.2.1 Structure and Thermal Stability

To investigate if the proteins had the expected α-helical structure, CD spectroscopy was performed. In Figure 9, variant T10A can be seen. Since all 11 mutants derived for the alanine scan showed the same α-helical structure, T10A has been chosen as a representation for them all, however, the rest can be found in Appendix, Figure B1. All are capable of refolding after being thermally denatured, regaining the same structure as before, just as the original binder (Figure 5).

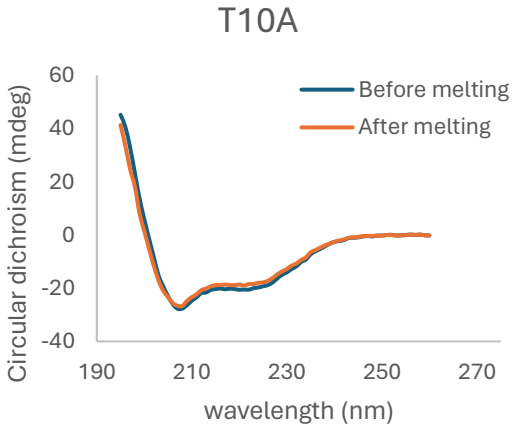

Figure 9. CD spectroscopy of alanine scan mutant T10A. The experiment was conducted twice, at room temperature, once before heat denaturation of the protein (in blue) and once after (in orange), to analyze the secondary structure of the protein. The α-helical structure can be seen due to dips at 208 and 222 nm. Complete refolding can be seen.

When studying the melting curve, the proteins were heated from 4ºC to 100°C. The results can be seen in Figure 10, comparing the results with the original binder, ADAPT(ABD035)_CD22_10. All alanine scan mutants display an S-curve, with D31A having quite a shallow one. The precise melting temperature of the proteins can be found in Table 4. For W11A, L14A, I15A, and D31A, the metling temperature has decreased to temperatures closer to, or even under, body temperature. W18A had a melting temperature of 44°V and Q21A one of 47°C. Except for these two plus the four prementioned, all others had the same temperature as the original binder, at 48ºC or above.

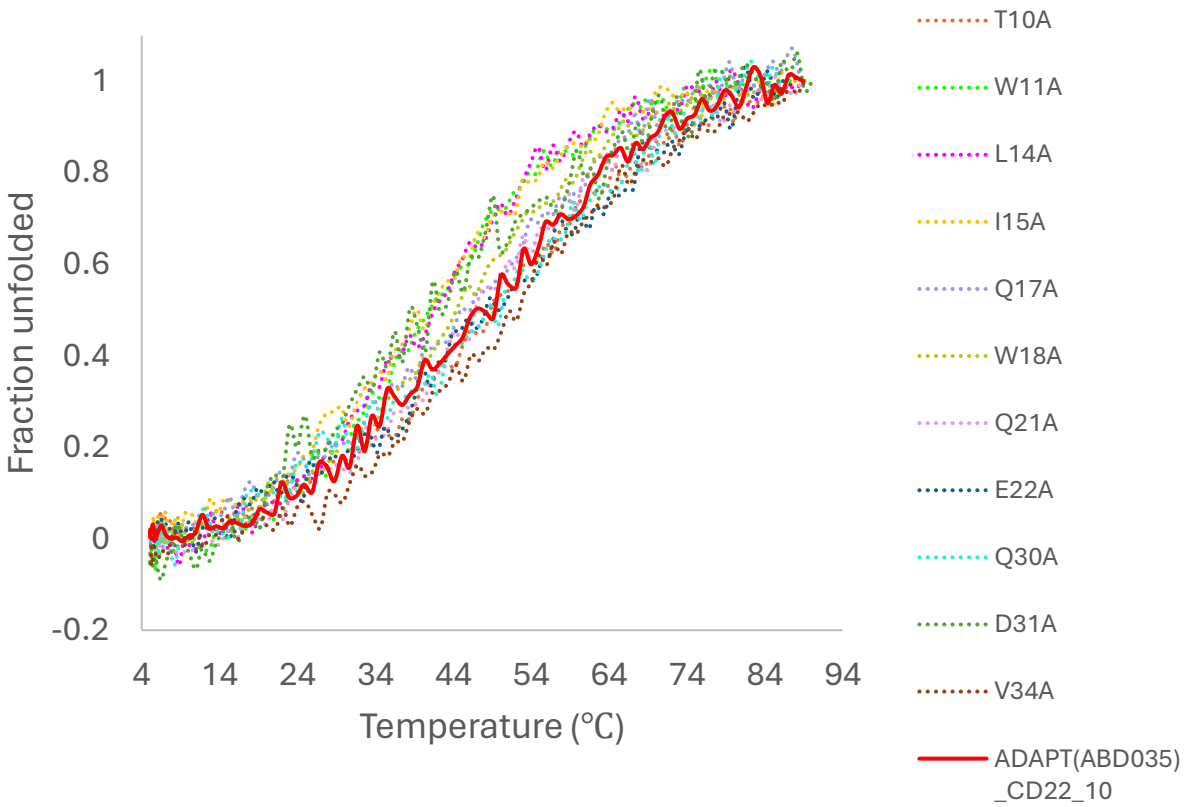

Figure 10. Variable temperature measurement (VTM), alanine scan's melting curve for mutants compared to ADAPT(ABD035)_CD22_10. The latter is marked in a solid line whilst the alanine scans are dotted lines, to make it easier to compare with the original binder.

In Table 4, a summary of the results can be found, including the amount of obtained protein measured by Qubit, and the molecular weight measured using MALDI MS. The results correspond to the theoretical weight for all but W11A, which lies about 70 Da above the expected. In Appendix, Figure B2, the spectra from the MALDI can be seen, for all but E22A, where the raw data of the result has been lost, thus marked as not detected (N/D) in Table 4. Moreover, a summary of the results from the SEC can be seen in Table 4. Some representative results from SEC can also be seen in Figure 11, where ADAPT(ABD035)_CD22_10 can be compared to T10A, which has been chosen as a representative chromatogram for all variants (all chromatograms can be found in Appendix, Figure B3). They all elute as monomers at the expected size just as the original binder, exception for E22A, which seems to have been degraded.

Table 4. Showing the amount of obtained protein, the measured molecular weight, the theoretical molecular weight (MW) of the protein, if the protein had an α-helical stucture at 20°C, if it had the ability to refold after heat denaturation, melting temperature and the result of SEC of the 11 alanine scan mutants as well as ADAPT(ABD035)_CD22_10. N/D – not detected.

Variant	Amount of obtained protein (mg protein / 100 ml culture)	MALDI MS (Da)	Theoretical MW (Da)	α-helical structure at 20°C (in CD)	Ability to refold after heat denaturation	Melting temp. (°C)	SEC
ADAPT(ABD035)_CD22_10_T10A	1.42	7033	7039	Yes	Yes	48	Monomer
ADAPT(ABD035)_CD22_10_W11A	1.52	7020	6954	Yes	Yes	40	Monomer
ADAPT(ABD035)_CD22_10_L14A	0.72	7020	7027	Yes	Yes	40	Monomer
ADAPT(ABD035)_CD22_10_I15A	0.31	7023	7027	Yes	Yes	40	Monomer
ADAPT(ABD035)_CD22_10_Q17A	0.75	7003	7012	Yes	Yes	48	Monomer
ADAPT(ABD035)_CD22_10_W18A	0.28	6954	6954	Yes	Yes	44	Monomer
ADAPT(ABD035)_CD22_10_Q21A	1.10	7000	7012	Yes	Yes	47	Monomer
ADAPT(ABD035)_CD22_10_E22A	0.23	N/D	7011	Yes	Yes	51	Degraded
ADAPT(ABD035)_CD22_10_Q30A	0.24	7000	7012	Yes	Yes	51	Monomer
ADAPT(ABD035)_CD22_10_D31A	0.46	7017	7025	Yes	Yes	36	Monomer
ADAPT(ABD035)_CD22_10_V34A	1.36	7031	7041	Yes	Yes	50	Monomer
ADAPT(ABD035)_CD22_10	0.68	7063	7069	Yes	Yes	48	Monomer

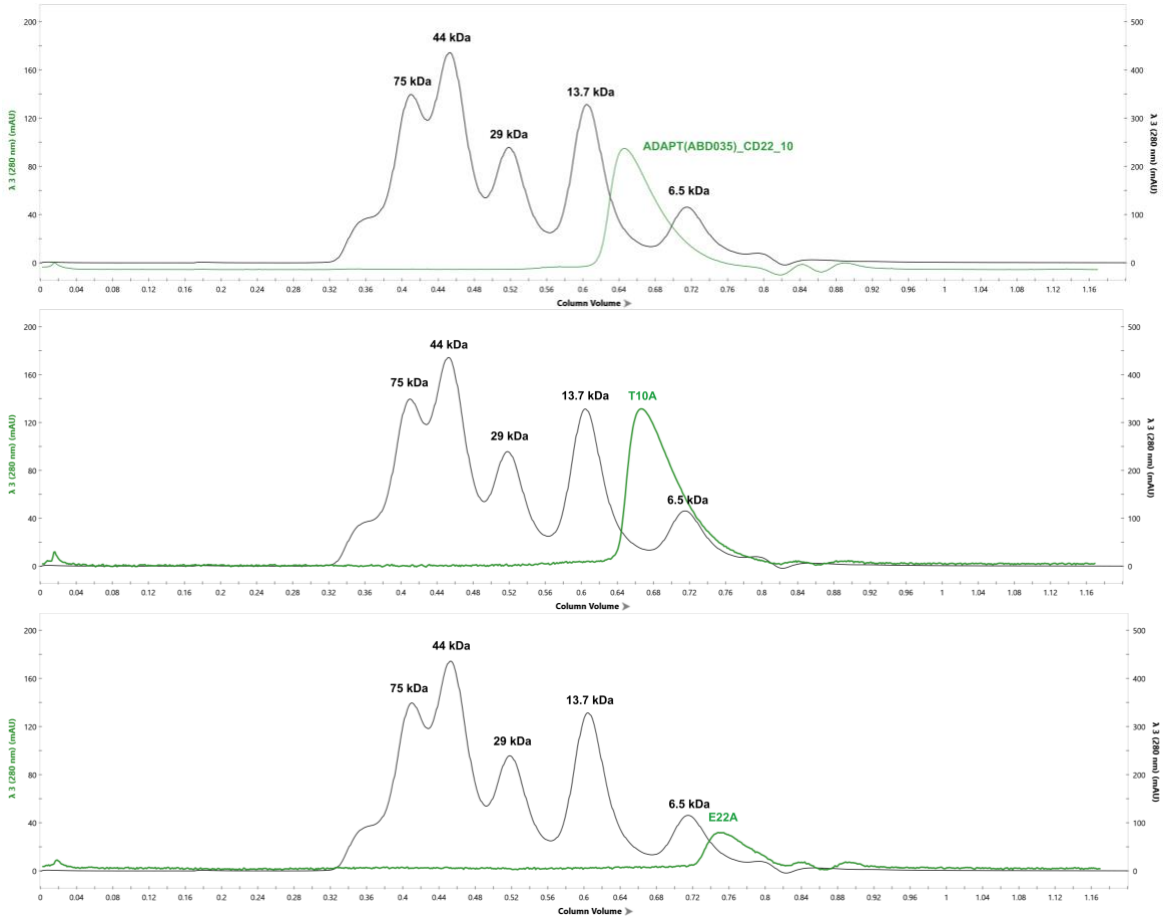

Figure 11. SEC of ADAPT(ABD035)_CD22_10, T10A and E22A, showing the column volume at which the protein is eluted. The calibrant curve can be seen in black, and includes Conalbumin (75 kDa), Ovalbumin (44 kDa), Carbonic anhydrase (29 kDa), Ribonuclease A (13.7 kDa) and Aprotinin (6.5 kDa), with the largest protein eluting first. For ADAPT(ABS035)_CD22_10 and T10A the peak can be seen between 6.5 and 13.7 kDa which is expected of a monomeric ADAPT of a size of approximately 7 kDa.

3.2.2 Affinity Towards HSA and CD22

Using SPR, the affinity (K_D) of the alanine scan mutants towards both CD22 and HSA could be measured, and the exact numbers for these can be found in the Appendix, Table B1. Gibbs free energy (ΔG) could be derived for each variant, which was then normalized against ΔG for ADAPT(ABD035)_CD22_10. These values can be seen in Figure 12. For W11A, L14A, I15A and Q17A, no binding to CD22 could be detected, whilst the rest have approximately the same, or a lower ΔG than the original binder. As expected, all variants showed affinity towards HSA, and a figure over ΔG for HSA can be found in the Appendix, Figure B4. However, these results does not consider how much CD22 that binds in or releases, only at which rate it happens. To take this into consideration, the binding signals for CD22 are visualized in Figure 13. Here a picture of the ADAPT is displayed, where the 11 positions that were changed to alanine during the alanine scan weremarked with different colors. The coloring depends on the binding signal measured between each alanine scan mutant and CD22, compared to the original binder. The green variants, Q21A, E22A, D31A and V34A, have quite a high binding signal, of at least 50% of the original binder. The one in yellow, T10A, had a signal of about 30% of the original, with the ones in orange, W18A and Q30A having under 20% of the original signal. No signal could be seen for W11A, L14A, I15A or Q17A, thus being painted in red. A sensogram showing the response units (RU) for all variants at 125 nM can be found in the Appendix, Figure B5.

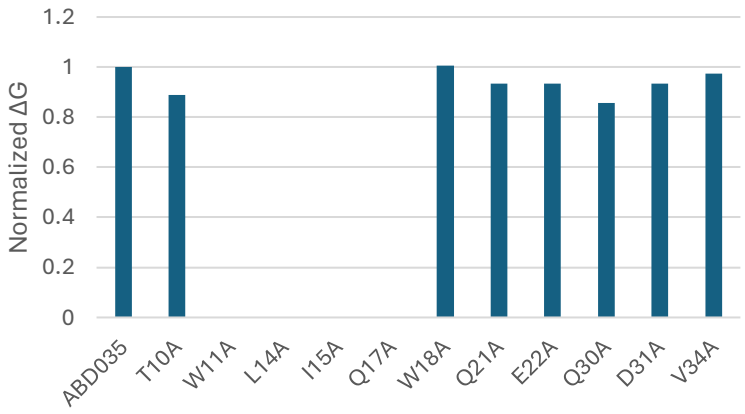

Figure 12. Gibbs free energy (ΔG), showing the binding energy between the ADAPT and CD22, has been normalized towards the ΔG of ADAPT(ABD035)_CD22_10 (in the graph only called ABD035) for all variants. W11A, L14A, I15A and Q17A did not show any binding towards CD22 and thus, no ΔG can be seen.

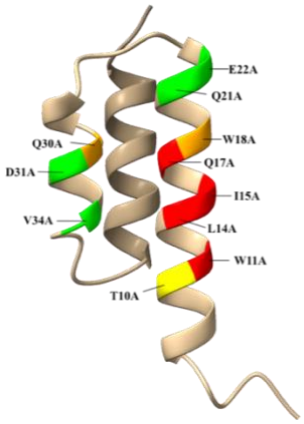

Figure 13. ADAPT structure obtained by homology modeling (to the wild-type albumin binding domain, PDB 1gjt) using SWISS-MODEL (23). The 11 positions varied during the alanine scan has been coloured based on binding signal to CD22 (in SPR) compared to the original binder, ADAPT(ABD035)_CD22_10. The green color indicates a capacity to bind of at least 50% of the original binder, yellow indicates a capacity to bind of about 30%, orange under 20% and red no capacity to bind at all.

3.3 Library Exploration

To explore how the library might be modified before designing the next maturation library, two positions were chosen to be examined closer. One was position 7, originally an asparagine (N), previously unexplored in library randomization. This position was chosen to see if it was possible to increase the number of variable positions when creating a new library. The position was investigated due to its potentially beneficial effect on CD22 binding due to it pointing outwards and laying close by the paratope, as identified by the alanine scan For this position, 16 different variants were meant to be explored, corresponding to all amino acids except for cysteine due to its ability to form disulfide bonds which can lead to dimerization of the ADAPT, as well as glycine and proline due to their disruption of α-helical structures. The second position to be explored was position 10, with a tyrosine (T), chosen as it had been locked when forming the maturation library. However, during the alanine scan, it seemed to have more flexibility than previously expected. T10 was exchanged to one type of amino acid from each group, namely the negatively charged glutamic acid (E), the positively charged arginine (R), the polar glutamine (Q), and the hydrophobic isoleucine (I) and the larger and aromatic tryptophan (W). This provided the variants T10E, T10I, T10W, T10Q and T10R. The positions of the varied amino acids can be seen in Figure 14.

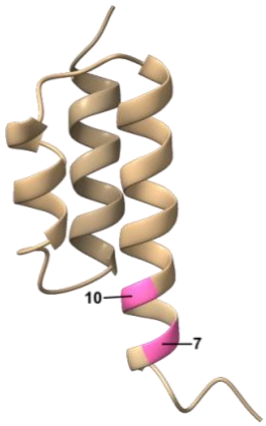

Figure 14. ADAPT structure obtained by homology modeling (to the wild-type albumin binding domain, PDB 1gjt) using SWISS-MODEL (23), with the two positions that are explored for the next maturation library highlighted in pink.

3.3.1 Evaluation of the N7 Variants

For the N7 variants, the introduction of 13 out of the 16 amino acids was successful. Variants N7D, N7H, and N7T were unsuccessfully cloned, and thus no results can be seen for these. Of the 13 created variants, between 0.57 and 1.78 mg of protein per 100 ml of culture could be obtained from each, as shown in Table 5. The purification step can be seen to have worked successfully, (Appendix, Figure C1). All had the expected molecular weight (Table 5 and Appendix, Figure C2), as well as an α-helical structure and the ability to refold after heat denaturation. The α-helical structure could be seen using the CD. In Figure 15, a representative sample has been chosen, N7E. Here it can be seen that the structure is the same both before and after thermal denaturation. The rest of the samples can be seen in Appendix, Figure C3.

Table 5. Showing the amount of obtained protein, the measured molecular weight, the theoretical molecular weight (MW) of the protein, if the protein had an α-helical stucture at 20°C, if it had the ability to refold after denaturation and melting temperature of the 13 N7 variants that were successfully produced.

Variant	Amount of obtained protein (mg protein / 100 ml culture)	MALDI MS (Da)	Theoretical MW (Da)	α-helical structure at 20°C (in CD)	Ability to refold after heat denaturation	Melting temp. (℃)
ADAPT(ABD035)_CD22_10_N7A	0.57	7021	7026	Yes	Yes	45
ADAPT(ABD035)_CD22_10_N7E	0.81	7079	7084	Yes	Yes	48
ADAPT(ABD035)_CD22_10_N7F	0.64	7096	7102	Yes	Yes	48
ADAPT(ABD035)_CD22_10_N7I	0.64	7063	7068	Yes	Yes	48
ADAPT(ABD035)_CD22_10_N7K	0.78	7078	7083	Yes	Yes	48
ADAPT(ABD035)_CD22_10_N7L	0.74	7062	7068	Yes	Yes	51
ADAPT(ABD035)_CD22_10_N7M	0.53	7080	7086	Yes	Yes	48
ADAPT(ABD035)_CD22_10_N7Q	0.86	7078	7083	Yes	Yes	48
ADAPT(ABD035)_CD22_10_N7R	0.73	7107	7111	Yes	Yes	48
ADAPT(ABD035)_CD22_10_N7S	0.53	7038	7042	Yes	Yes	48
ADAPT(ABD035)_CD22_10_N7V	0.81	7049	7054	Yes	Yes	46
ADAPT(ABD035)_CD22_10_N7W	1.78	7137	7141	Yes	Yes	54
ADAPT(ABD035)_CD22_10_N7Y	0.77	7117	7118	Yes	Yes	47

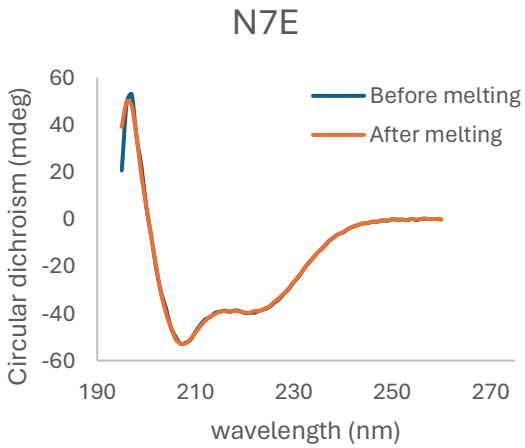

Figure 15. CD spectroscopy of N7E. The experiment was conducted twice at room temperature, once before heat denaturation of the protein (in blue) and once after (in orange), to see the secondary structure of the protein. The α-helical structure can be seen due to dips at 208 and 222 nm. The protein can be seen to have refolded entirely.

Examination of the melting temperature of the proteins resulted in two different types. Most showed the standard S-curve, indicating that the protein is pure and has a distinct denaturation temperature, see Figure 16. However, except for N7A and N7V, all amino acids with a hydrophobic side chain showed very little or no S-curvature, Figure 17. For these, the melting temperatures in Table 5 are not as reliable.

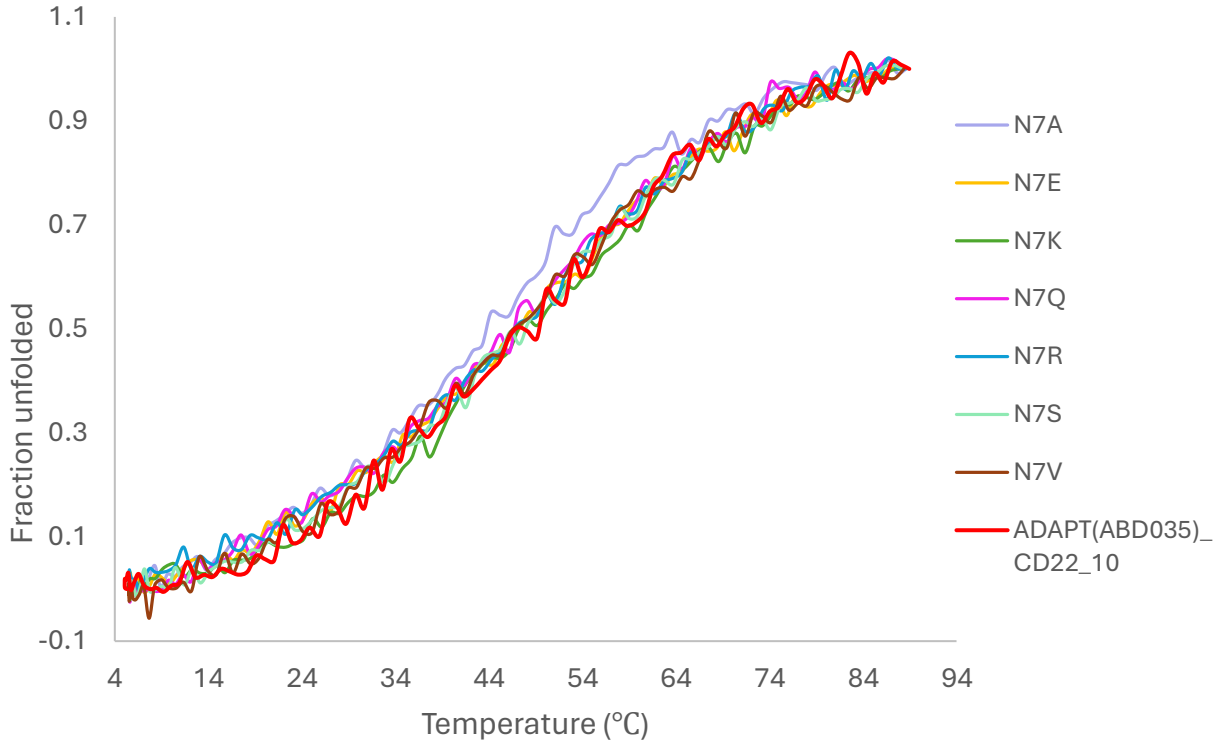

Figure 16. Variable temperature measurement (VTM), showing the melting curves for N7-variants with a clear S-curvature. The results of N7-variants with an S-curvature can be seen and compared to ADAPT(ABD035)_CD22_10.

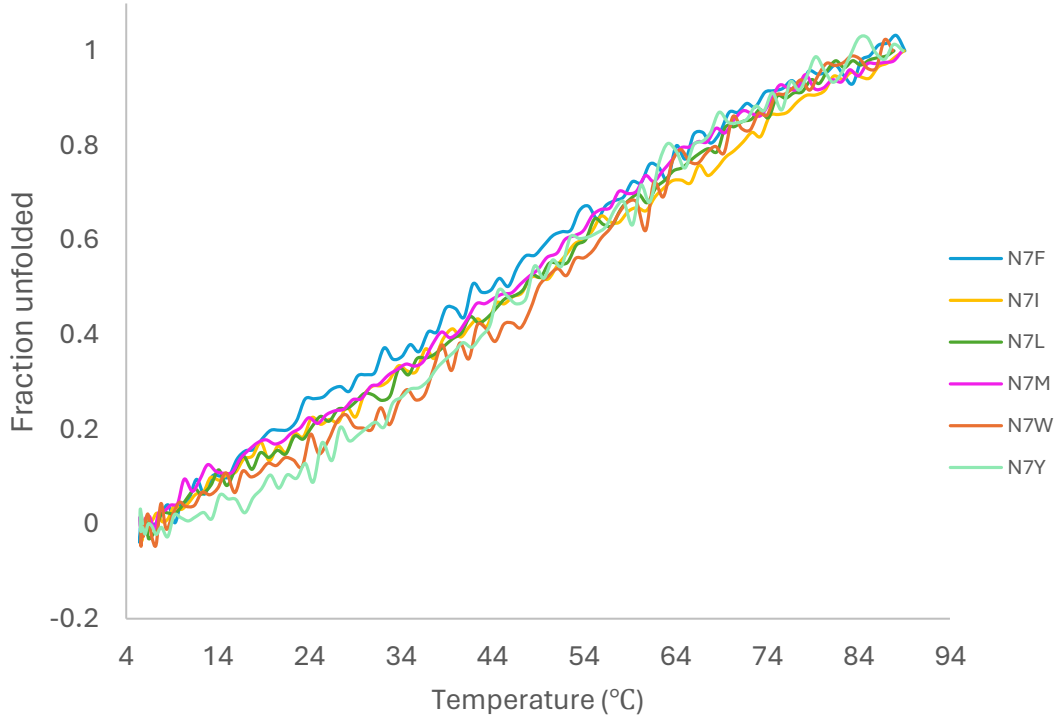

Figure 17. Variable temperature measurement (VTM), showing the melting curves for N7-variants without a clear S-curvature.

Analysis of the binding towards CD22, using BLI, showed that there is no significant difference in affinity when exchanging asparagine (N) towards any of the other amino acids. The results have been divided based on the amino acids' side chains. For the affinity of the amino acids

with charged side chains, see Figure 18. Hydrophobic and polar side chains are shown in Figure 19 and Figure 20 respectively. The capacity of binding CD22 can be seen to vary a bit, with N7F, N7I, N7V and N7W showing lower binding signals than the rest (see Figure 19).

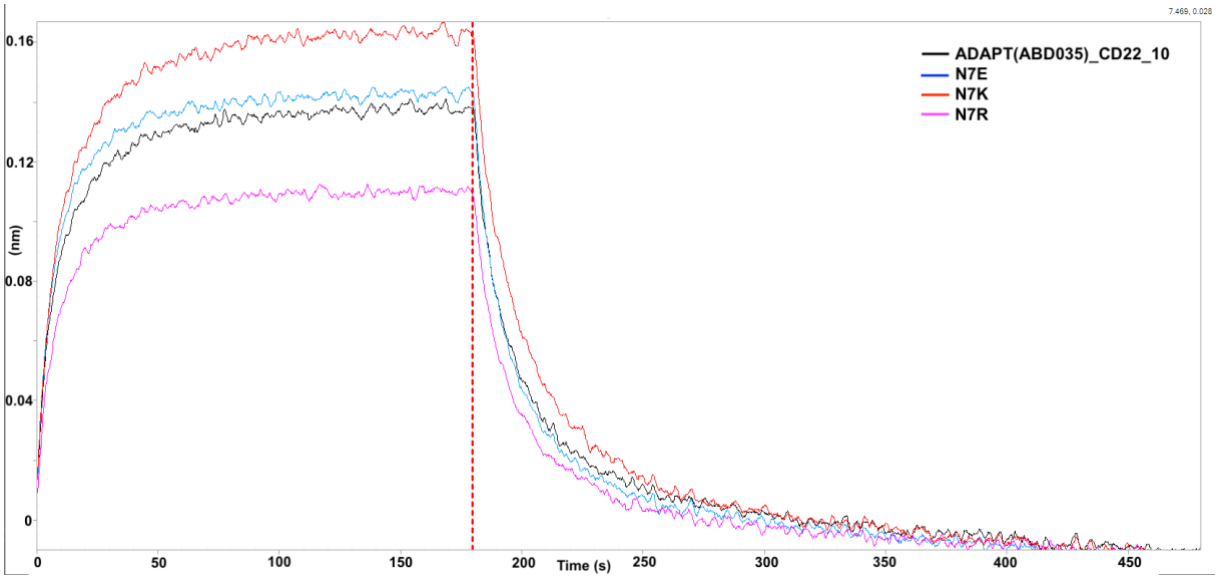

Figure 18. The binding profile of the produced variants with electrically charged side chains, compared to the original binder, towards CD22. The sensograms show the binding of ADAPT (captured on anti-His biosensors) when dipped into CD22 (500 nM). At the red, dotted line, after 300s, the sensors are dipped into buffer to measure how fast CD22 releases from the ADAPT.

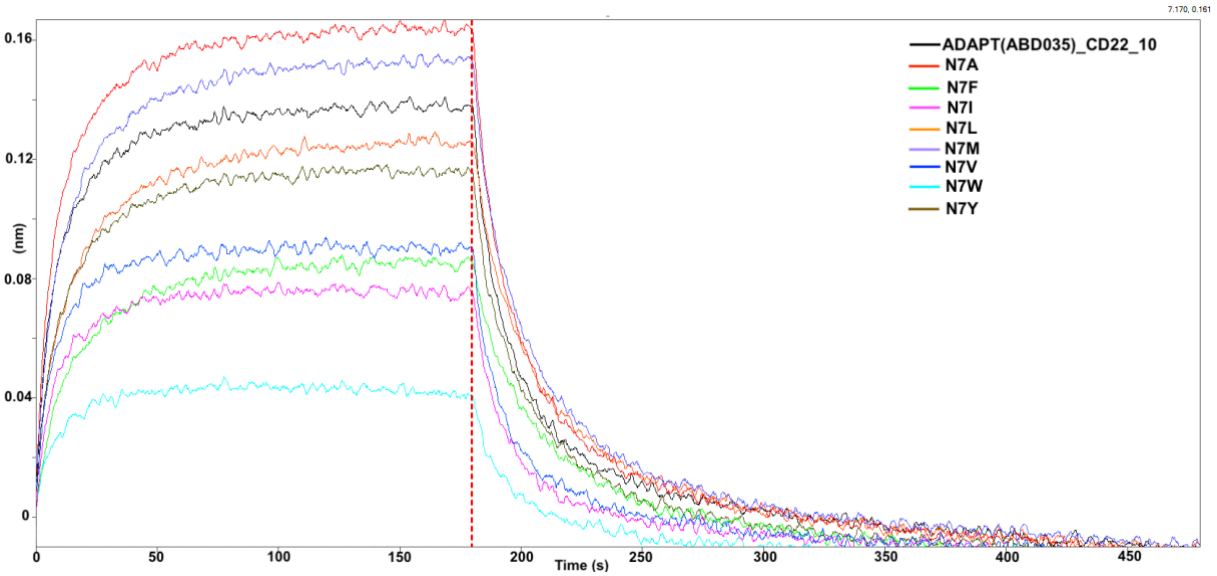

Figure 19. The binding profile of the amino acids with hydrophobic side chains, compared to the original binder, towards CD22. The sensograms show the binding of ADAPT (captured on anti-His biosensors) when dipped into CD22 (500 nM). At the red, dotted line, after 300s, the sensors are dipped into buffer to measure how fast CD22 releases from the ADAPT.

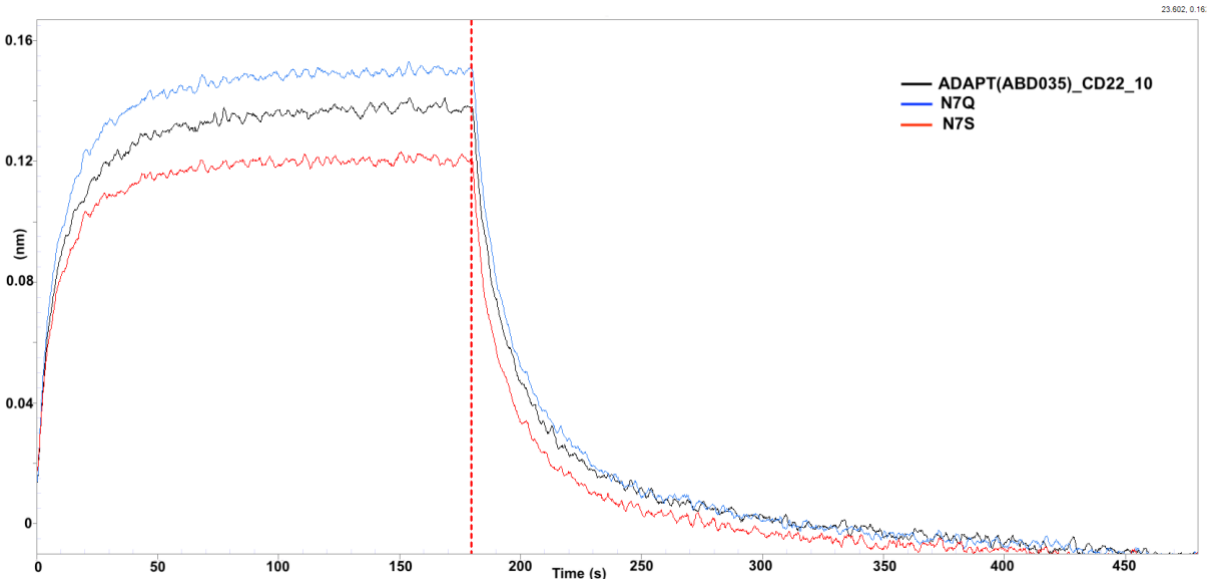

Figure 20. The binding profile of the amino acids with polar uncharged side chains, compared to the original binder, towards CD22. The sensograms show the binding of ADAPT (captured on anti-His biosensors) when dipped into CD22 (500 nM). At the red, dotted line, after 300s, the sensors are dipped into buffer to measure how fast CD22 releases from the ADAPT.

3.3.2 Evaluation of the T10 Variants

For the four T10 variants that were successfully cloned and produced (Appendix, Figure C1) between 0.75 and 1.11 mg of protein per 100 ml culture could be obtained. They also showed the expected molecular weight in MS (Table 6, Appendix, Figure C2). The QuickChange mutagenesis for T10R was unsuccessful; thus, no results can be seen.

Table 6. Showing the amount of obtained protein, their measured molecular weight and the theoretical molecular weight (MW) of the protein, for the ones where T10 was successfully exchanged to another amino acid.

Variant	**Amount of obtained protein (mg protein / 100 ml culture)**	**MALDI MS (Da)**	**Theoretical MW (Da)**
ADAPT(ABD035)_CD22_10_T10E	0.91	7095	7097
ADAPT(ABD035)_CD22_10_T10I	1.07	7076	7081
ADAPT(ABD035)_CD22_10_T10Q	1.11	7093	7096
ADAPT(ABD035)_CD22_10_T10W	0.75	7150	7154

The binding towards CD22, measured using BLI, can be seen to have been reduced for T10E, T10Q and T10W, compared to the original binder, ADAPT(ABD035)_CD22_10. For T10I, the affinity does not seem to be affected (Figure 21).

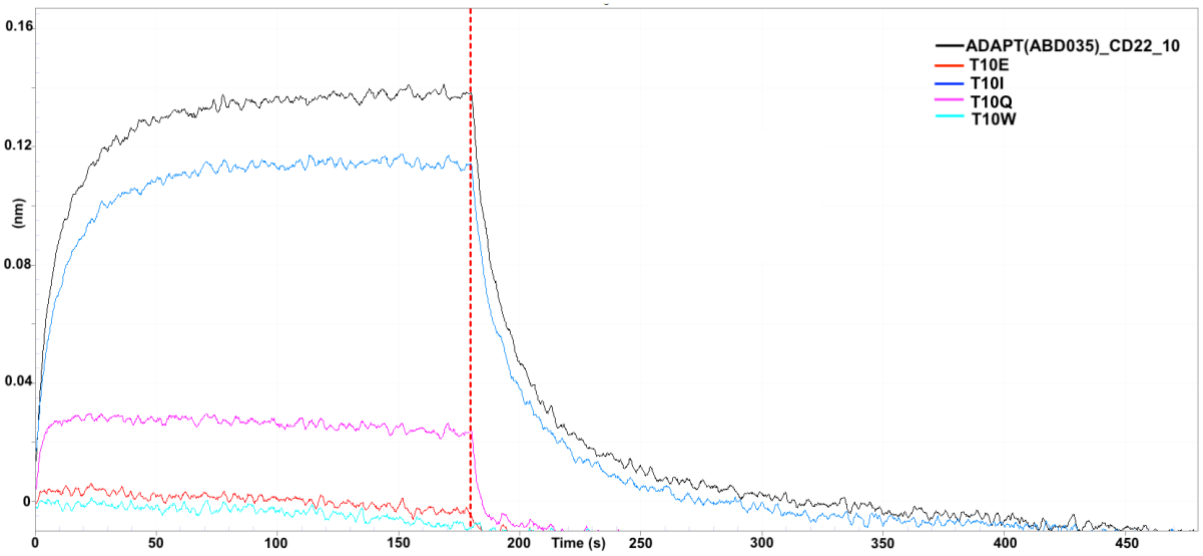

Figure 21. The binding profile of the four variants of T10, compared to the original binder, towards CD22. The sensograms show the binding of ADAPT (captured on anti-His biosensors) when dipped into to CD22 (500 nM). At the red, dotted line, after 300s, the sensors are dipped into buffer to measure how fast CD22 releases from the ADAPT.

4. Discussion and Conclusions

The aim of this project has been to increase the affinity of an ADAPT towards CD22 while preserving its ability to bind HSA simultaneously. This is in hopes of creating an ADAPT which could be used in targeted cancer therapy of B-cell malignancies, since CD22 is exclusively found on the surface of B-cells. An original binder called ADAPT(ABD035)_CD22_10 had previously been developed, which an affinity maturation library was based on to create variants that would hopefully have lower off rates. Since no improvements were found among these variants, an alanine scan was made to elucidate the paratope and investigate which positions are of importance for the affinity towards CD22 as well as the stability of the ADAPT. Lastly, one position was explored further, as well as one previously unexplored position, to evaluate if they would be of interest to include when creating a new maturation library.

The specific aim of the previously performed affinity maturation selection was to find a binder with a slower off rate, thus improving the affinity. However, all 20 variants from the maturation selection showed similar or faster off rate from CD22 compared to the original ADAPT(ABD035)_CD22_10. Two reasons as to why the affinity might have been lowered will be discussed. The first being the exchange to ABDstab as the scaffold in creation of the maturation library. ABDstab is more thermally stable than ABD035, and ABDstab is therefore expected to be more susceptible to mutations without causing stability issues. However, ABDstab has a lower affinity towards HSA. When comparing the two scaffolds for the original binder in this study, the melting temperature did increase with 13°C for ADAPT(ABDstab)_CD22_10 compared to ADAPT(ABD035)_CD22_10 (Table 2), and as expected, affinity decreased for ADAPT(ABDstab)_CD22_10 (Table 3) towards HSA. The K_D went from 0.72 nM for ADAPT(ABD035)_CD22_10 to 21 nM for ADAPT(ABDstab)_CD22_10. More surprisingly, when examining the affinity and the binding signal towards CD22, this could be seen to be lower as well (Table 3 and Appendix, Figure A4). The negative effect on the CD22 affinity was not expected since the scaffold positions that differ between ABDstab and ABD035 are located far from the CD22 binding surface and might not motivate the thermostable abilities gained by the exchange of scaffold. Another reason for the low affinity of the variants from the maturation selections could be that I15 was switched out for all variants compared to the original binder (Table 1). When examining the alanine scan, switching isoleucine (I) to an alanine (A) meant that I15A lost all affinity towards CD22, thus indicating the importance of that precise amino acid in this position. This is further strengthened by isoleucine and alanine having quite similar properties, both having hydrophobic side chains of relatively small size, yet the change still rendered significant difference in affinity. When doing the alanine scan only one position was exchanged. However, multiple changes were made to the variants from the maturation selection. Thus, the result of the affinity will not be dependent only on that single position, but on all the exchanged positions. This will likely affect why some of the variants from the maturation selection still have affinity towards CD22, even though the isoleucine has been removed. However, an amino acid of such an importance should probably be kept as it is and not exchanged even though it is still possible to gain affinity.

Generally, the results from the alanine scan showed quite positive results. All variants were successfully produced. They all had an α-helical structure and the ability to refold after heat denaturation. However, some variations in results could be seen. W11A, L14A, I15A and Q17A all lost their binding to CD22 (Figure 12) whilst the others retained the affinity to varying degrees. During the alanine scan it could be seen that W11A, L14A, I15A and D31A all had a prominent decrease in melting temperature, being 40°C for the three first mentioned and 36°C for D31A. Since the final aim is to use the ADAPT for therapy, temperatures so close to the

human body temperature are unsuitable. For W11A, L14A and I15A, these positions were previously deemed unchangeable when creating the maturation library due to their suggested importance for CD22 binding, thus this is not too much of an issue. However, for D31A, this is more troubling. D31A had quite high affinity towards CD22, indicating it being a position that could be varied when designing future maturation libraries, in order to find the optimal amino acid for CD22 binding. Yet, the low melting temperature suggests that this position is affecting the stability of the ADAPT, which could cause problems if exchanged. E22A however had a high melting point of 51°C (three degrees higher than ADAPT(ABD035)_CD22_10). However, it was the only variant which seemed to have degraded when doing SEC. Furthermore, the MS data from this variant was lost and when a new trial was made on the remaining protein after about a month, no protein could be detected by MS. In contrast, CD spectroscopy showed an α-helical structure, both before and after heat denaturation of the protein. Both D31 and E22 seem to have the potential of being exchanged in terms of CD22 affinity, but when changed for an alanine both had a reduction in stability. Changes of these position could still be explored but should be done with more care, having the issue with stability in mind. Maybe amino acids with a charged or polar side chain would be more beneficial for the stability then that of the hydrophobic alanine.

For W11A the wrong size was seen when doing the MALDI MS. The theoretical size being 6954 Da, with the one from the MALDI being 7020 Da. Why this has occurred is unclear. The sequence was, just as all the others, sent in for sequence confirmation, which showed that the desired exchange had been created. Since the original binder has a size of 7063 Da, it is not likely that no change has occurred either. The mass should be further examined with a more sensitive MS to be confident in the result.

Both Q21A and V34A seem to be good candidates to switch out for other amino acids whilst maintaining affinity towards CD22, providing high melting temperatures and the ability to refold after denaturation (Table 4). Even though Q30A and W18A show quite a negative effect on the binding towards CD22 (less than 20% of the signal as ADAPT(ABD035)_CD22_10), they still show some binding which suggest that these positions are part of the paratope and have the potential to impact the binding strength. Identifying the optimal amino acids for CD22 interaction in these positions may lead to an improved affinity, and they should therefore be opened to randomization in a future maturation library.

When doing the alanine scan it could be seen that the positions that had been locked when creating the maturation library (positions 10, 11, 14 and 17), did indeed lower the affinity towards CD22 when exchanged. However, for W11A, L14A and Q17A, the change meant that no affinity at all could be detected towards CD22, which was not the case for T10A. T10A had a binding signal of approximately 30% compared to that of ADAPT(ABD035)_CD22_10, and a K_D of 630 nM, compared to 110 nM for ADAPT(ABD035)_CD22_10. Due to this, position T10 was further explored, exchanging it to amino acids from different classification groups (hydrophobic, polar, positively charged, and negatively charged), to see if this could be a position susceptible to randomization when designing future maturation libraries. The exploration showed that neither T10E or T10Wshowed any affinity towards CD22, and only a very low affinity could be seen for T10Q, indicating that they would not make good candidates for exchange (Figure 21). Since threonine (T) and glutamine (Q) are part of the same group, having polar uncharged side chains, this indicates that the larger size of glutamine might be disadvantageous. For T10I on the other hand, the affinity at large looked the same. Isoleucine and threonine are part of different groups with isoleucine having a hydrophobic side chain, but quite a similar size. This once again indicates the importance of the size of the amino acid in

this position. Tryptophan (W) belongs to the same hydrophobic group as isoleucine. However, it was not a sustainable option, supposedly due to its large size. Unfortunately, no variant using an amino acid with a positively charged side group was successfully cloned so it is unknown how that would have affected it. Glutamic acid (E), which has a negatively charged side chain as well as being quite large also had a negative effect on the affinity. Since the alanine scan, where threonine was exchanged for alanine, also showed a retained affinity towards CD22, just as T10I, as well as having an acceptable thermostability profile with a melting temperature of 48°C and ability to refold after heat denaturation (Table 4), this indicates that in creation of a future maturation library, it may be possible to exchange T10 towards other small amino acids.

Since the affinity maturation did not result in any improved binders, and the alanine scan confirmed a reasonable design of the used affinity maturation library, an attempt to broaden the ADAPT paratope and increase the library size was explored. Here, position N7, a previously untouched position in the present ADAPT libraries, was investigated. N7 is positioned in the beginning of helix 1, close to the positions which have been deemed necessary for the binding towards CD22. This position was thus exchanged to every amino acid (excluding cysteine, glycine and proline), to see how this affects the affinity as well as stability of ADAPT(ABD035)_CD22_10. Since N7D, N7H and N7T could not be successfully cloned, no conclusions can be drawn about these. All the 13 variants which was successfully produced had quite high melting temperatures, comparable to that of the original binder (48°C) or above, except for three variants of 45, 46 and 47°C respectively. Moreover, they all had the expected α-helical structure, and the ability to refold after thermal denaturation (Table 5). However, even though both N7A and N7V have nice S-shaped melting curves, for N7I and larger amino acids with hydrophobic sides chains, the melting curve does not have the desired S-curve formation, but instead show a linear behavior (Figure 17). This usually indicates non-cooperative unfolding, meaning that instead of having a specific temperature at which the full structure completely denatures, parts of the structure denature one by one, continuously, as the temperature increases. Due to these stability concerns, hydrophobic amino acids with a larger side chain than valine are not great alternatives even though they show affinity towards CD22. However, since this position does not seem to affect the affinity, it is most likely placed outside of the paratope. This means it can be varied in future libraries towards CD22, but this will probably not lead to any substantial improvement in affinity.

It can be concluded that the previous affinity maturation selections did not provide variants with improved affinity to CD22, which was initially the hope. However, more information about the paratope of the original binder has been gathered, which can be used for future endeavors. Among this information it should be noted that the ABD035 scaffold seem more beneficial to use compared to ABDstab for this binder. ABD035 will cause a lower thermal stability compared to ABDstab. However, during these experiments the original binder was shown to have an acceptable stability. It has been susceptible to changes without ever losing its structure, most variants have had melting temperatures above 47°C and all have been able to refold after heat denaturation. It should therefore be a suitable scaffold to keep for future maturation libraries. The positions of W11, L14, I15 and Q17 should not be varied in a future library since they are crucial for CD22 binding. W18, Q21, Q30 and V34 seem susceptible to randomization, and T10 could maybe be an alternative if changed to amino acids of similar size. Position D31 is important for thermostability and E22A for a general stability, these could potentially be selectively randomized with caution (e.g. avoiding hydrophobic amino acids), and it could be beneficial to explore these positions in more depth. Lastly, a new position that could be varied in the library has been examined, N7. This position seems to be possible to vary, however large amino acids with hydrophobic side chains should be avoided for stability reasons. Using these

conclusions, it should be possible to derive a new affinity maturation library which could possibly provide new variants with a lower off rate and thus increase the affinity towards CD22. The differences between the old library and the suggested new one can be seen in Figure 22. The aim of increasing the affinity is of great importance in obtaining a protein that would bind CD22 long enough to be of use for therapeutic targeting.

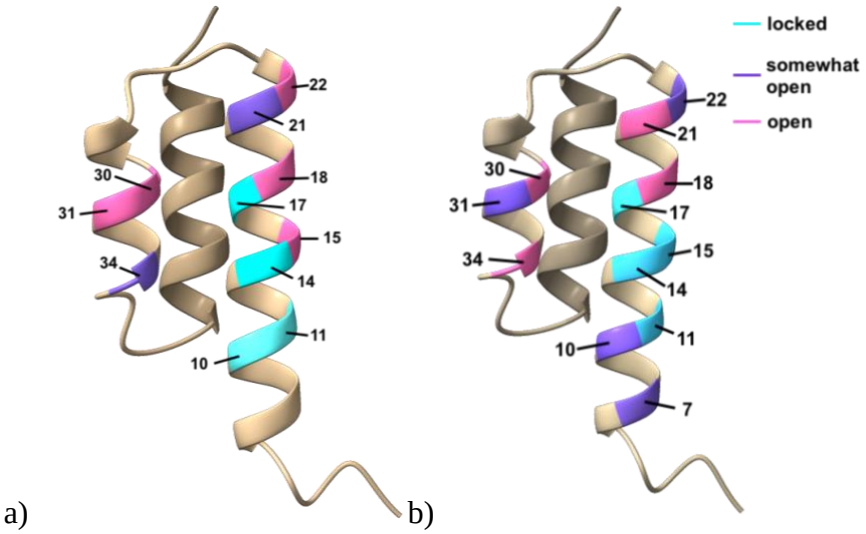

a) b)

Figure 22. a) The locked and opened positions in the old maturation library. b) The locked and opened positions in the new suggestion of a library. The turquoise suggests locked positions and the pink open positions. The purple highlights positions which were or should be kept somewhat open but exchanged with extra care. The N7 position has been marked as somewhat open in B) due to not having a significant impact on the affinity.

5. References

1. Bhojwani D, Yang JJ, Pui CH. Biology of childhood acute lymphoblastic leukemia. Vol. 62, Pediatric Clinics of North America. W.B. Saunders; 2015. p. 47–60.
2. Terwilliger T, Abdul-Hay M. Acute lymphoblastic leukemia: a comprehensive review and 2017 update. Vol. 7, Blood Cancer Journal. Springer Nature; 2017.
3. Lennmyr E, Karlsson K, Ahlberg L, Garelius H, Hulegårdh E, Izarra AS, et al. Survival in adult acute lymphoblastic leukaemia (ALL): A report from the Swedish ALL Registry. Eur J Haematol. 2019 Aug 1;103(2):88–98.
4. Hunger SP, Raetz EA. How I treat relapsed acute lymphoblastic leukemia in the pediatric population [Internet]. 2020. Available from: http://ashpublications.org/blood/article-pdf/136/16/1803/1761205/bloodbld2019004043c.pdf
5. Fielding AK, Richards SM, Chopra R, Lazarus HM, Litzow MR, Buck G, et al. Outcome of 609 adults after relapse of acute lymphoblastic leukemia (ALL); an MRC UKALL12/ECOG 2993 study. 2007; Available from: http://ashpublications.org/blood/article-pdf/109/3/944/1287586/zh800307000944.pdf
6. O'Leary MC, Lu X, Huang Y, Lin X, Mahmood I, Przepiorka D, et al. FDA Approval summary: Tisagenlecleucel for treatment of patients with relapsed or refractory b-cell precursor acute lymphoblastic leukemia. Vol. 25, Clinical Cancer Research. American Association for Cancer Research Inc.; 2019. p. 1142–6.
7. Vormittag P, Gunn R, Ghorashian S, Veraitch FS. A guide to manufacturing CAR T cell therapies. Vol. 53, Current Opinion in Biotechnology. Elsevier Ltd; 2018. p. 164–81.
8. Xu J, Luo W, Li C, Mei H. Targeting CD22 for B-cell hematologic malignancies. Vol. 12, Experimental Hematology and Oncology. BioMed Central Ltd; 2023.
9. Sterner RC, Sterner RM. CAR-T cell therapy: current limitations and potential strategies. Vol. 11, Blood Cancer Journal. Springer Nature; 2021.
10. Li W, Ding L, Shi W, Wan X, Yang X, Yang J, et al. Safety and efficacy of co-administration of CD19 and CD22 CAR-T cells in children with B-ALL relapse after CD19 CAR-T therapy. J Transl Med. 2023 Dec 1;21(1).
11. Niu J, Qiu H, Xiang F, Zhu L, Yang J, Huang C, et al. CD19/CD22 bispecific CAR-T cells for MRD-positive adult B cell acute lymphoblastic leukemia: a phase I clinical study. Vol. 13, Blood Cancer Journal. Springer Nature; 2023.
12. Shah NN, Sokol L. Targeting CD22 for the treatment of B-cell malignancies. Vol. 10, ImmunoTargets and Therapy. Dove Medical Press Ltd; 2021. p. 225–36.
13. Haso W, Lee DW, Shah NN, Stetler-Stevenson M, Yuan CM, Pastan IH, et al. Anti-CD22-chimeric antigen receptors targeting B-cell precursor acute lymphoblastic leukemia. Blood [Internet]. 2013;121(7):1165–74. Available from: http://ashpublications.org/blood/article-pdf/121/7/1165/1367991/zh800713001165.pdf
14. Shah NN, Stevenson MS, Yuan CM, Richards K, Delbrook C, Kreitman RJ, et al. Characterization of CD22 expression in acute lymphoblastic leukemia. Pediatr Blood Cancer. 2015 Jun 1;62(6):964–9.
15. Lamb YN. Inotuzumab Ozogamicin: First Global Approval. Drugs. 2017 Sep 1;77(14):1603–10.
16. Huang CJ, Lin H, Yang X. Industrial production of recombinant therapeutics in Escherichia coli and its recent advancements. Vol. 39, Journal of Industrial Microbiology and Biotechnology. 2012. p. 383–99.
17. Von Witting E, Lindbo S, Lundqvist M, Möller M, Wisniewski A, Kanje S, et al. Small Bispecific Affinity Proteins for Simultaneous Target Binding and Albumin-Associated Half-Life Extension. Mol Pharm. 2021 Jan 4;18(1):328–37.

18. Knudsen Sand KM, Bern M, Nilsen J, Noordzij HT, Sandlie I, Andersen JT. Unraveling the interaction between FcRn and albumin: Opportunities for design of albumin-based therapeutics. Vol. 6, Frontiers in Immunology. Frontiers Media S.A.; 2015.
19. Nilvebrant J, Hober S. The albumin-binding domain as a scaffold for protein engineering. In: Computational and Structural Biotechnology Journal. Elsevier B.V.; 2013. p. e201303009.
20. Jonsson A, Dogan J, Herne N, Abrahmsén L, Nygren PÅ. Engineering of a femtomolar affinity binding protein to human serum albumin. Protein Engineering, Design and Selection. 2008 Aug;21(8):515–27.
21. Gü lich S, Linhult M, Nygren ke, Uhlén M, Hober S. Stability towards alkaline conditions can be engineered into a protein ligand [Internet]. Vol. 80, Journal of Biotechnology. 2000. Available from: www.elsevier.com/locate/jbiotec
22. Jarmoskaite I, Alsadhan I, Vaidyanathan PP, Herschlag D. How to measure and evaluate binding affinities. Elife. 2020 Aug 1;9:1–34.
23. Waterhouse A, Bertoni M, Bienert S, Studer G, Tauriello G, Gumienny R, et al. SWISS-MODEL: Homology modelling of protein structures and complexes. Nucleic Acids Res. 2018 Jul 2;46(W1):W296–303.

Appendix A – Variants from Maturation Selection

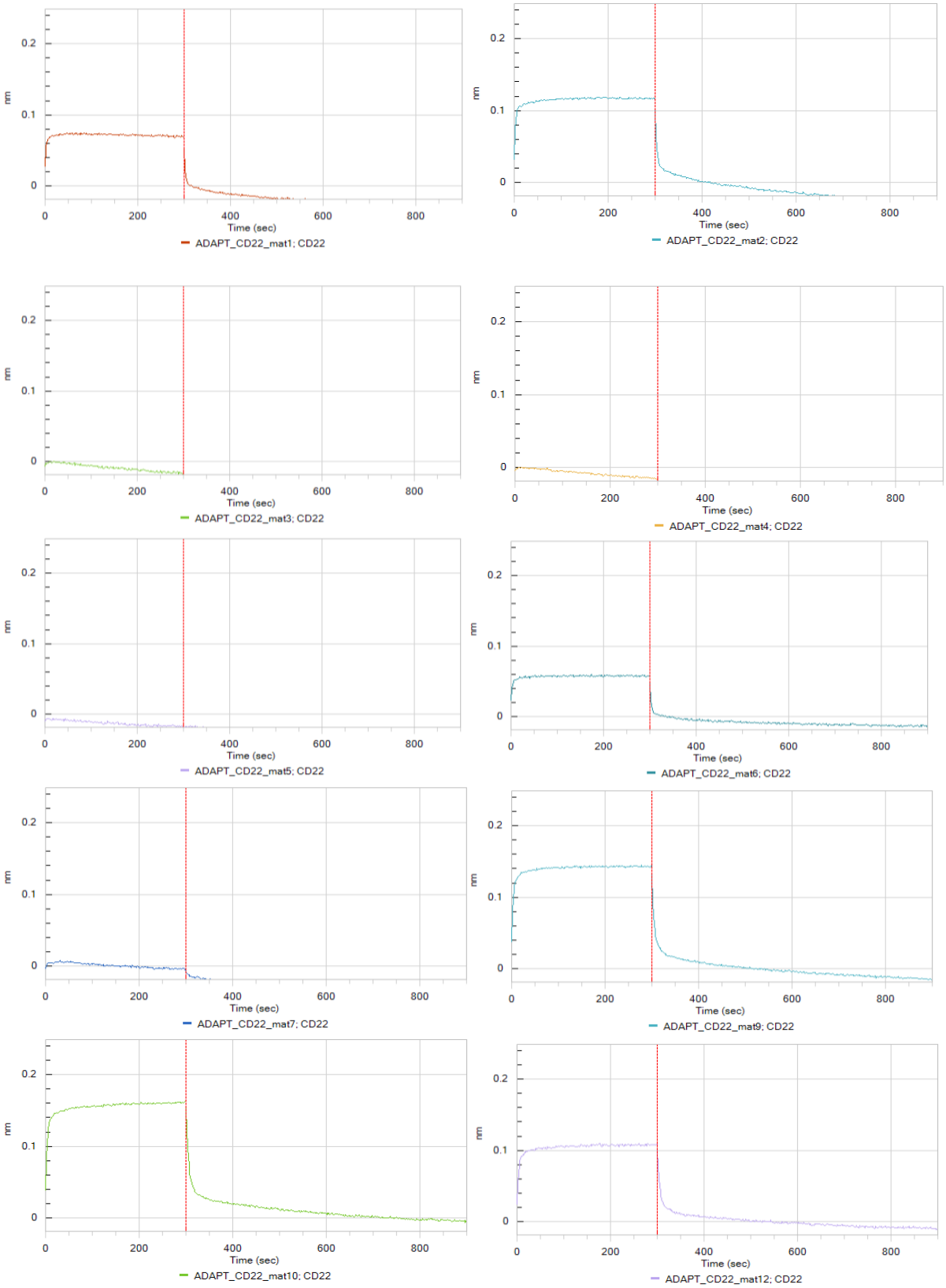

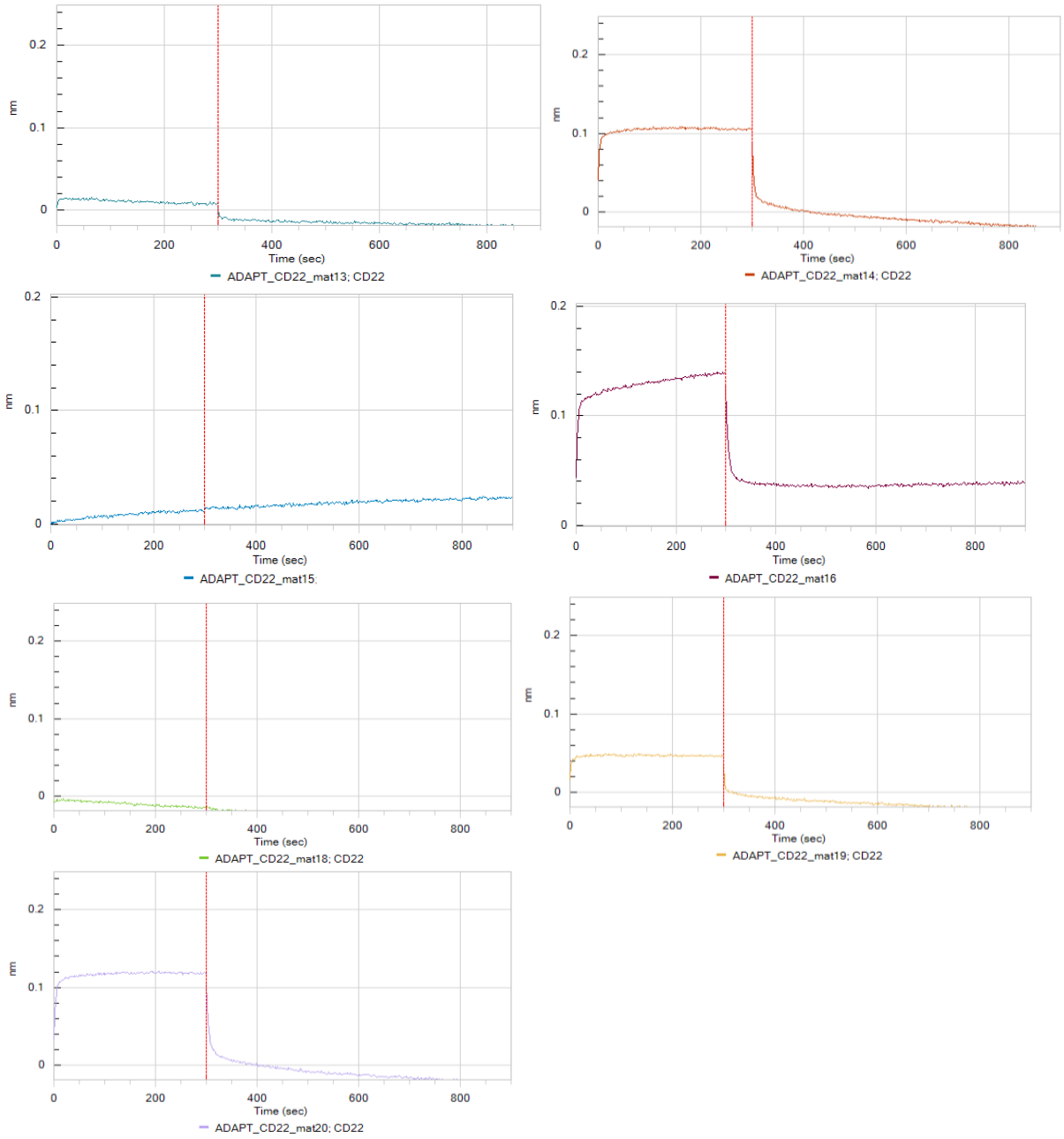

Figure A1. Octet results for the variants from the maturation selection, showing binding of captured ADAPT to CD22 (1000 nM) in solution. mat8, mat11, mat17 and ADAPT(ABD035)_CD22_10 can be seen in Figure 2.

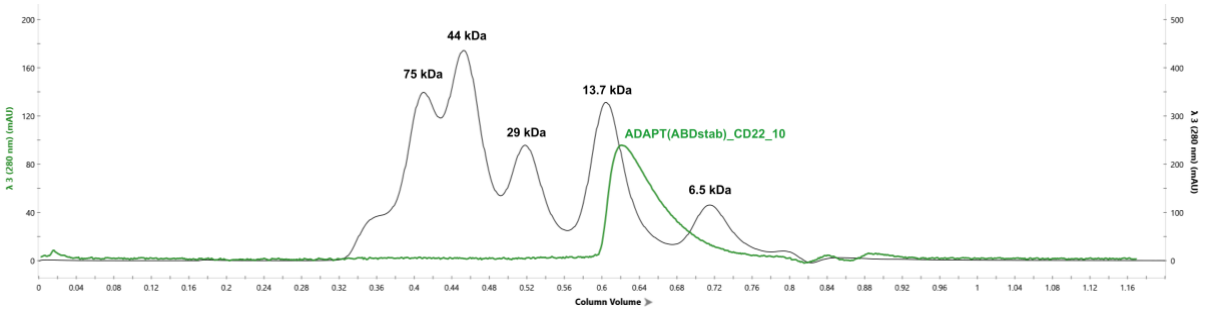

Figure A2. SEC of ADAPT(ABDstab)_CD222_10, showing the column volume at which the protein is eluted. The calibrant curve can be seen in black, and uses Conalbumin (75 kDa), Ovalbumin (44 kDa), Carbonic anhydrase (29 kDa), Ribonuclease A (13.7 kDa) and Aprotinin (6.5 kDa), with the largest protein eluting first. The peak can be seen between 6.5 and 13.7 kDa which is expected of a protein of a size of approximately 7 kDa.

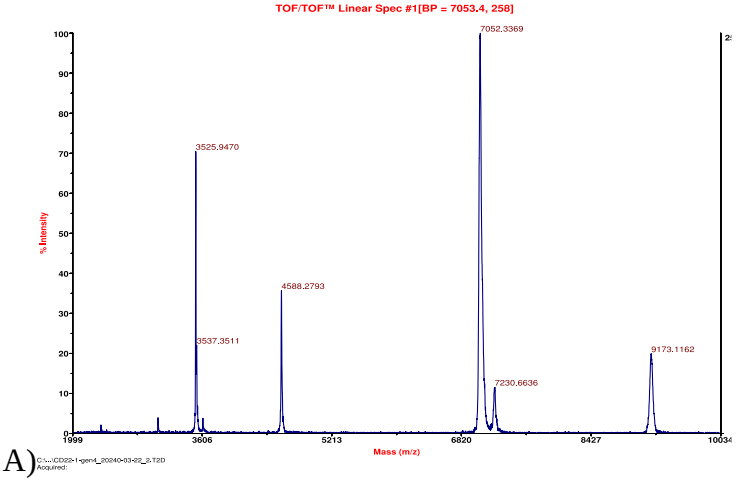

A)

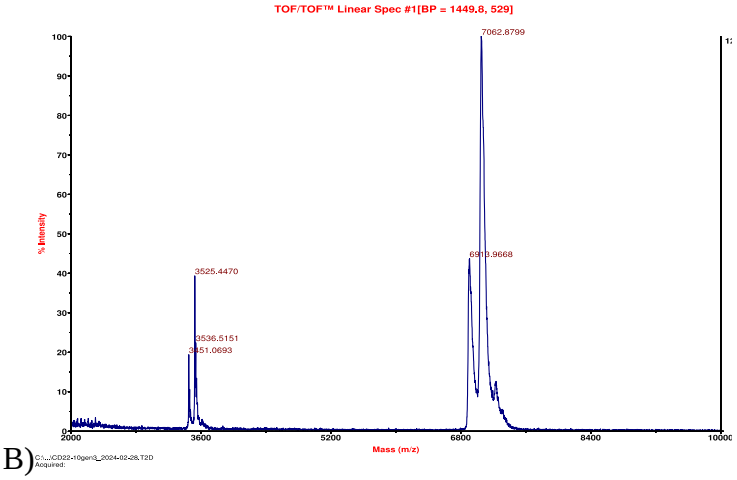

B)

Figure A3. Mass spectra obtained using MALDI MS for A) ADAPT(ABDstab)_CD22_10 and B) ADAPT(ABD035)_CD22_10). The mass obtained corresponds to the theoretical values.

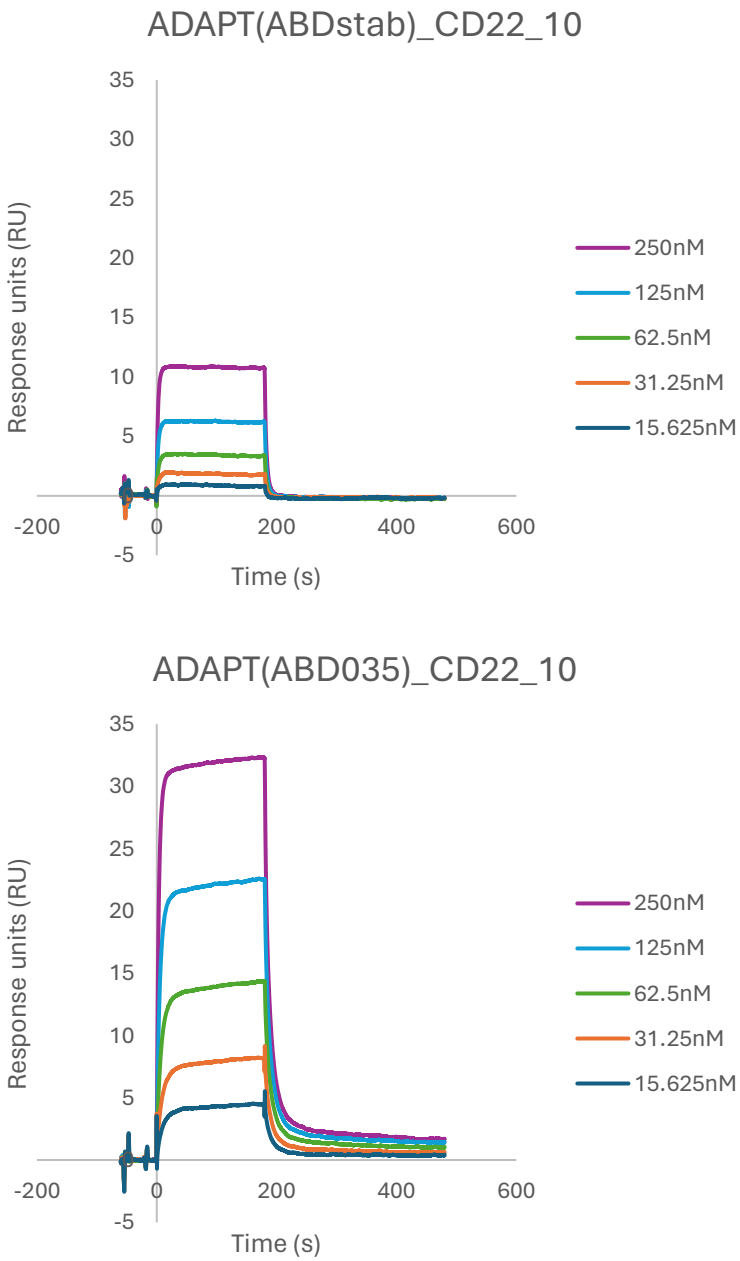

Figure A4. SPR data of the ADAPT binding to immobilized CD22 in a multi-cycle kinetics setup. The obtained K_D value can be seen in Table 3.

Appendix B – Alanine Scan

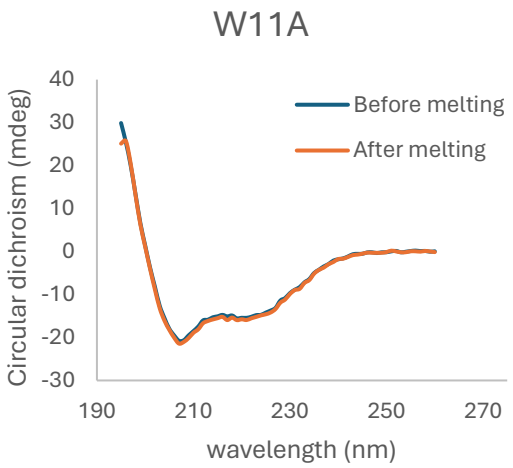

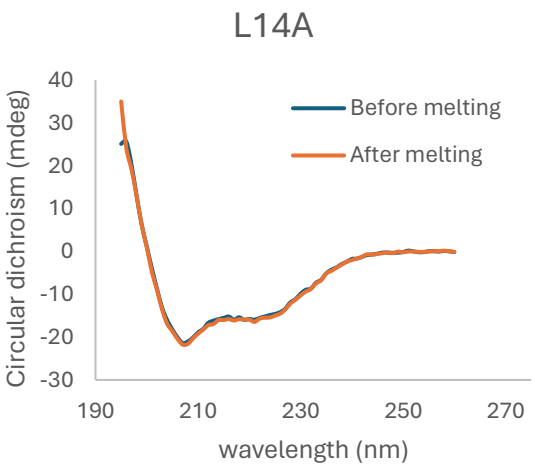

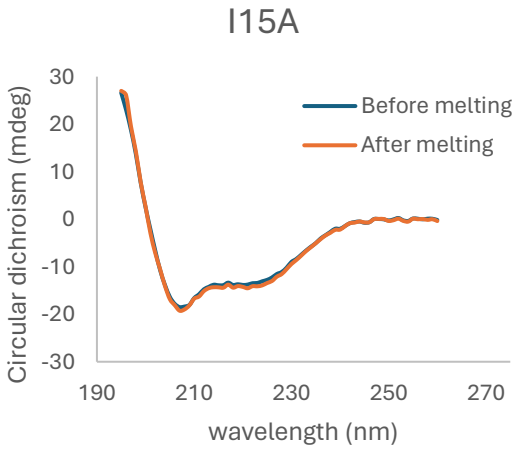

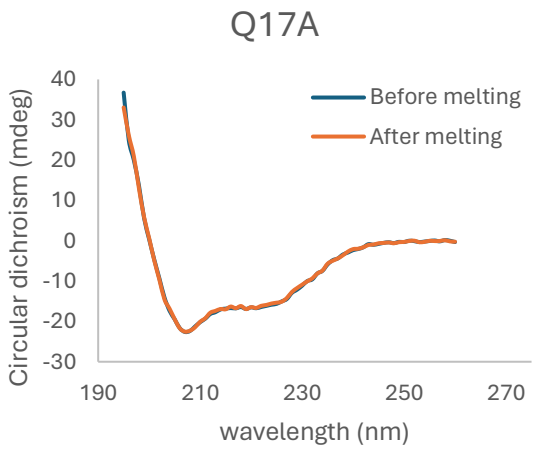

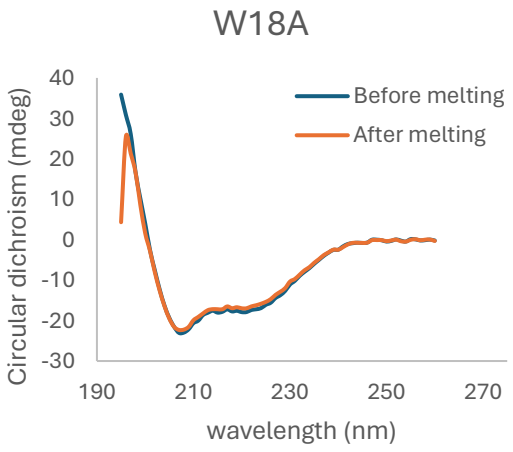

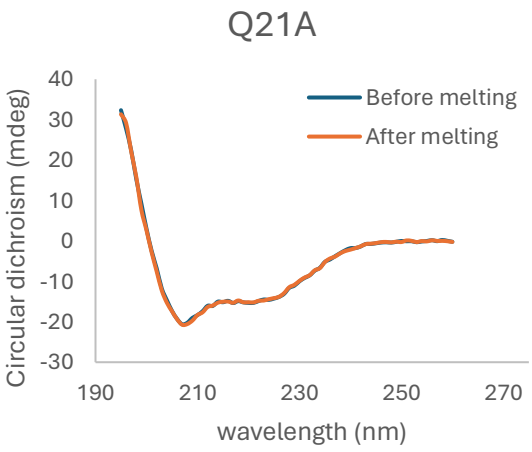

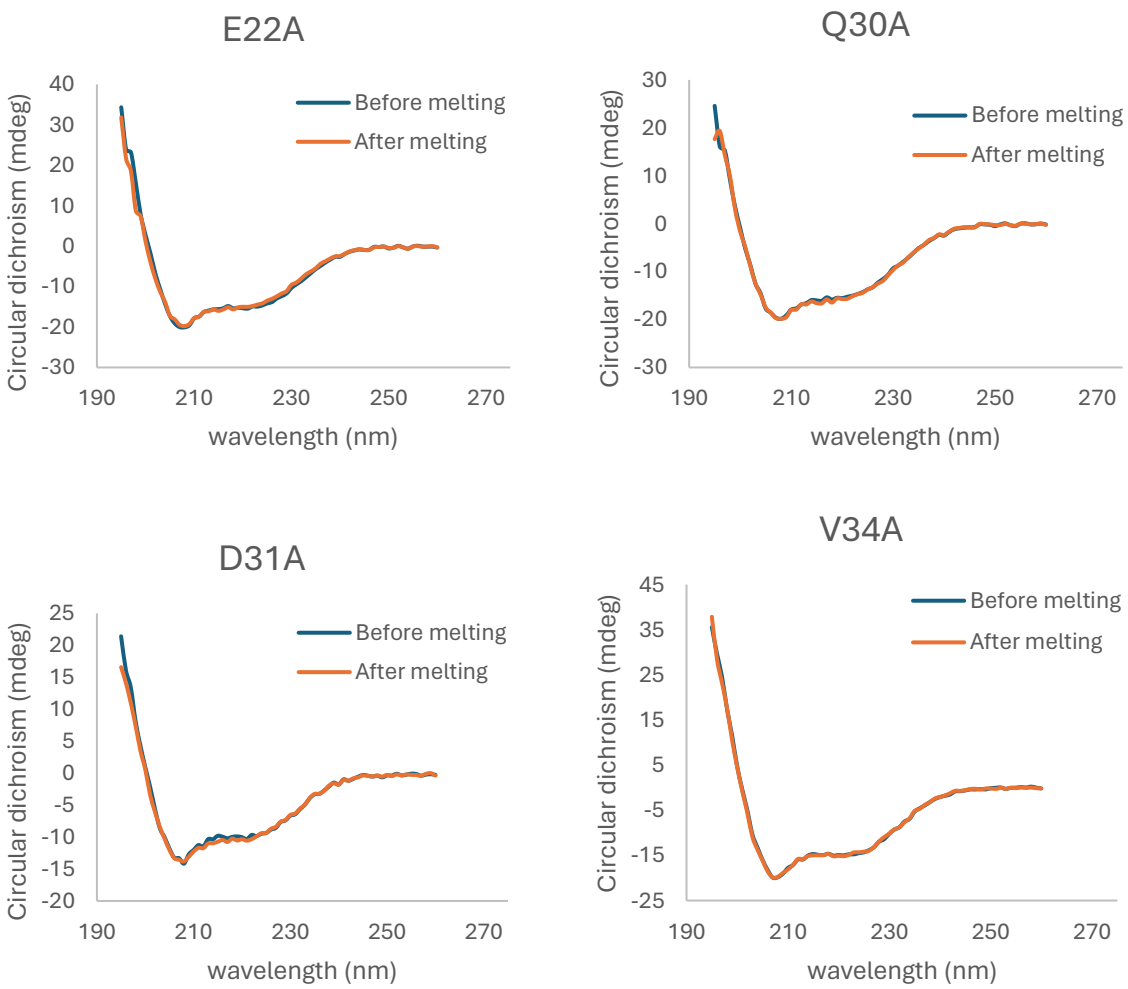

Figure B1. CD spectra for the alanine scan. The experiment was made twice, at room temperature, once before heat denaturation of the protein (in blue) and once after (in orange), to see the secondary structure of the protein. The α-helical structure can be seen due to dips at 208 and 222 nm. A total refolding can be seen for all variants. CD spectra of the variants W11A to V34A, T10A can be seen in Figure 7.

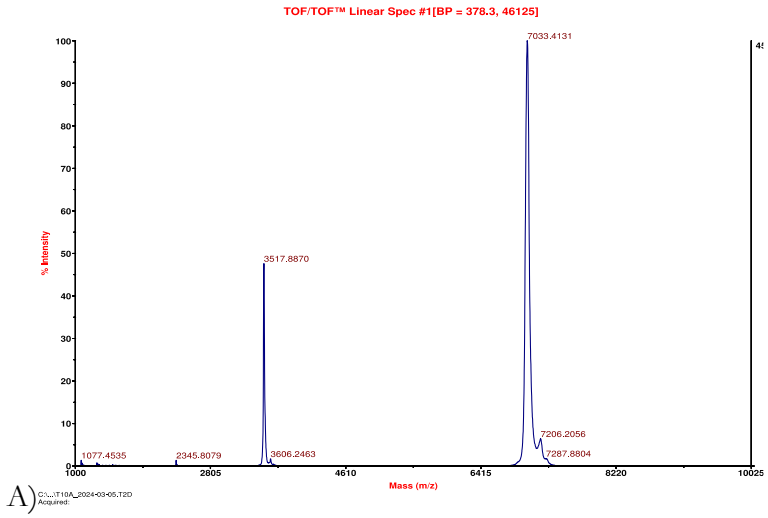
TOF/TOF™ Linear Spec #1[BP = 378.3, 46125]
% Intensity
Mass (m/z)
7033.4131
3517.8870
7206.2056
7287.8804
1077.4535
2345.8079
3606.2463
1000
2805
4610
6415
8220
10025

A)

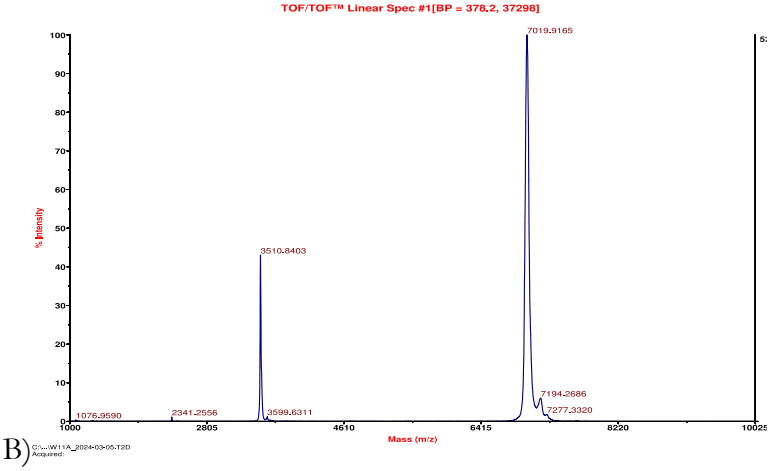
TOF/TOF™ Linear Spec #1[BP = 378.2, 37298]
% Intensity
Mass (m/z)
7019.9165
3510.8403
7194.2686
7277.3320
1076.9590
2341.2556
3599.6311
1000
2805
4610
6415
8220
10025

B)

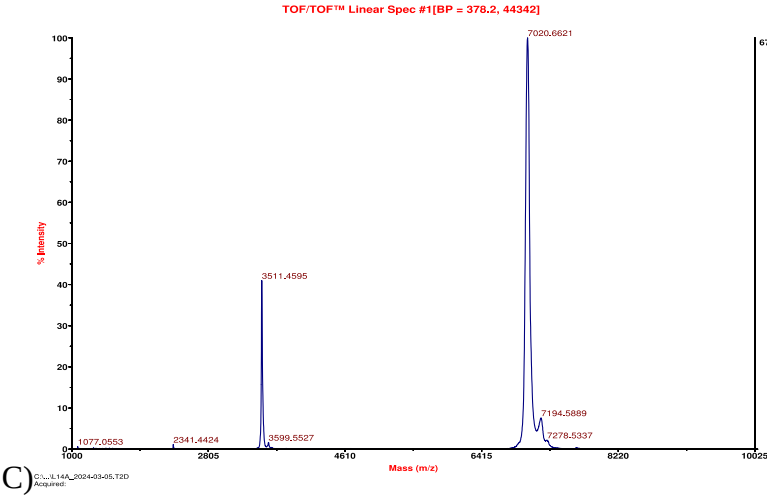
TOF/TOF™ Linear Spec #1[BP = 378.2, 44342]
% Intensity
Mass (m/z)
7020.6621
3511.4595
7194.5889
7278.5337
1077.0553
2341.4424
3599.5527
1000
2805
4610
6415
8220
10025

C)

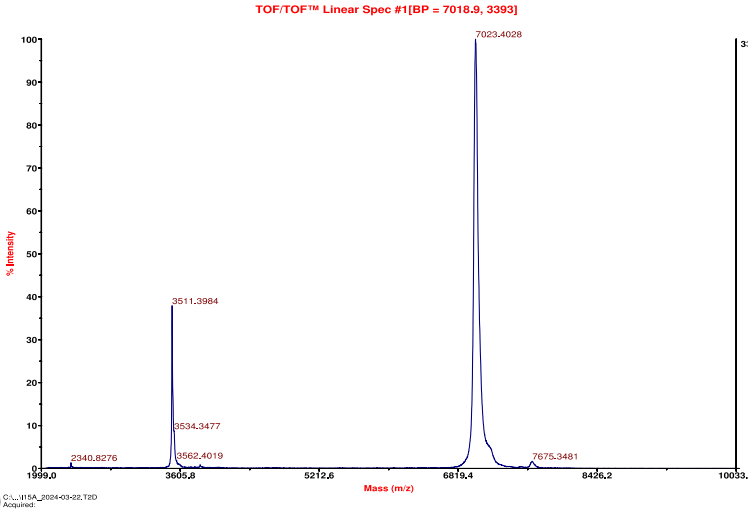
TOF/TOF™ Linear Spec #1[BP = 7018.9, 3393]
% Intensity
Mass (m/z)
7023.4028
3511.3984
3534.3477
3562.4019
2340.8276
7675.3481

D)

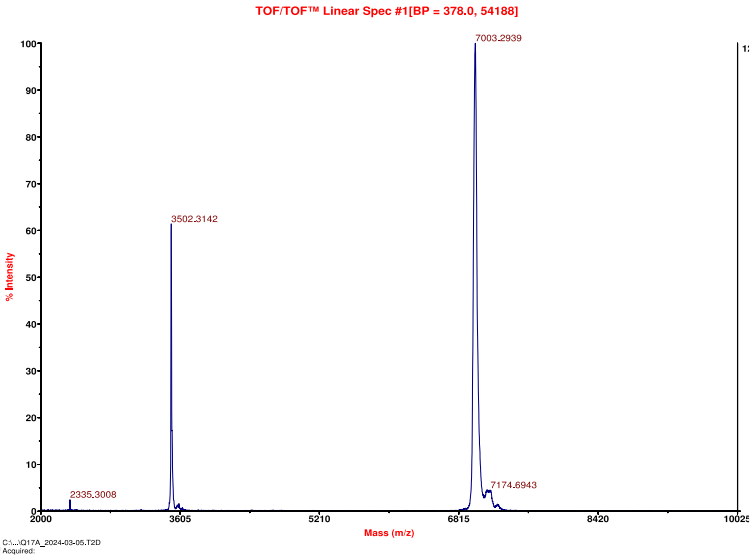
TOF/TOF™ Linear Spec #1[BP = 378.0, 54188]
% Intensity
Mass (m/z)
7003.2939
3502.3142
2335.3008
7174.6943

E)

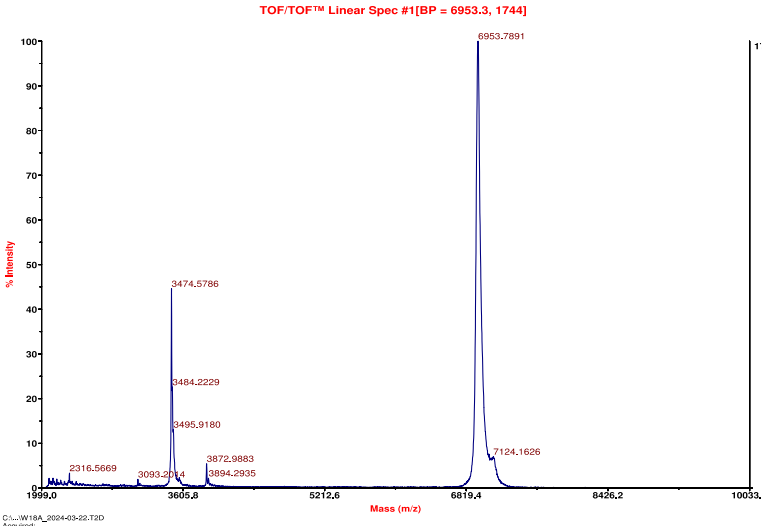
TOF/TOF™ Linear Spec #1[BP = 6953.3, 1744]
% Intensity
Mass (m/z)
6953.7891
3474.5786
3484.2229
3495.9180
2316.5669
3872.9883
3894.2935
7124.1626

F)

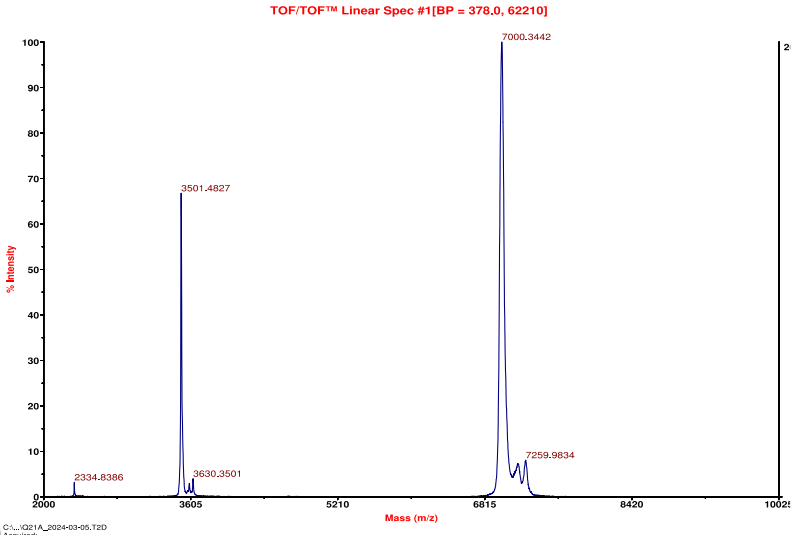
TOF/TOF™ Linear Spec #1[BP = 378.0, 62210]
7000.3442
3501.4827
2334.8386
3630.3501
7259.9834
% Intensity
Mass (m/z)
100
90
80
70
60
50
40
30
20
10
0
2000
3605
5210
6815
8420

G)

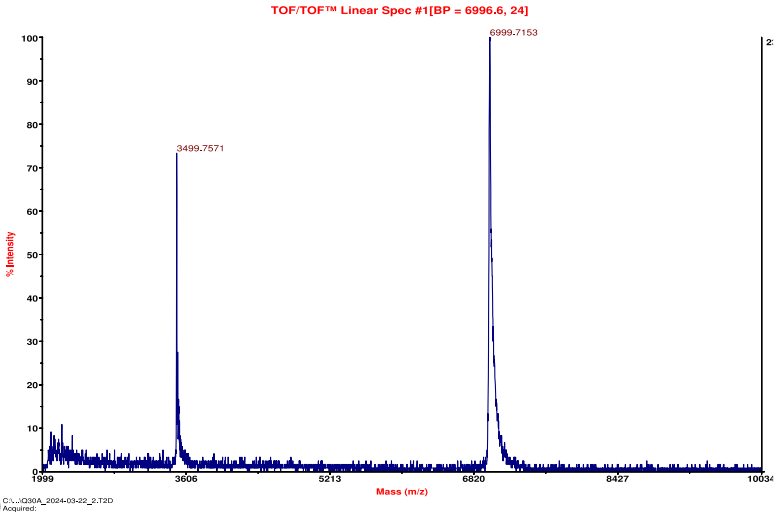
TOF/TOF™ Linear Spec #1[BP = 6996.6, 24]
6999.7153
3499.7571
% Intensity
Mass (m/z)
100
90
80
70
60
50
40
30
20
10
0
1999
3606
5213
6820
8427

H)

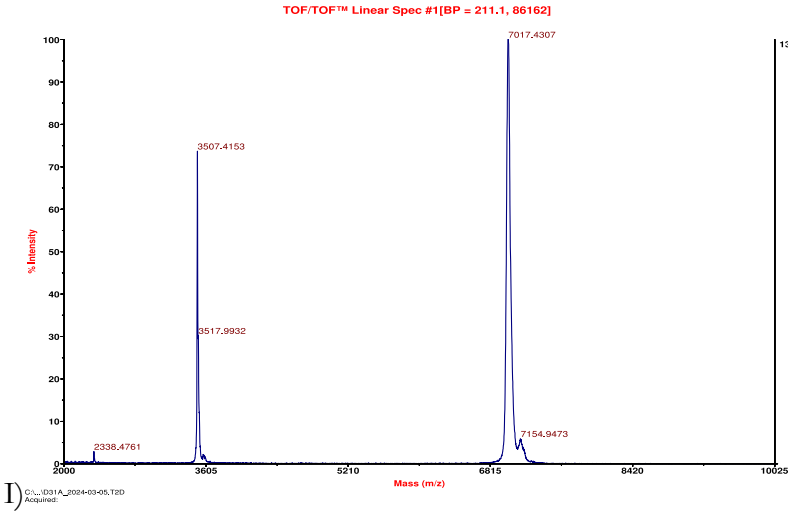

I)

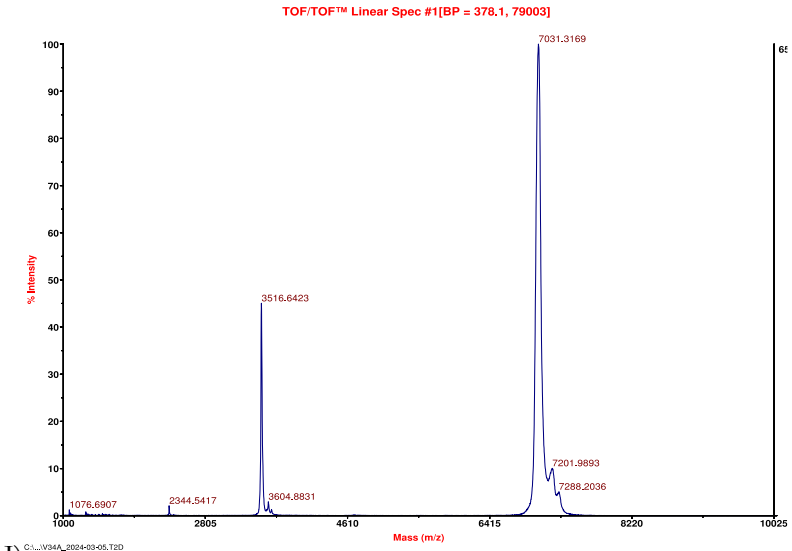

J)

Figure B2. Mass spectra obtained using MALDI MS for A) W11A, B) L14A, C) I15A, D) Q17A, E) W18A, F) Q21A, G) E22A, H) Q30A, I) D31A and J) V34A. The mass obtained corresponds to the theoretical values for all but W11A.

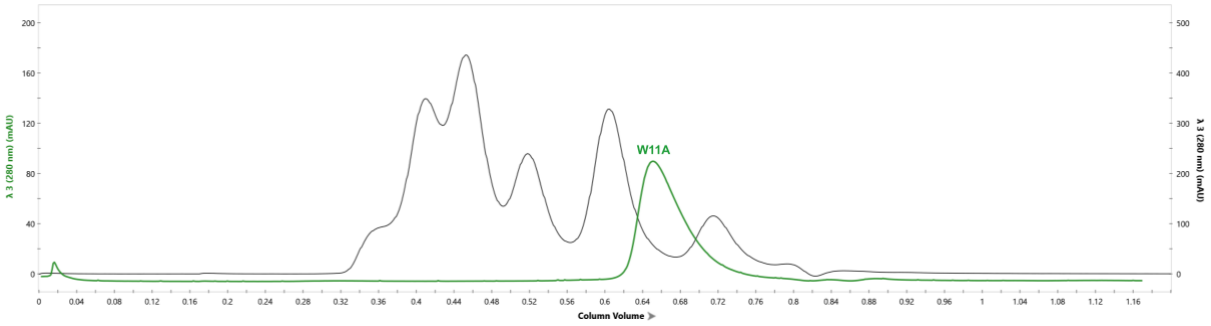
W11A
λ 3 (280 nm) (mAU)
Column Volume

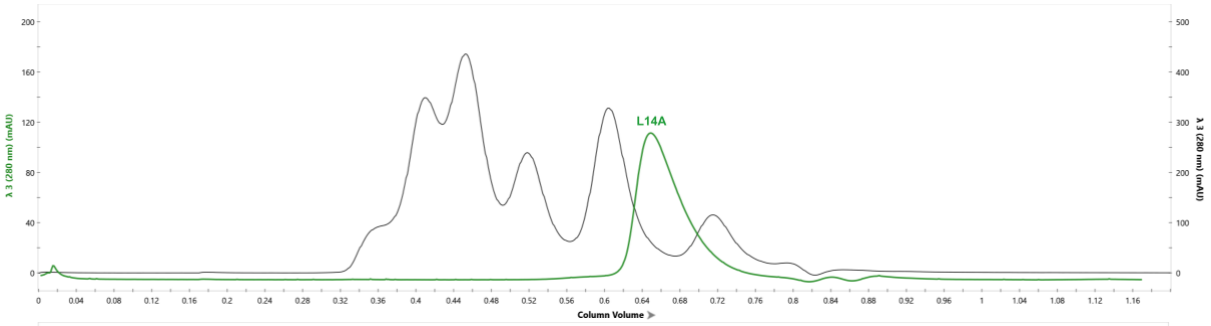
L14A
λ 3 (280 nm) (mAU)
Column Volume

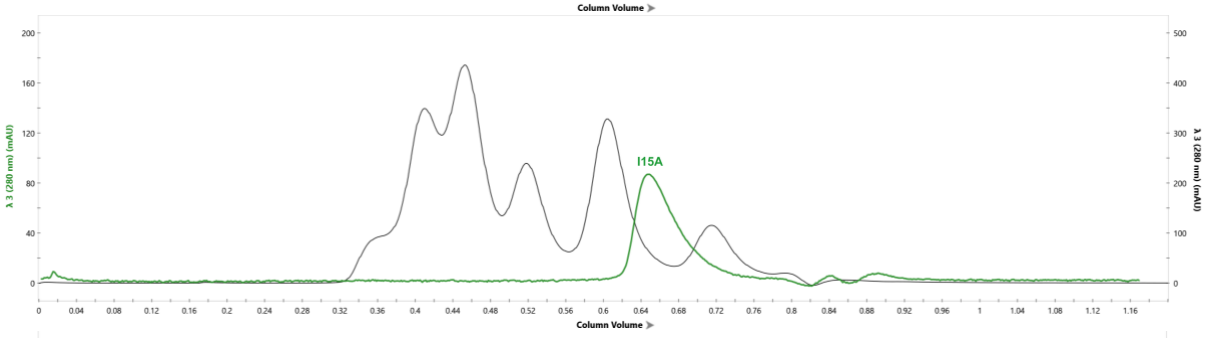
I15A
λ 3 (280 nm) (mAU)
Column Volume

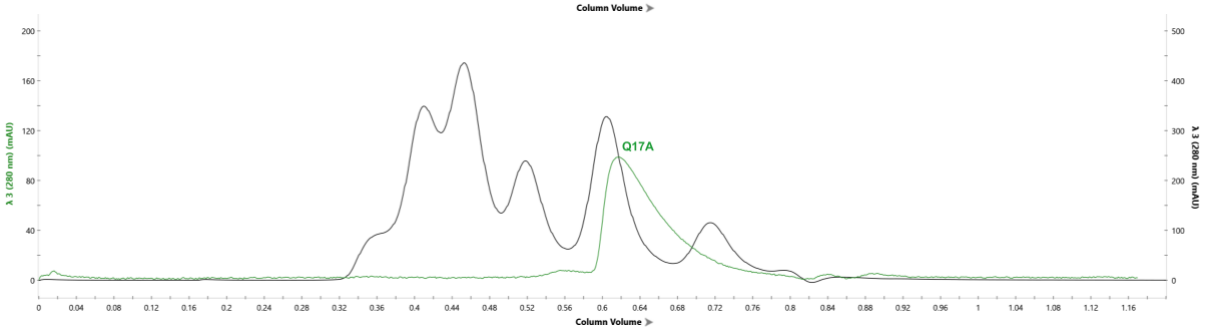
Q17A
λ 3 (280 nm) (mAU)
Column Volume

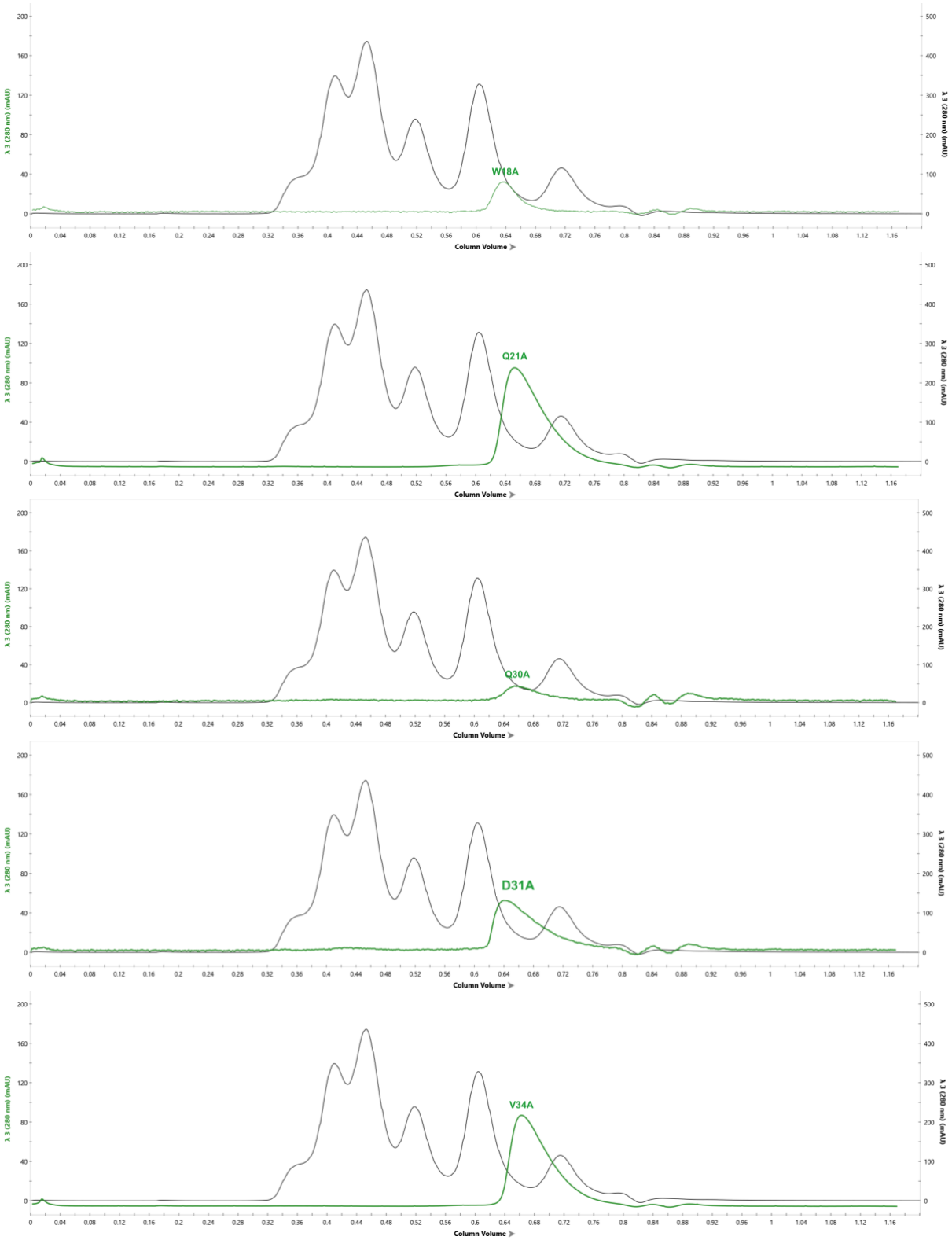

Figure B3. SEC of all alanine scan variants except for T10A and E22A, which can be seen in Figure 9, showing the column volume at which the protein is eluted. The calibrant curve can be seen in black, and uses Conalbumin (75 kDa), Ovalbumin (44 kDa), Carbonic anhydrase (29 kDa), Ribonuclease A (13.7 kDa) and Aprotinin (6.5 kDa), with the largest protein eluting first. The peaks can be seen between 6.5 and 13.7 kDa which is expected of a protein of a size of approximately 7 kDa.

Table B1. Table over the affinity for the alanine scan variants, as well as for ADAPT(ABD035)_CD22_10, towards CD22 and HSA determined using Biacore T200. ND – not detected. The values have been used to make Figure 10 and Appenix, Figure B4.

Variant	**Affinity for CD22, K_D (M)**	**Affinity for HSA, K_D (M)**
ADAPT(ABD035)_CD22_10_T10A	6.3E-07	3.7E-10
ADAPT(ABD035)_CD22_10_W11A	N/D	2.0E-10
ADAPT(ABD035)_CD22_10_L14A	N/D	1.5E-10
ADAPT(ABD035)_CD22_10_I15A	N/D	1.3E-09
ADAPT(ABD035)_CD22_10_Q17A	N/D	9.1E-10
ADAPT(ABD035)_CD22_10_W18A	9.5E-08	2.0E-09
ADAPT(ABD035)_CD22_10_Q21A	3.1E-07	6.5E-10
ADAPT(ABD035)_CD22_10_E22A	3.1E-07	9.4E-10
ADAPT(ABD035)_CD22_10_Q30A	1.1E-06	4.0E-09
ADAPT(ABD035)_CD22_10_D31A	3.1E-07	3.7E-10
ADAPT(ABD035)_CD22_10_V34A	1.6E-07	3.6E-10
ADAPT(ABD035)_CD22_10	1.1E-07	2.1E-08

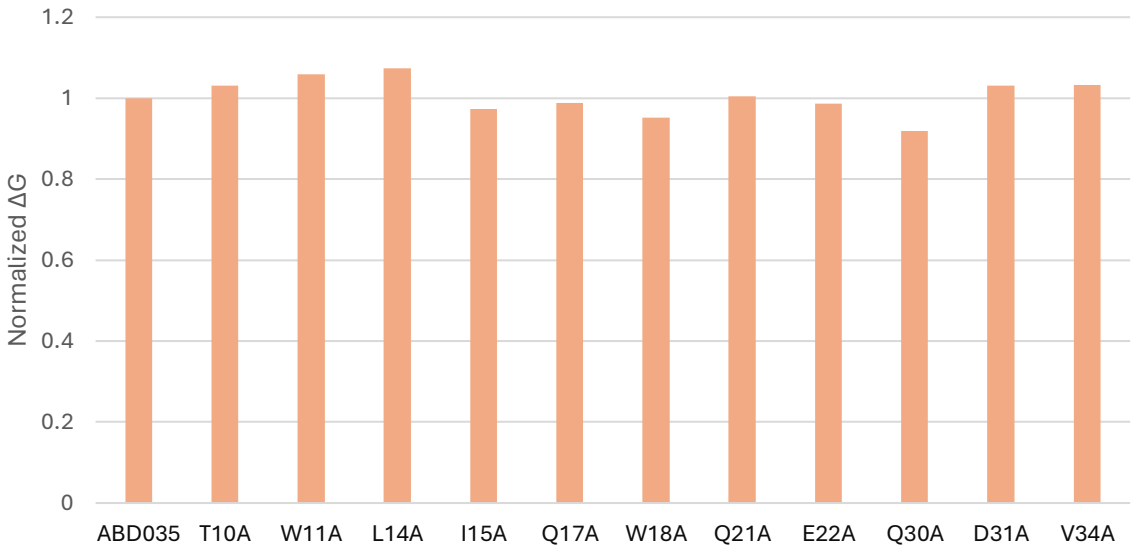

Figure B4. Gibbs free energy (ΔG), showing the binding energy between the ADAPT and HSA, has been normalized towards the ΔG of ADAPT(ABD035)_CD22_10 (in the graph only called ABD035) for all variants, showing the affinity of the ADAPTs towards HSA. Values from Table B1.

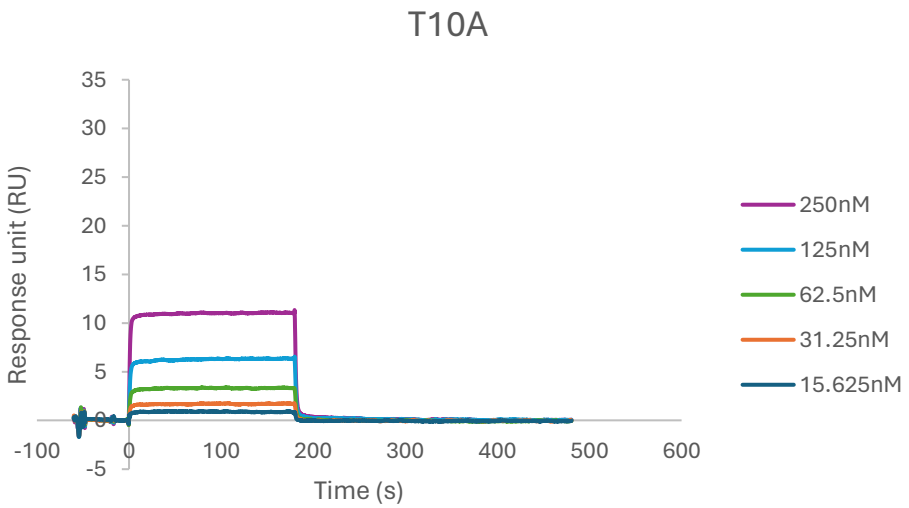
T10A
Response unit (RU)
35
30
25
20
15
10
5
0
-5
-100
0
100
200
300
400
500
600
Time (s)
250nM
125nM
62.5nM
31.25nM
15.625nM

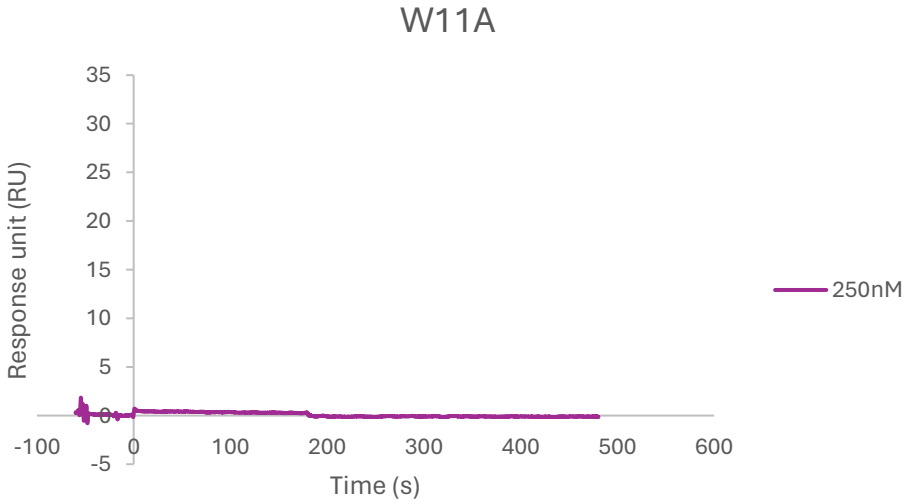
W11A
Response unit (RU)
35
30
25
20
15
10
5
0
-5
-100
0
100
200
300
400
500
600
Time (s)
250nM

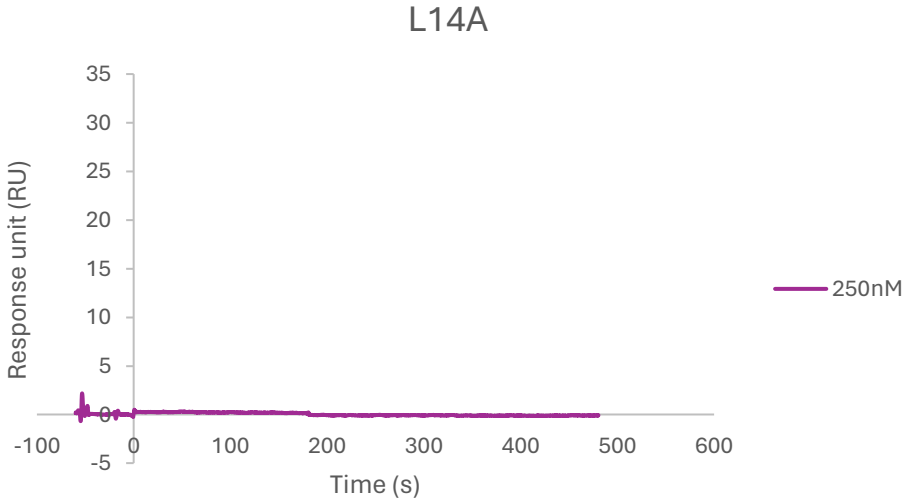
L14A
Response unit (RU)
35
30
25
20
15
10
5
0
-5
-100
0
100
200
300
400
500
600
Time (s)
250nM

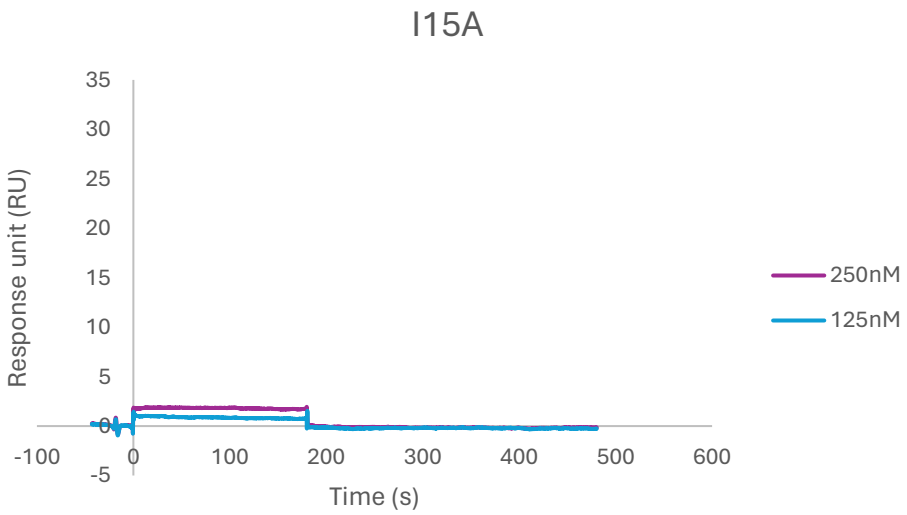
I15A
Response unit (RU)
35
30
25
20
15
10
5
0
-5
-100
0
100
200
300
400
500
600
Time (s)
250nM
125nM

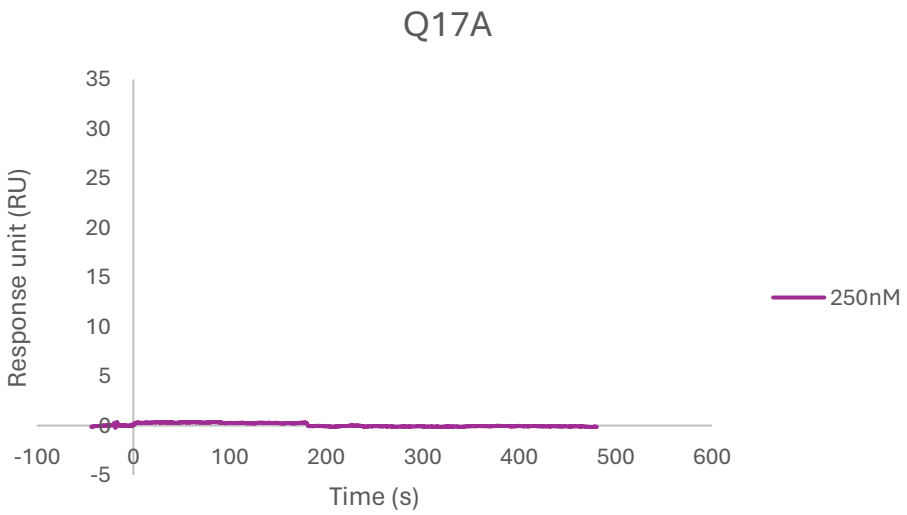
Q17A
Response unit (RU)
35
30
25
20
15
10
5
0
-5
-100
0
100
200
300
400
500
600
Time (s)
250nM

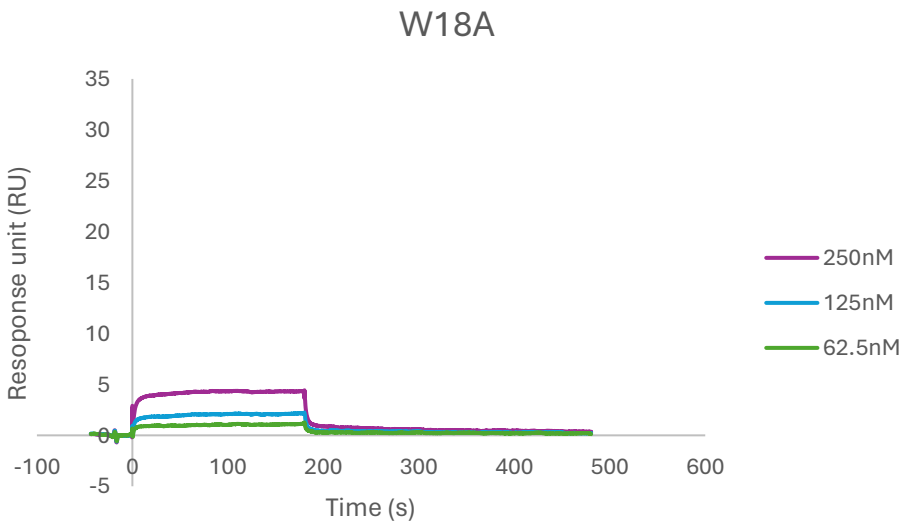
W18A
Resoponse unit (RU)
35
30
25
20
15
10
5
0
-5
-100
0
100
200
300
400
500
600
Time (s)
250nM
125nM
62.5nM

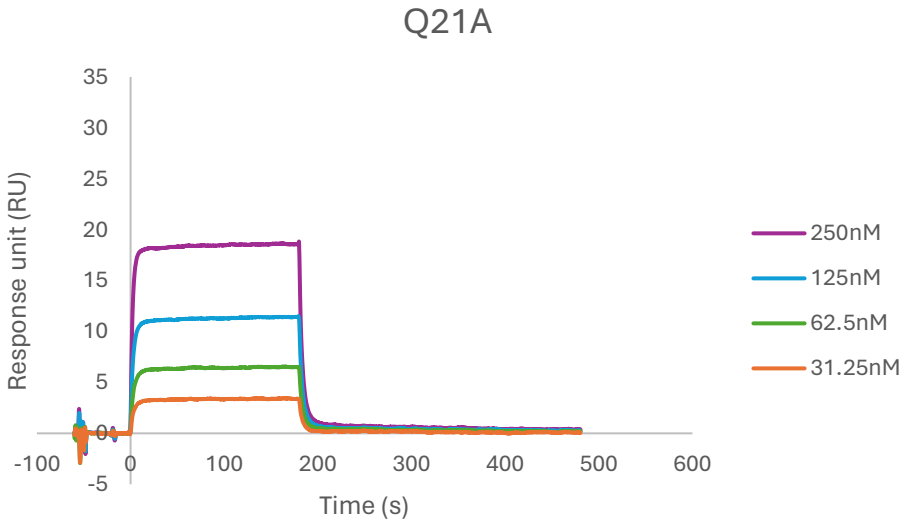
Q21A
Response unit (RU)
35
30
25
20
15
10
5
0
-5
-100
0
100
200
300
400
500
600
Time (s)
250nM
125nM
62.5nM
31.25nM

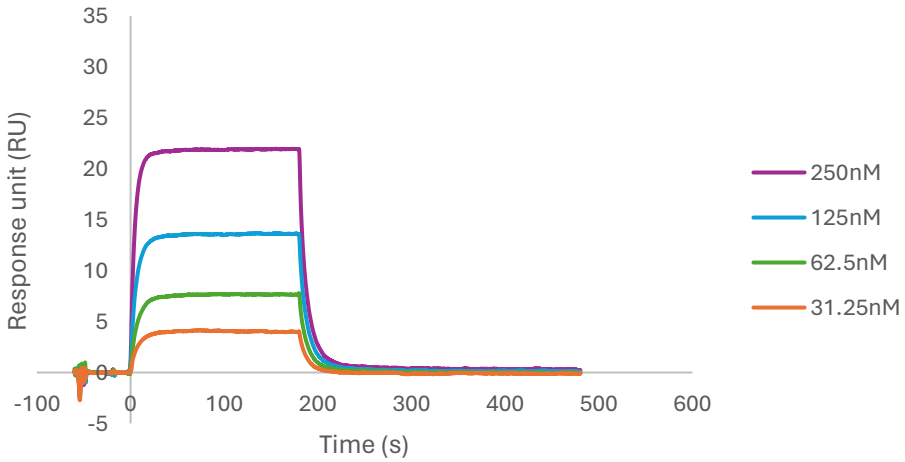
E22A
Response unit (RU)
35
30
25
20
15
10
5
0
-5
-100
0
100
200
300
400
500
600
Time (s)
250nM
125nM
62.5nM
31.25nM

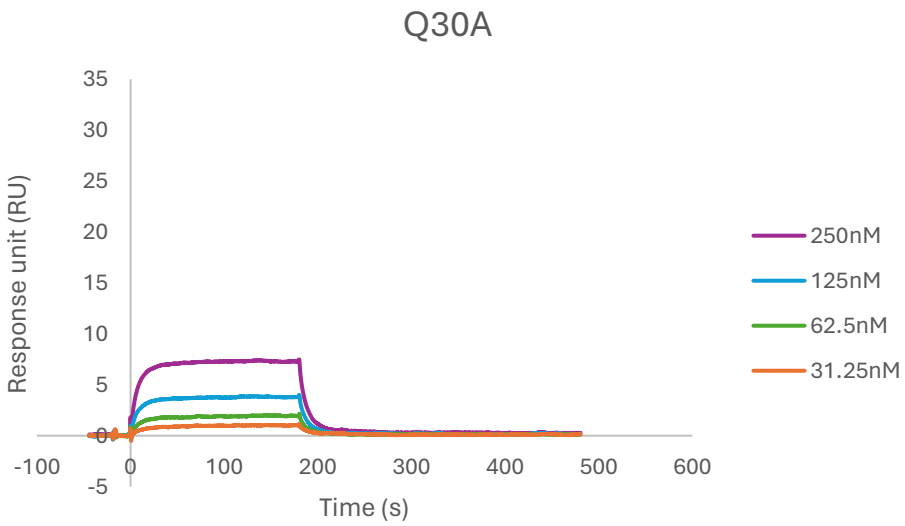
Q30A
Response unit (RU)
35
30
25
20
15
10
5
0
-5
-100
0
100
200
300
400
500
600
Time (s)
250nM
125nM
62.5nM
31.25nM

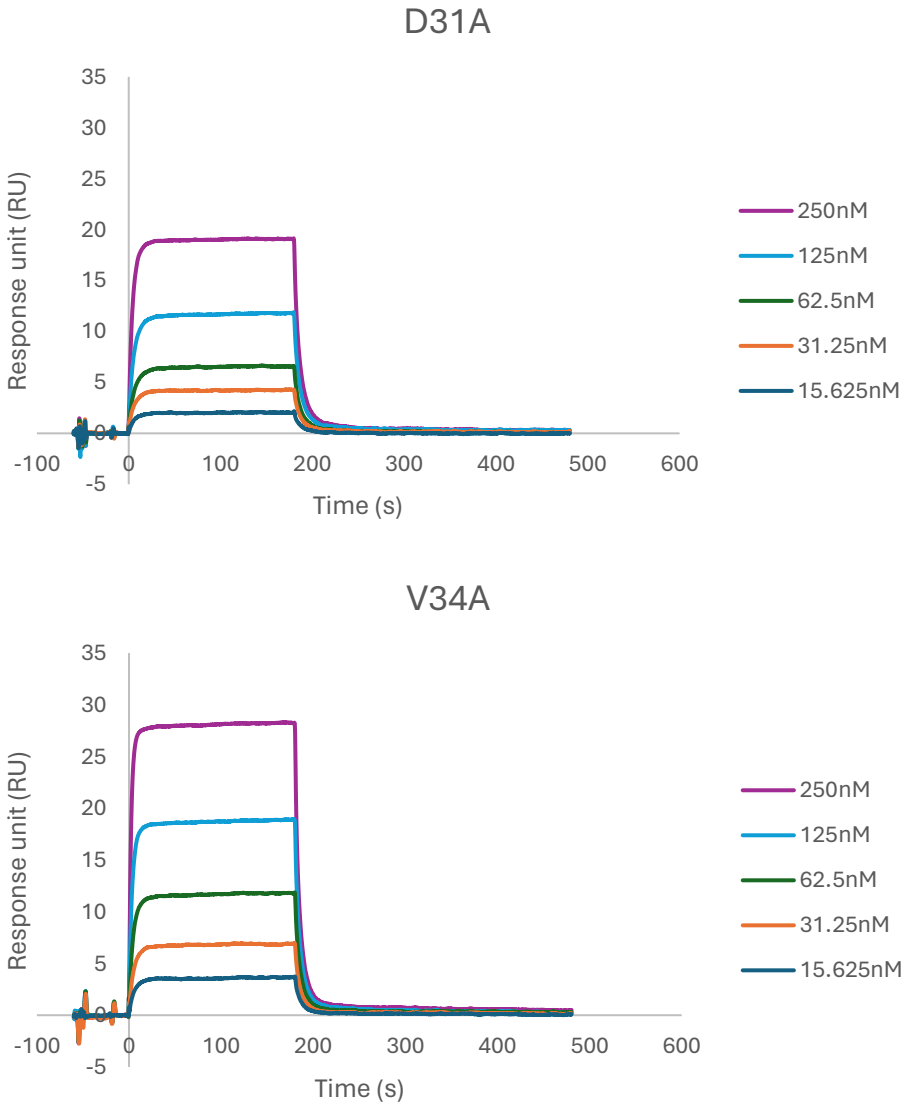

Figure B5. SPR data of for all alanine scan variants, showing the ADAPT binding to immobilized CD22 in a multi-cycle kinetics setup. The samples were diluted 1:1 from 250nM to 15.62nM. Some show fewer dilutions due to no detectable signal for the lower dilutions. The obtained K_D values can be seen in table B1. Figure 11 has been colored based on the response units in these sensograms.

Appenidx C – Library Exploration

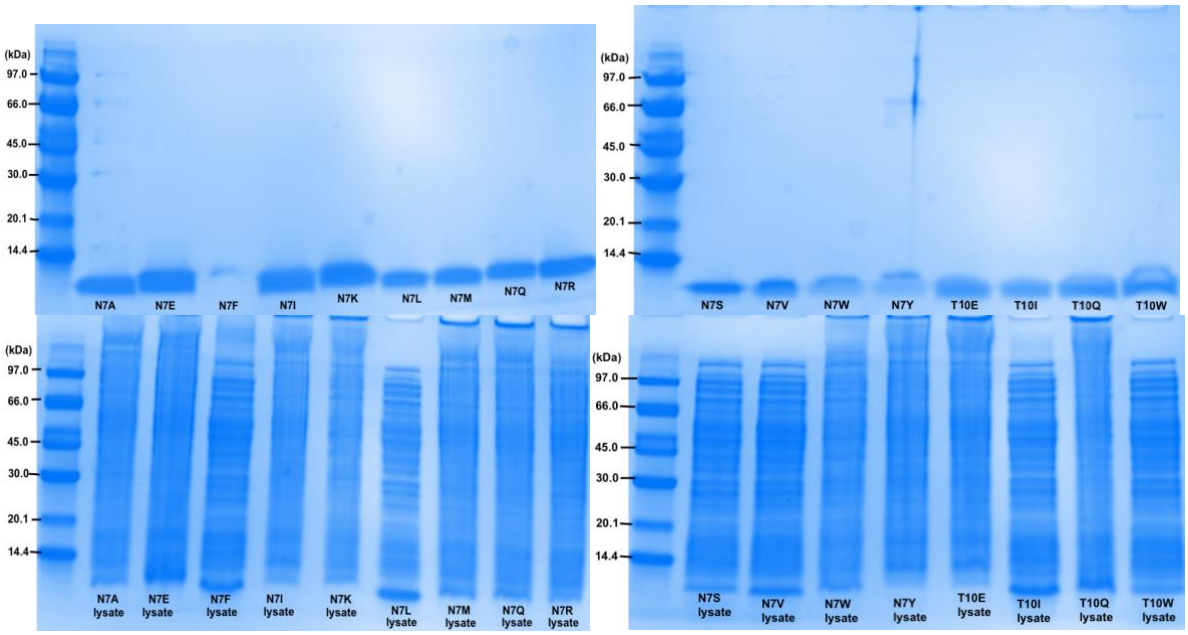

Figure C1. SDS-PAGE showing either the purified samples or the lysate of the library exploration variants. Most purified results can be seen to have a clear line, of a size under 14.4 kDa, even though some lysates show faint lines at this size. N7F has a very faint line due to no sample being loaded in the well, however some overloading happened.

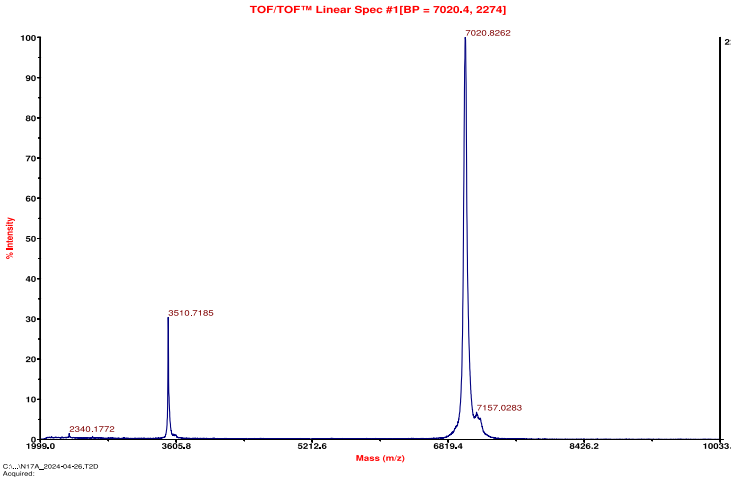
TOF/TOF™ Linear Spec #1[BP = 7020.4, 2274]
7020.8262
3510.7185
7157.0283
2340.1772
% Intensity
Mass (m/z)
1999.0
3605.8
5212.6
6819.4
8426.2
10033.

A)

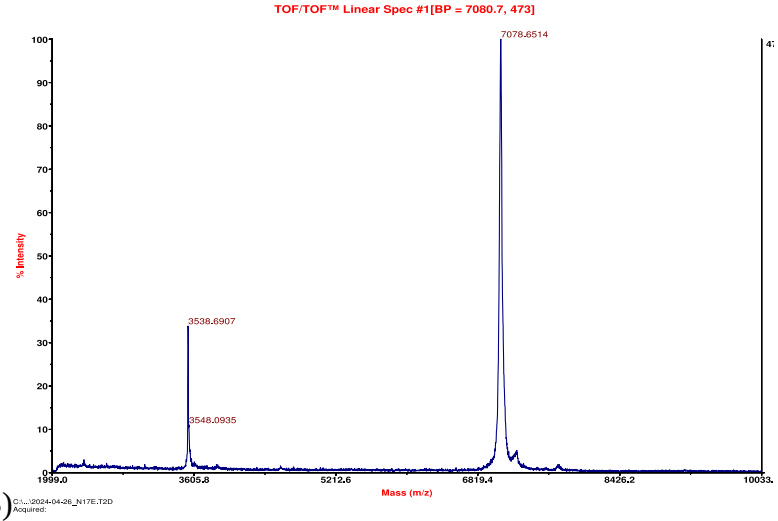
TOF/TOF™ Linear Spec #1[BP = 7080.7, 473]
7078.6514
3538.6907
3548.0935
% Intensity
Mass (m/z)
1999.0
3605.8
5212.6
6819.4
8426.2
10033.

B)

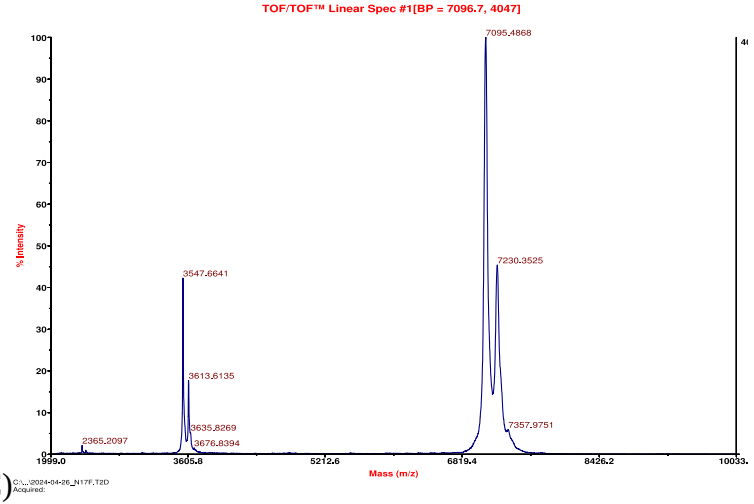
TOF/TOF™ Linear Spec #1[BP = 7096.7, 4047]
7095.4868
3547.6641
7230.3525
3613.6135
3635.8269
3676.8394
7357.9751
2365.2097
% Intensity
Mass (m/z)
1999.0
3605.8
5212.6
6819.4
8426.2
10033.

C)

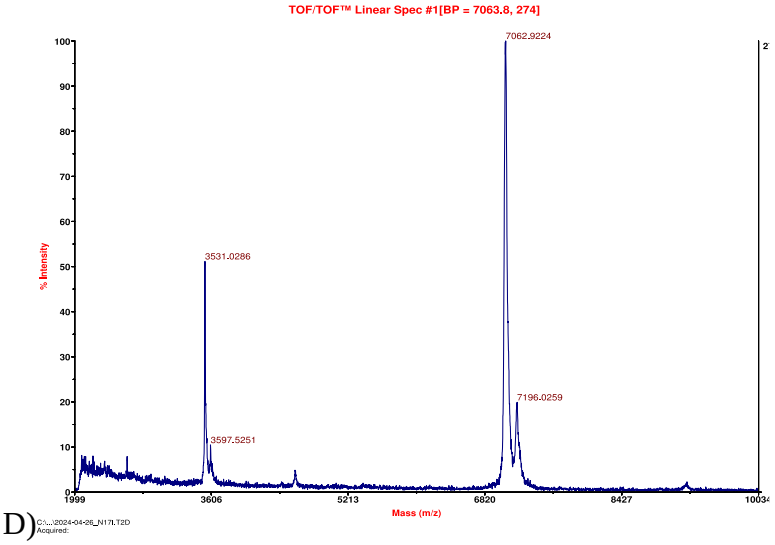
TOF/TOF™ Linear Spec #1[BP = 7063.8, 274]
7062.9224
3531.0286
7196.0259
3597.5251
% Intensity
Mass (m/z)
1999
3606
5213
6820
8427

D)

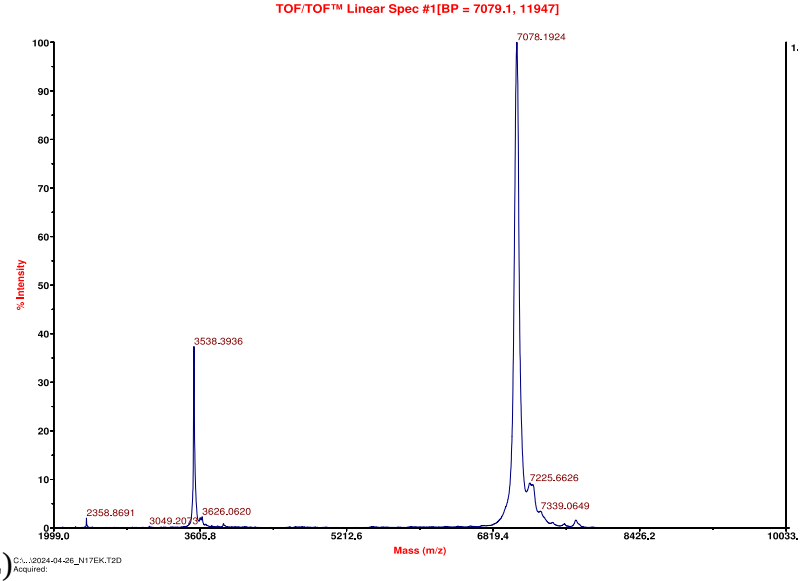
TOF/TOF™ Linear Spec #1[BP = 7079.1, 11947]
7078.1924
3538.3936
7225.6626
7339.0649
2358.8691
3626.0620
% Intensity
Mass (m/z)
1999.0
3605.8
5212.6
6819.4
8426.2

E)

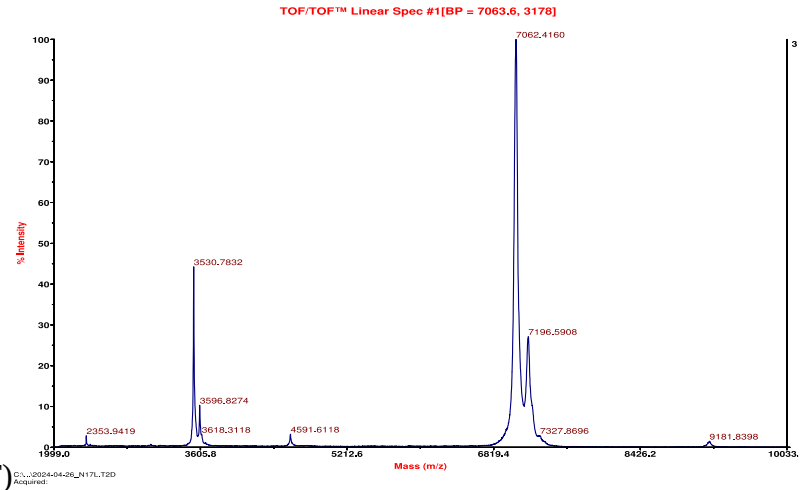
TOF/TOF™ Linear Spec #1[BP = 7063.6, 3178]
7062.4160
3530.7832
7196.5908
3596.8274
2353.9419
3618.3118
4591.6118
7327.8696
9181.8398
% Intensity
Mass (m/z)
1999.0
3605.8
5212.6
6819.4
8426.2

F)

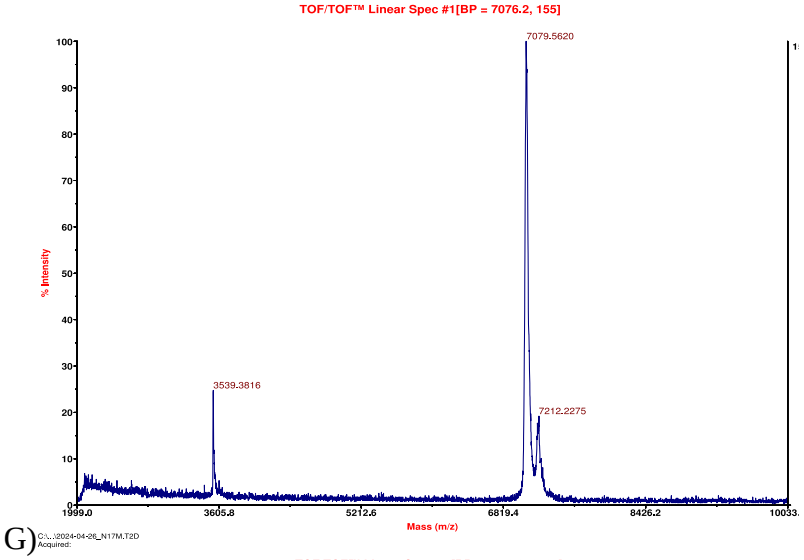
TOF/TOF™ Linear Spec #1[BP = 7076.2, 155]
7079.5620
3539.3816
7212.2275
% Intensity
Mass (m/z)
1999.0
3605.8
5212.6
6819.4
8426.2
10033.
C:\..\2024-04-26_N17M.T2D
Acquired:

G)

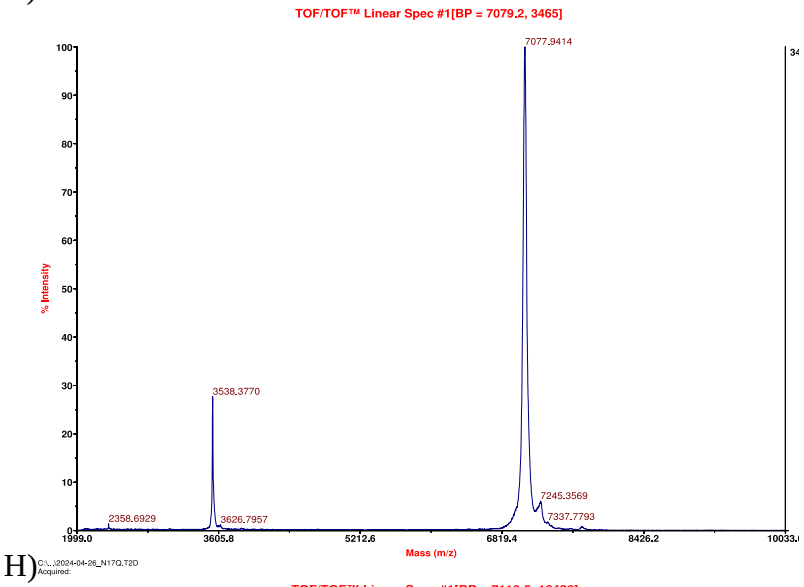
TOF/TOF™ Linear Spec #1[BP = 7079.2, 3465]
7077.9414
3538.3770
2358.6929
3626.7957
7245.3569
7337.7793
% Intensity
Mass (m/z)
1999.0
3605.8
5212.6
6819.4
8426.2
10033.
C:\..\2024-04-26_N17Q.T2D
Acquired:

H)

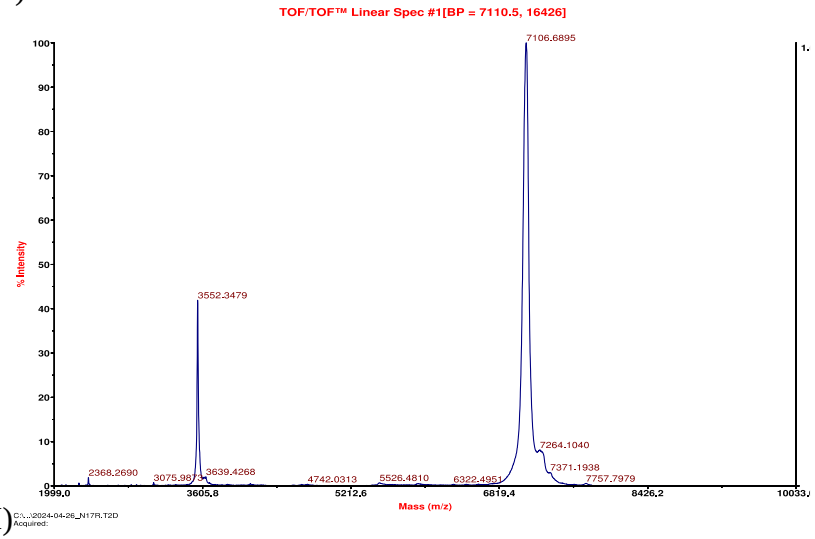
TOF/TOF™ Linear Spec #1[BP = 7110.5, 16426]
7106.6895
3552.3479
2368.2690
3075.9873
3639.4268
4742.0313
5526.4810
6322.4951
7264.1040
7371.1938
7757.7979
% Intensity
Mass (m/z)
1999.0
3605.8
5212.6
6819.4
8426.2
10033.
C:\..\2024-04-26_N17R.T2D
Acquired:

I)

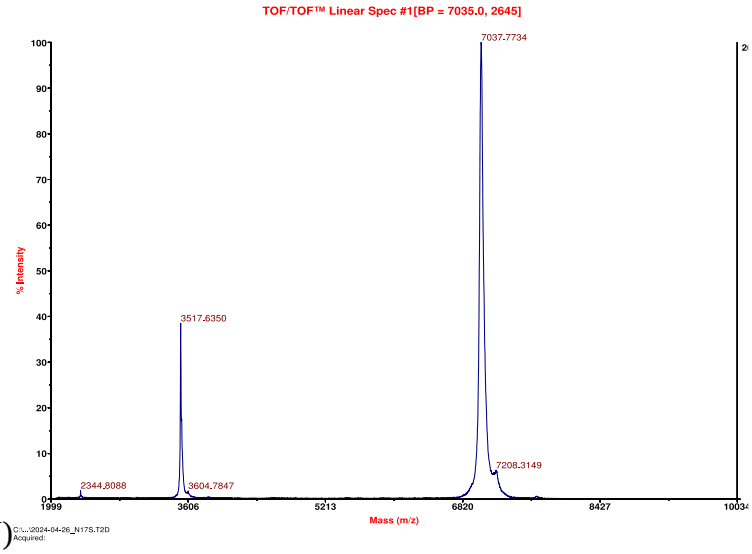

J) C:\...\2024-04-26_N17S.T2D
Acquired:

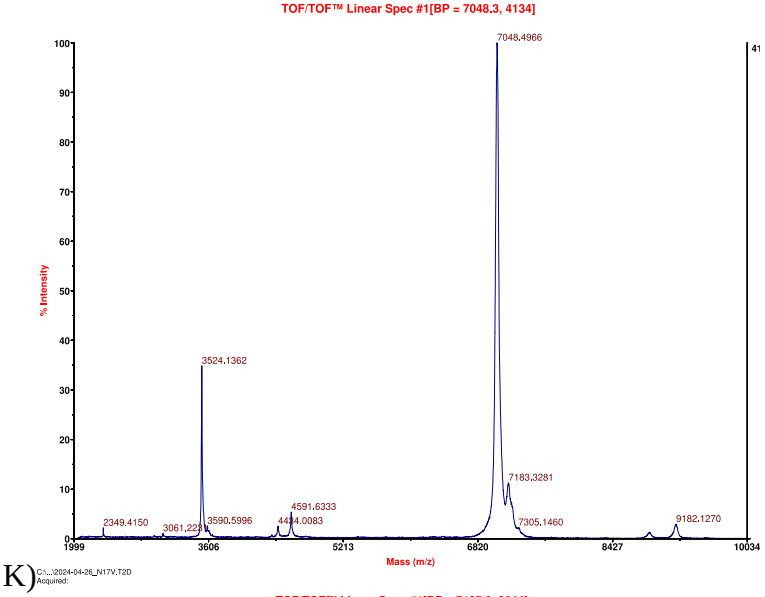

K) C:\...\2024-04-26_N17V.T2D
Acquired:

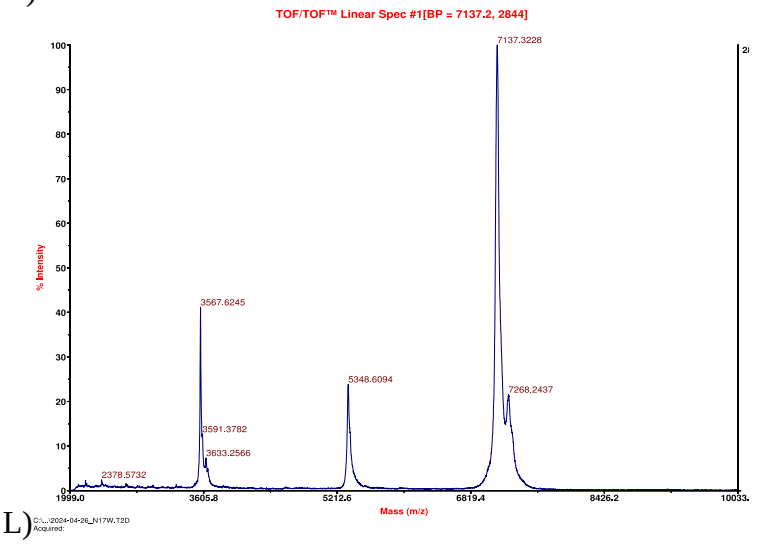

L) C:\...\2024-04-26_N17W.T2D
Acquired:

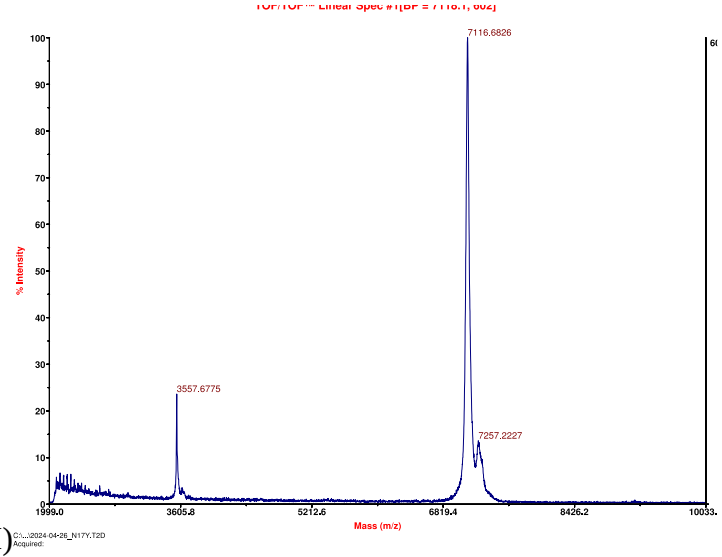
7116.6826
3557.6775
7257.2227
% Intensity
Mass (m/z)

M)

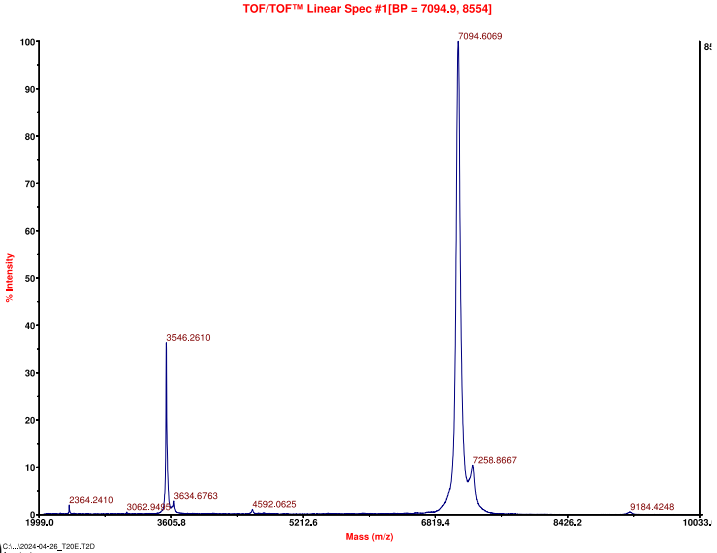
TOF/TOF™ Linear Spec #1[BP = 7094.9, 8554]
7094.6069
3546.2610
7258.8667
2364.2410
3634.6763
4592.0625
9184.4248
% Intensity
Mass (m/z)

N)

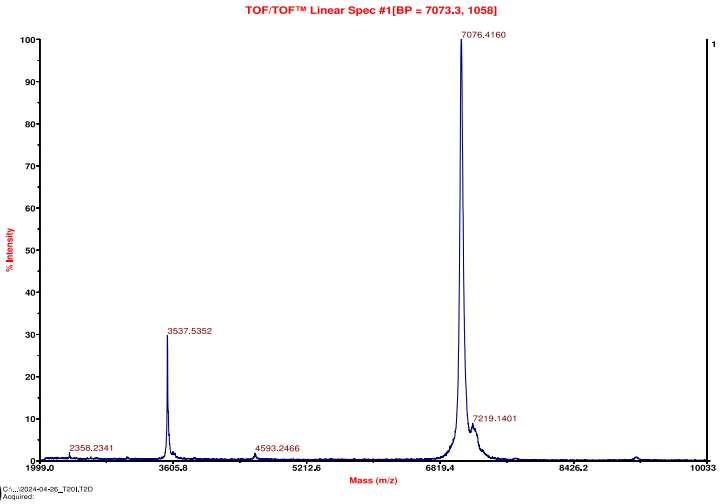
TOF/TOF™ Linear Spec #1[BP = 7073.3, 1058]
7076.4160
3537.5352
7219.1401
2358.2341
4593.2466
% Intensity
Mass (m/z)

O)

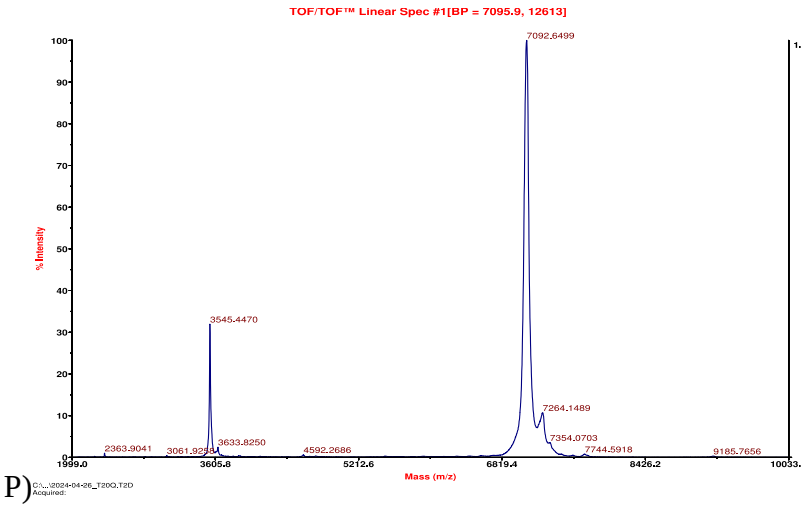

P)

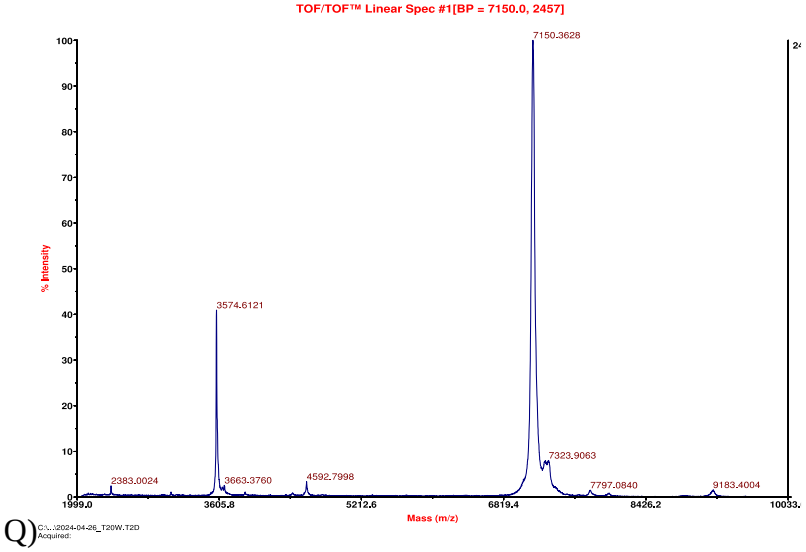

Q)

Figure C2. Mass spectra obtained using MALDI MS for A) N7A, B) N7E, C) N7F, D) N7I, E) N7K, F) N7L, G) N7M, H) N7Q, I) N7R, J) N7S, K) N7V, L) N7W, M) N7Y, N) T10E, O) T10I, P) T10Q AND Q) T10W. The mass obtained corresponded to the theoretical values.

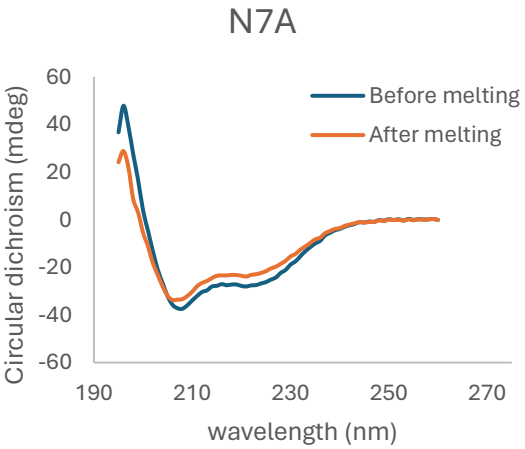
N7A
Circular dichroism (mdeg)
60
40
20
0
-20
-40
-60
190
210
230
250
270
wavelength (nm)
Before melting
After melting

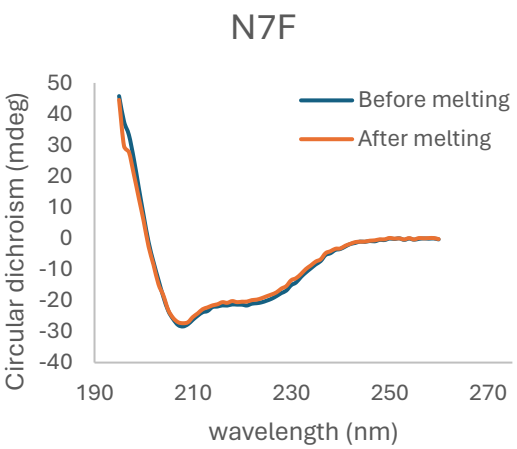
N7F
Circular dichroism (mdeg)
50
40
30
20
10
0
-10
-20
-30
-40
190
210
230
250
270
wavelength (nm)
Before melting
After melting

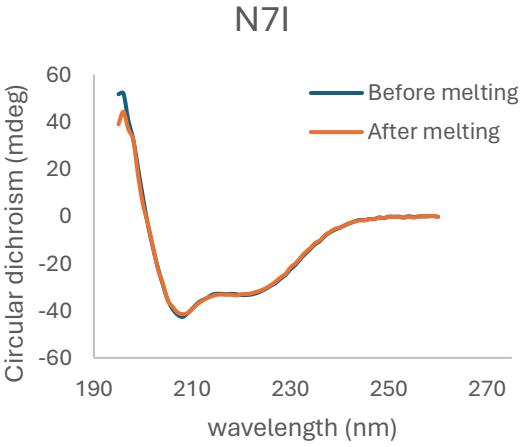
N7I
Circular dichroism (mdeg)
60
40
20
0
-20
-40
-60
190
210
230
250
270
wavelength (nm)
Before melting
After melting

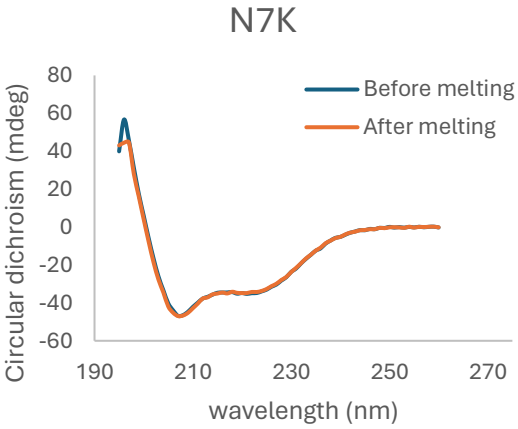
N7K
Circular dichroism (mdeg)
80
60
40
20
0
-20
-40
-60
190
210
230
250
270
wavelength (nm)
Before melting
After melting

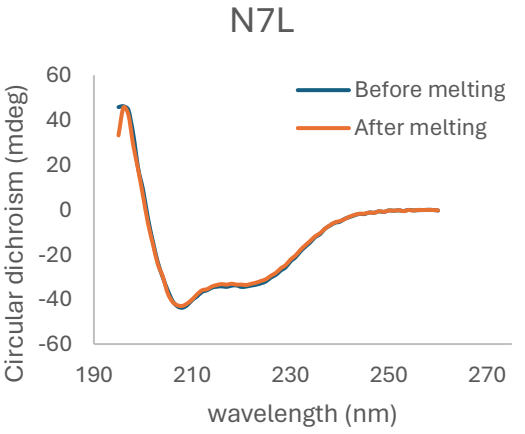
N7L
Circular dichroism (mdeg)
60
40
20
0
-20
-40
-60
190
210
230
250
270
wavelength (nm)
Before melting
After melting

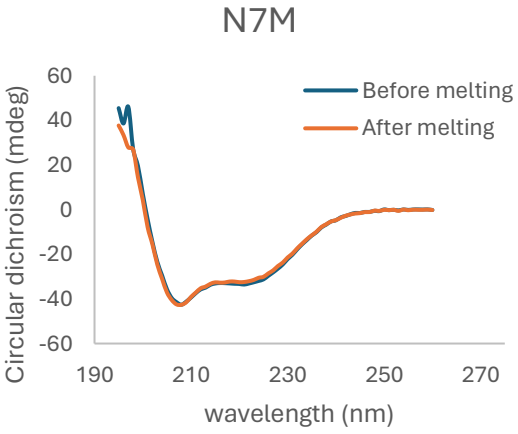
N7M
Circular dichroism (mdeg)
60
40
20
0
-20
-40
-60
190
210
230
250
270
wavelength (nm)
Before melting
After melting

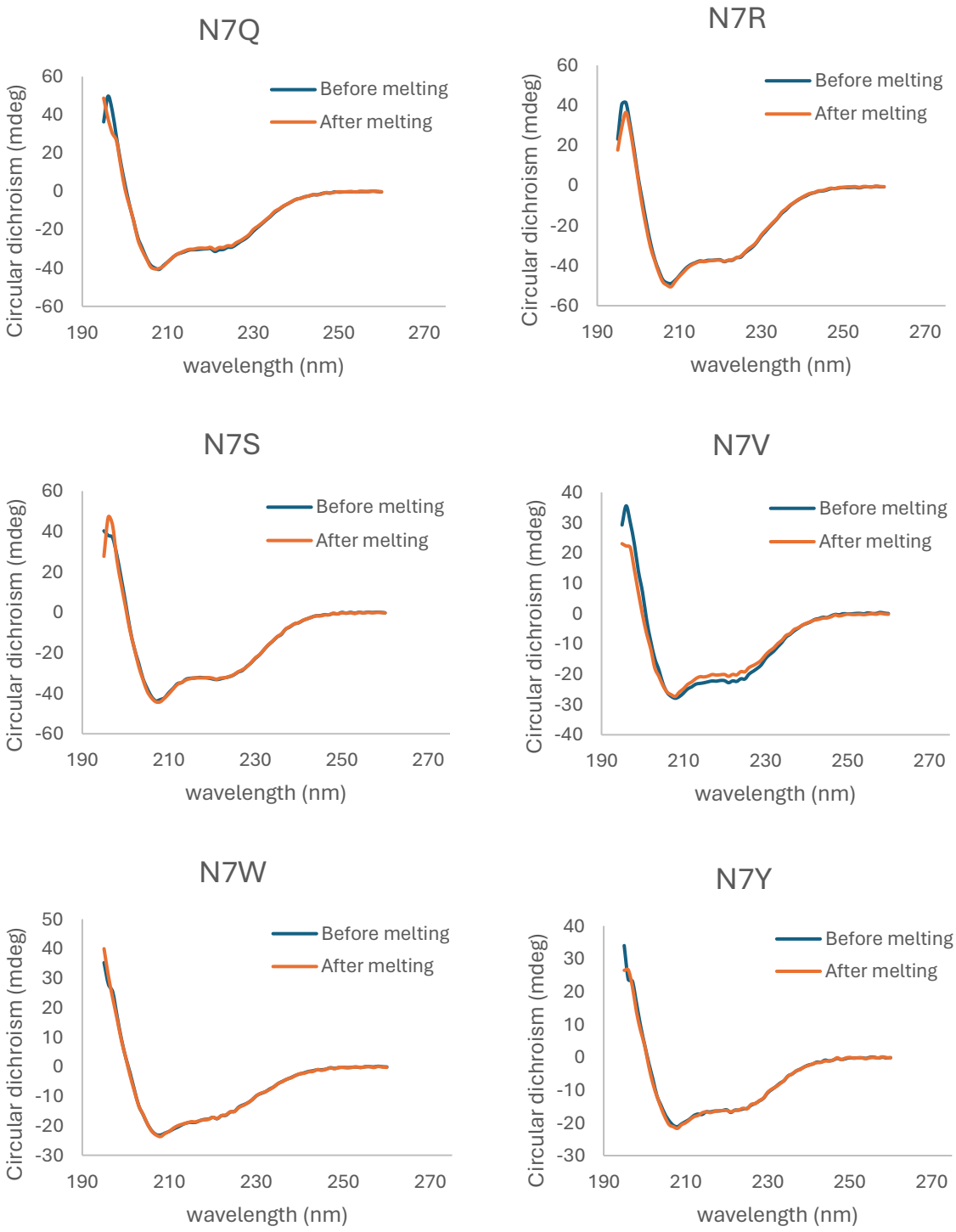

Figure C3. CD spectroscopy of the library explorations, N7E can be seen in Figure 13. The experiment was conducted twice, at room temperature, once before heat denaturation of the protein (in blue) and once after (in orange), to see the secondary structure of the protein. The α-helical structure can be seen due to dips at 208 and 222 nm. A total refolding can be seen for all variants.